PETROLOGY OF THE BONDLA MAFIC - ULTRAMAFIC COMPLEX, USGAON, GOA, WITH SPECIAL REFERENCE TO CHROMITE MINERALISATION

Thesis submitted to **Goa University**
for the degree of

DOCTOR OF PHILOSOPHY

in

GEOLOGY

by

DILIP BHIVA AROLKAR

M.Sc.

Department of Geology
Goa University
1995

CERTIFICATE

This is to certify that the thesis entitled "Petrology of the Bondla mafic-ultramafic complex, Usgaon, Goa, with special reference to chromite mineralisation" submitted by Shri. Dilip Bhiva Arolkar for the award of the degree of Doctor of Philosophy in Geology is based on the work carried out by the candidate under my supervision. The thesis or any part thereof has not previously been submitted for the award of any other degree or diploma of any other University or Institute. The material obtained from other sources has been duly acknowledged in the thesis.

Department of Geology,

Goa University,
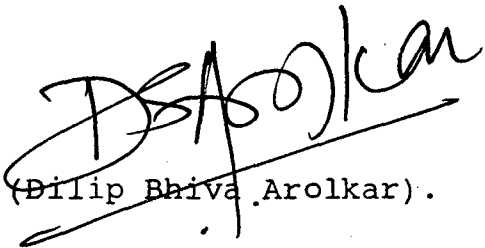
Taleigao Plateau,

Goa 403205.

(Dr. A.G. Dessai),

Research Supervisor.

Prof. Dr. A. G. DESSAI
M. Sc. Ph. D.
Research Supervisor
Department of Geology
GOA UNIVERSITY

STATEMENT

I declare that the thesis entitled " Petrology of the Bondla mafic-ultramafic complex, Usgaon, Goa, with special reference to chromite mineralisation " is my original contribution and that the thesis or any part thereof has not been peviously submitted for the award of any other degree or diploma of any University or Institute. To the best of my knowledge, the present study is the first comprehensive study of its kind from this area.

The literature pertaining to the problem investigated, has been duly cited. Facilities availed from other sources are duly acknowledged.

Department of Geology,

Goa University,

Taleigaon Plateau,

Goa 403205.

(Dilip Bhiva Arolkar).

ACKNOWLEDGEMENTS

CONTENTS

CHAPTER I

INTRODUCTION

CHAPTER I

INTRODUCTION

Prologue

The western Dharwar Craton of south India is cha-
racterised by profuse development of greenstones which are
associated with a number of mafic-ultramafic complexes.
The latter have been variously interpreted as Alpine-type
intrusions (Pichamuthu, 1956; Varadarajan, 1970; Karuna-
karan, 1970), submarine extrusives (Naqvi and Hussein,
1979), primordial rocks of komatiitic chemistry (Vishwa-
nathan, 1974 ; Naqvi and Hussein, 1979; Sudhakar, 1980),
and as layered intrusives (Varadarajan , 1970 ; Nijagu-
nappa and Naganna, 1983; Srikantappa et al.,1980).

The coastal belt of Goa and northern Karnataka
contains a number of N-S trending mafic-ultramafic com-
plexes which are included under Goa-Shimoga schist belt.
The Bondla mafic-ultramafic complex is one such complex
located in central Goa about which little geological
information is available. The complex is emplaced into

1

supracrustal rocks which host some of the important iron ore deposits of the country. The latter being economically important have been subjected to detailed scrutiny. Considerable information on the geology of these deposits has accumulated particularly during the post - liberation period. The associated mafic-ultramafic rocks on the contrary have remained largely neglected. Consequently, little information on the geological setting, structural features, petrography, geochemistry and mineralisation characteristics of these rocks is available, that could be utilised in understanding the petrogenesis and ore potential of these rocks. In an attempt to rectify the dearth of information, the author decided to study the geology of the mafic-ultramafic complex at Bondla in central Goa.

Previous Work

The schistose rocks occurring in southern Mahratta and Karnataka were designated as "Dharwars" (Foote 1876). Three such bands of schistose rocks were described by Foote (1876) from this area. Maclaren (1904) gave the name "Castle Rock Band" to one of the bands described by Foote (1876). This band consists of dolomitic limestones and

quartzites which occasionally grade into quartz-schist.

In the classic work on manganese ore deposits of India, Fermor (1909) has briefly described the manganese ores of Goa. References to the manganese ores are also listed in the memoirs on manganese ores of India (Dunn, 1942). Most of the information available till 1950 has been summarised by Pascoe (1965). The Dharwars constituting the `Castle Rock Band' are represented by quartzites, magnetite-quartzites, haematite-quartzites, limonite-quartzites, sericite- quartz-schists, fine grained biotite-quartz-schists, phyllites, fine grained grey limestones and basic igneous rocks (Pascoe, 1965). According to Dhepe (1963) the `Castle Rock Band' begins in North Canara (Karnataka), runs northwards along the Western Ghats through Goa until it disappears under the Deccan Traps in Belgaum, while small portions extend in south Ratnagiri district of Maharashtra.

Oertal (1958) made a brief mention of the occurrence of iron and manganese ore deposits and published the first geological map of Goa. The iron ore deposits of Goa

3

have been studied by Gokulam (1972) and their mineralogy

has been investigated by Majumdar (1965); Sahu and Gurav

(1972) and Dessai (1980).

A systematic study of manganese ores of south Goa

has been carried out by Dessai and Deshpande (1977a;

1977b; 1978; 1979a). A concise account of the geology of

the manganese ores of south Goa is available in (Dessai,

1985a). The mineralogy of clays from Sanvordem (Dessai,

1985b) and Colva (Dessai and Warrier, 1986) and of litho-

marges from parts of Goa has also been investigated

(Dessai, 1984). Rocks of komatiitic chemistry have been

reported from south Goa by Dessai and Deshpande (1979b;

1979c).

A revised geological map of Goa is published by

Gokul et al., (1985). The rock formations from Goa have

been included under the Goa Group (Gokul et al., 1985),

which has been correlated with the Chitradurga Group of

the Dharwar Supergroup. Dhoundiyal et al., (1987) have

studied the geochronology and geochemistry of the granitic

rocks of Goa. Brief descriptions on petrography of the

granitic rocks are also available in Gopalkrishna (1976) and Gokul and Srinivasan (1976). Geology and structure of central Goa have been described by Dessai and Peshwa (1982), Jena (1985) and Balakrishnan et al., (1992). Sulphide minerals in the greenstones from Tisk-Usgaon is investigated by Vidyadharan and Abbas (1989), and Dessai et al.,(1994).

The Area

An area around Bondla extending from Usgaon in the north to Durgini in the south, in central Goa (Fig.1.1) where mafic-ultramafic rocks are best exposed, was selected for study. It is included in Survey of India topographic sheet No.48 I/3 and is bounded by latitudes 15o 22' 11" and 15o 27'52" N and longitudes 74o 04'20" and 74o 10' 00"E. Towards the east the area is bounded by the foothills of the Western Ghats, towards the west and south it is delimited by the northwesterly flowing Dudhsagar river. The northern boundary is marked by the Madai river and its northwesterly flowing tributary - the Ragada. The Ragada and Dudhsagar are both tributaries of the westerly flowing Mandovi.
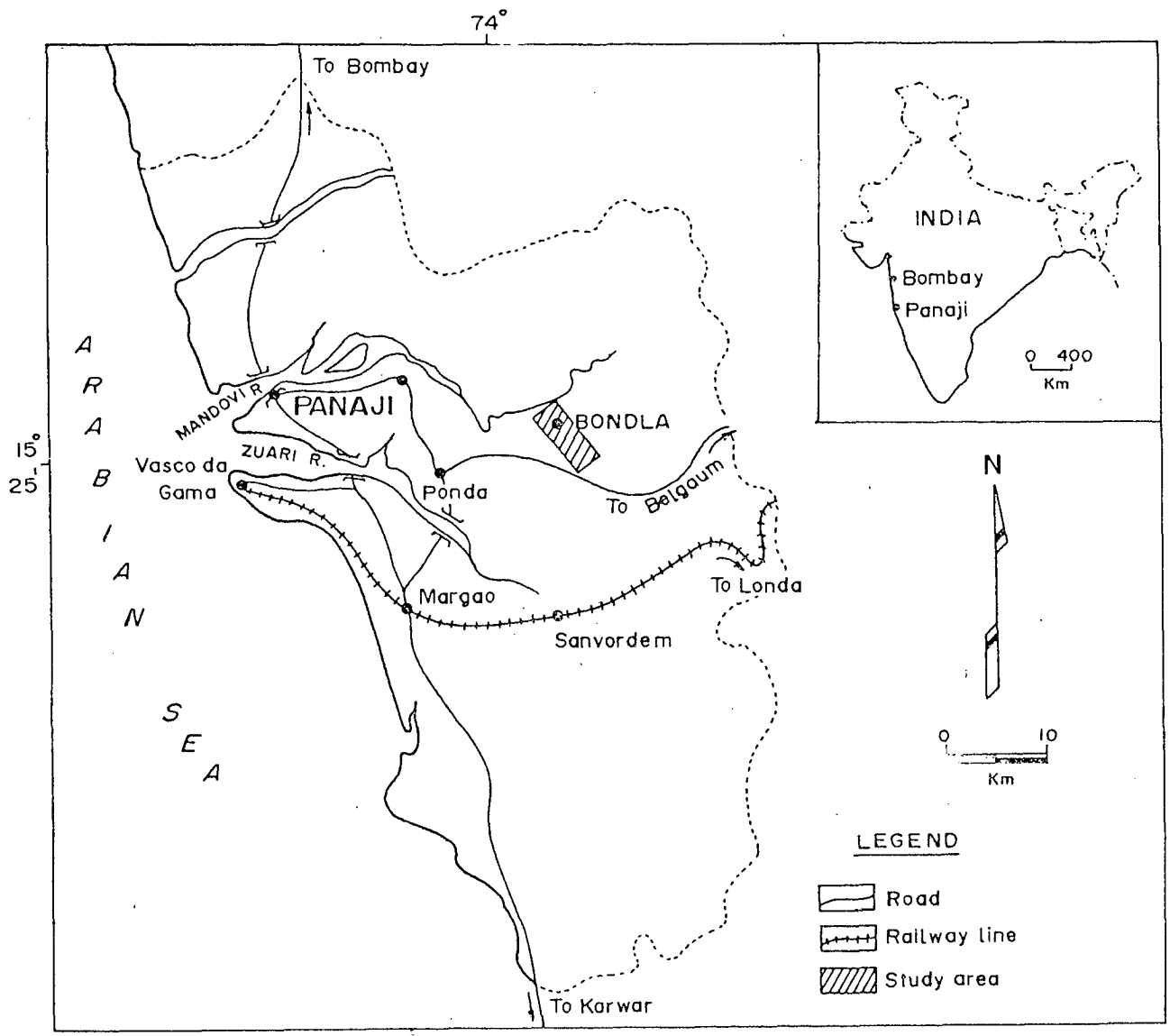
Fig. 1.1 Location map.

The nearest railway station is Sanvordem which is located to the south of the area . It is connected to Usgaon - the major township in the north by an all weather road. The Panaji-Belgaum national highway-NH4A passes along the southern and western parts of the area. Tisk is an important market place in the southern part of the area located on the national highway. Ponda is the nearest major township which is about 10 km west of Tisk. Ponda is connected to other important townships such as the capital Panaji to the northwest and Margao to the southwest by all weather roads. Panaji is situated about 40 km by road from Tisk and Margao about 28 km. Important localities in the area are Bondla, Ganje, Nanus, Dharbandora, Durgini and Poikul which are all interconnected by metal roads.

Physiography

The area around Bondla is a hilly terrain. The major portion of the area is occupied by hill ranges running NW-SE. The hills are densely vegetated. The maximum elevation in the central part of the area around Dharbandora is 461 m above M.S.L. and in the southeastern

part at Durgini it is 396 m above M.S.L. Other peaks in
the northwestern part show elevations varying between 250
and 375 m.

The major water divide runs NW-SE. The streams
originating from this divide flow either due NE or SW.
Those flowing due NE meet the Ragada which is a north
westerly flowing tributary of the Madai. The Ragada
meets Madai at Konkere. Further, the Madai follows a
westerly course for about 14 km upto Sonarwada. From
Sonarwada the river takes a sharp turn and flows north-
westerly. From here onwards it is known as the Mandovi.
The streams flowing due SW meet the Dudhsagar river. After
flowing over a distance of about 5-6 km, the Dudhsagar
follows a northwesterly course upto Sonarwada where it
meets the Mandovi. The Mandovi follows a northwesterly
course for a distance of about 40-45 km until it meets the
Arabian sea at Panaji - the capital of Goa. The river
Mandovi is navigable in the lower reaches and hence used
as a water-way to transport iron and manganese ores mined
in the hinterland.

Methodology

The study was undertaken to investigate the geological setting, the structure, petrography, geochemistry, the mineral chemistry and the petrogenesis of the mafic-ultramafic rocks and associated chromite mineralisation.

The area was geologically mapped on 1:25,000 scale. The structure of the area was studied with the help of aerial photographs on 1:60,000 scale followed by field checks. During the field work, the attitude of structural elements such as foliations, lineations, joints, faults, shear zones were studied and recorded. Similarly the layering shown by the mafic-ultramafic rocks was also studied and the attitude of layering was recorded. The representative samples of all rock types and the associated chromite were collected. The rock samples were subjected to laboratory investigations. Microsections and polished sections of rocks and ore minerals were studied in transmitted and incident light. Modal analyses of all rock types were carried out with James-Swift automatic mechanical point counter. The optical properties of the silicate minerals were determined with the 4-Axes Univer-

sal Stage. The anorthite content was determined with the help of Universal Stage using Slemmons (1962) Curves. A number of polished sections of chromite and sulphide minerals were studied in incident light under a Leitz ore microscope. Representative rock samples were chemically analysed for major, trace and rare earth elements. The major elements were analysed by rapid analysis technique of Shapiro and Brannock (1962) using USGS silicate rock standards (Flanagan, 1967). Repeat analyses were carried by Atomic Absorption Spectro-photometer at Deccan College, Pune. Some of the samples were analysed by X-Ray Flourescence Spectroscopy (XRF) at the National Geophysical Research Institute (NGRI), Hyderabad and the analytical results were cross checked at the C.S.I.R.O. Australia. Trace and rare earth element analyses were carried out at N.G.R.I. by Inductively Coupled Plasma Spectroscopy (ICP-MS). Additional samples were analysed by INAA at C.S.I.R.O., Australia.

Mineral analyses were carried by GEOL, Electron-probe Analyser under standard conditions at CSIRO, Australia, using synthetic and natural standards at accelerating voltage of 15 kv and a specimen current of 3 nA.

CHAPTER II

GEOLOGICAL SETTING

CHAPTER II

GEOLOGICAL   SETTING

The chapter deals with the geological setting of
the Bondla mafic-ultramafic complex.   An outline of the
regional geological framework is followed by a concise
account of the geology of Goa.   Lastly,   the geology of
the area is described.

Regional Geological Framework

The area under study forms a part of the Karnataka
Craton of Peninsular India.   The craton is predominantly
occupied by granitic gneisses,   granites,   and schistose
supracrustal rocks.   The former constitute the Peninsular
Gneissic Complex whereas,   the schistose rocks have been
included by Foote (1876) under the Dharwar System.   The
gneisses and the schists together constitute the Archaean
of Peninsular India.

10

Fermor (1936) was amongst the earlier workers who first divided the Archaean province of India into two sub-divisions. The charnockitic region to the south and the non-charnockitic region to the north. This early idea was later developed by Radhakrishna (1983) who recognised two types of metamorphic terrains in south India : (i) the southern high-grade Granulite terrain and (ii) the northern low-grade Granite-Greenstone terrain. Within the latter two types of provinces are recognised - the western and the eastern. These are separated by the N-S running Closepet Granite batholith. The western province is referred to as the iron- manganese Shimoga province and the eastern as the Kolar Gold Field province (Radhakrishna, 1983). These two provinces are also referred to as the western Dharwar Craton and the eastern Dharwar Craton respectively (Naqvi and Rogers, 1987). The area under study forms a part of the western Dharwar Craton.

The western Dharwar Craton is constituted of schistose supracrustal rocks consisting of a volcano- sedimentary assemblage. The rocks occur as bands of greenstone which are separated from one another by intervening gneissic and granitic rocks. Number of such bands have been

described from the craton. They are considered to be the remnants of the Dharwar metavolcanics and metasediments which formerly covered a large part of the craton and which have escaped denudation as they formed synclinal strips folded-in with the gneisses (Krishnan, 1968).

The schists and the gneisses exhibit a complicated interrelation with each other. In some areas, the schists appear to rest on the gneisses whereas in others a reverse relationship is observed. Opinions differ among various workers as regards the basement cover relationship which has led to a major debate on the Archaean rocks of peninsular India. Hence, different workers have proposed various schemes of classification for the Dharwars of south India (Smeeth, 1916; Rama Rao, 1940; 1962; Nautiyal, 1967; Pichamuthu, 1968; Radhakrishna, 1974 ; 1983 ; Swami Nath *et al.*, 1976).

Three views on the classification of Dharwars are widely prevalent : (i) the Dharwar greenstone suite is younger than the Peninsular Gneiss (ii) the Dharwar schistose rocks belong to one stratigraphic suite which is older than the Peninsular Gneiss and (iii) the Dharwar

12

supracrustals belong to a number of different suites whose ages overlap those of gneissic rocks.

Various attempts have been made to resolve the schist-gneiss controversy by radiometrically dating the components of the Peninsular Gneiss. The latter includes a complex suite of tonalite-trondhjemite gneiss with a wide variety of screens and inclusions of other rock types. Some of these enclaves are engulfed remnants of older schists, whereas, others may be metasedimentary and/or metavolcanic rocks formed on the gneisses and not connected to the schists. The gneiss suite includes former sedimentary, volcanic and intrusive rocks, metamorphosed and emplaced granite. These various components are so closely and finely intermixed that their discrimination is not possible.

The radiometric ages of the Peninsular Gneiss suite therefore, vary greatly between 3400 and 3000 Ma (Naqvi and Rogers, 1987). Some of the oldest ages are provided by the Gorur Gneiss - 3358 ± 60 Ma (Beckinsale, et al.,1980) and Anmod Ghat Trondhjemitic Gneiss - 3400± 140 Ma (Dhoundiyal, et al., 1987). By and large it is agreed

13

that the 30.00 Ma period represents the time of emplacement of trondhjemitic gneiss and corresponds to the cratonisation of the western Dharwar Craton (Naqvi and Rogers, 1987). Towards the eastern part of the craton a suite of potassic granite known as the Closepet Granite occurs whose ages vary betwen 2500 and 2300 Ma. e.g. Chitradurga Granite and Arsikeri Granite.

In recent years, Radhakrishna (1974) and Swami Nath et al., (1976) suggested that the Peninsular Gneiss formation is an event separating two Archaean greenstone sequences. The older sequence is included under the Sargur Group (Swami Nath and Ramakrishnan, 1981) whereas, the younger one constitutes the Dharwar Supergroup (Swami Nath and Ramakrishnan, 1981). The general stratigraphic scheme for the western Dharwar Craton is as follows (after Swami Nath and Ramakrishnan, 1981):

```
Middle to Late Proterozoic              Kaladgi, Badami

(Helikian & Hadrynian)                  and Bhima Groups.


                                        ----- UNCONFORMITY-----

Late Archaean

(Kenoran)                               _

to Early Proterozoic                    |  Chitradurga

(Aphebian)          DHARWAR             |  Group

(2400 - 2600 Ma)    SUPERGROUP          |---Unconformity---

                                        |  Bababudan

                                        |_ Group

                                           -----UNCONFORMITY-----


                                        _

Middle Archaean                         |  Migmatites,

                    PENINSULAR|            gneisses,

(2900 - 3000 Ma)    GNEISS              |_ granitoids


                                        _

Early to Middle                         |  Several

Archaean                                |  unclassified

                    SARGUR              |  associations

                    GROUP               |  of supra-

(> 3000 Ma)                             |  crustal

                                        |_rocks

                        Basement   not seen

                        (3400 Ma gneisses)
```

15

Geology of Goa

Major portion of Goa is occupied by the rocks of the Dharwar System (Foote, 1876). Maclaren (1904) described the rocks from Castle Rock along the eastern border of Goa and assigned them to "Castle Rock Band" which occupies a major portion of Goa and extends northwards into the Konkan region of Maharashtra. Towards the south it extends into North Canara district of Karnataka. The "Castle Rock Band" comprises magnetite-, haematite-quartzite, biotite-quartz-schist, phyllites, grey limestones, basic igneous rocks and granitic gneisses. A summary of information available till 1950 is found in Pascoe (1965). He has referred to the Goa rocks as northward extensions of the Upper Chloritic Division of Dharwar System (Smeeth, 1916). Oertal (1958) carried out systematic mapping of Goa and published the first geological map of the region. He divided the Dharwarian rocks into: (i) Lower Intra- conglomerate group and (ii) Upper Metalliferous group of schistose rocks. The granitic rocks were considered by him to be intrusive into the schist.

During the post -liberation period, the Geological Survey of India carried out systematic geological mapping and a revised geological map was published (Gokulam, 1972). Except for a small area in the northeast which is covered by Deccan Traps (late Cretaceous to Eocene), the rest of the state is occupied by greenstones of Archaean to Proterozoic age. The rocks in general trend NW-SE conforming to the regional Dharwarian trend in Peninsular India. Gokul *et al.*, (1985) assigned these rocks to the Goa Group which in their opinion, is broadly comparable and correlatable to the Chitradurga Group of the Dharwar Supergroup. The Goa Group consists of four formations. The detailed stratigraphic succession is as follows (after Gokul *et al.*, 1985):

SUB-RECENT | Sea sand and
TO RECENT |_Laterite

UPPER CRETACEOUS   DECCAN TRAP | Basalt
TO LOWER EOCENE

PROTEROZOIC ?   BASIC | Dolerite,
                        INTRUSIVES |_Gabbro

```
                                              _
                                             | Pegmatite,
                                             | Vein quartz,
                                             | Porphyritic
                             ACID            | granite,
PROTEROZOIC                                  | Hornblende
                             INTRUSIVES      | granite,
                                             | Felspathic
                                             | gneiss,
                                             |_Granite gneiss


                             _               _
PROTEROZOIC                 |Vagheri        | Metabasalt
                            |Formation      |_Metagreywacke
                            |
                            |                 _
                            |                | Banded
                            |                | ferruginous
                            |                | quartzite
                            |                | Manganiferous
                            |                | chert breccia
```

18

		Bicholim Formation	with pink ferruginous phyllite
			Limestone
ARCHAEAN	D H A		Pink ferruginous phyllite
TO	R W A R		Quartz-chlorite-amphibole schist
PROTERO-ZOIC			
	GOA		
	GROUP		
		Sanvordem Formation	Argillite
			Quartzite
	S U P E R G R O		Tilloid
			Metagreywacke
			Metagabbro
			Peridotite
			Talc-chlorite-schist
			Variegated phyllite

```
U          |Barcem         | Quartz-
P          |Formation      | chlorite-
           |               | schist
           |               | Quartz-
           |               | sericite-
           |               | schist
           |               | Red phyllite
           |               | Quartz
           |               | porphyry
           |               | Massive,
           |               | Schistose,
           |               | Vesicular
           |_              |_metabasalt
```

The Barcem Formation is predominantly constituted
of metabasalts which are schistose, vesicular and mas-
sive. These are intercalated with metasediments. Argil-
lites and metagreywackes dominate the Sanvordem Formation
whereas pink ferruginous phyllites with banded-haematite-
quartzites predominate in the Bicholim Formation. The
youngest Vagheri Formation comprises metagreywacke and
metabasalt. This volcano- sedimentary sequence is intrud-
ed by granitic gneisses which are exposed in three differ-

ent areas of the state. Dhoundiyal *et al.*, (1987) carried out Rb-Sr whole rock radiometric dating of the granitic gneisses from Goa. The Anmod Ghat Trondhjemitic Gneiss which outcrops in the eastern part of the state has yielded a Rb-Sr whole rock isochron age of 3400 $\pm$ 140 Ma (Dhoundiyal *et al.*,1987). This gneiss is analogous to the Gorur Gneiss of Karnataka which has also provided some of the oldest ages (3358 $\pm$ 67 Ma; Beckinsale *et al.*, 1980) so far recorded in south India. The Anmod Ghat Trondhjemitic Gneiss therefore, could represent the basement for the Goa Group of rocks (Dhoundiyal *et al.*, 1987). The other granitic gneisses from Goa such as the syntectonic Chadranath Granite from central Goa has been dated to 2650 $\pm$100 Ma and the post -tectonic Canacona Granite Porphyry from south Goa has given Rb-Sr whole rock age of 2395 $\pm$ 390 Ma (Dhoundiyal *et al.*, 1987).

A number of basic intrusives represented by gabbroic plutons and dolerite dykes intrude the schistose rocks. The mafic-ultramafic complex at Bondla near Usgaon is one such intrusive complex in central Goa (Jena, 1985; Balakrishnan *et al.*, 1992). All rocks in general except the granitic gneisses and the intrusive mafic-ultramafic

complexes exhibit a thick laterite cover which varies in thickness from a couple of metres to over 25 metres.

Structurally, the area is complex and exhibits at least three cycles of deformation during which the rocks have been subjected to folding and faulting. During the first phase of deformation the rocks were folded along an E-W axis with folds plunging due west. Such folds are seen in the southern part of Goa. The Chandranath Granitic Gneiss occupies the core of an antiformal structure related to this fold movement (Gokul, 1985).

The above deformational episode was followed by the second fold movement which was the strongest phase of deformation along a NE-SW compression. The resulting folds trend NW-SE and are best exposed in the central and northern parts of Goa. The folds are tightly appressed, isoclinal to overturned to the SW and doubly plunging by 20 to 40º due NW and SE (Gokul, 1985). A number of NW-SE and NE-SW trending faults and shear zones traverse the rocks. One of the NW-SE trending shear zones traverses the rocks of the western part of the area under investigation.

Geology of the Area

The area under study where the mafic-ultramafic complex is exposed, exhibits a thick laterite and soil cover which supports dense vegetation (Plate I Photo 1). This has hindered field observations to a considerable extent. It was observed that the metasediments exhibit the thickest laterite cover followed in decreasing order by the peridotites. The gabbroic rocks in particular are least lateritised.

Mapping of the lithological ~~the~~ units and delineating their boundaries had to be done on the basis of the detached remnant outcrops. Hence, the boundaries of the different lithological units are inferred. Fresh outcrops were available along road cuttings, stream cuttings, quarry and mining pits and unlateritised remnants. Help was also taken of black and white aerial photographs on 1:60,000 scale to demarcate the boundaries of the lithological units and to study the structure of the area.

Aerialphoto interpretation followed by ground truth collection showed that the metasediments are folded into a NW-SE trending anticline. It is overturned towards SW and is plunging due NW (Dessai and Peshwa, 1982). A prominent shear zone traverses the western limb of the fold. The shear zone extends over a length of 15 km from Kusumwada in NW to Gurkhem in SE. Its maximum width is about 2 km (Balakrishnan et al., 1992). The shear zone can be examined to the east of Usgaon-Tisk road (Plate I Photo 2). The rocks are crushed and mylonitised. This is related to the second episode of folding (Gokul, 1985). Along the shear zone, the rocks of the mafic-ultramafic complex have been fractured. Away from the shear zone, the effects of shearing are subdued. It appears therefore, that the shearing may have been synchronous with the emplacement of the complex.

The metasediments are foliated parallel to the direction of shearing. The foliation trends N305⁰ and dips 35-40⁰ due N45⁰. The shear zones are often conjugated with dextral and sinistral displacement on sub-vertical shear surfaces. The metasediments are traversed by four sets of fractures. They trend (i) N335⁰ and dip 40-

24

45o towards N235o (ii) N275o dip 40-42o towards N5o (iii)

N255o dip 70-80o towards N165o and (iv) N230o dip 70o

towards N320o.

These fractures are filled by quartz-calcite veins

which belong to three episodes. The quartz veins of the

first episode trend N335o and N275o. They are cut by

veins trending N255 to 265o which belong to the second

episode. The veins of both these episodes are very thin

(5 mm - 1 cm in thickness). The veins of the second

episode are lenticular. The lenticles exhibit sinistral

en echelon pattern. At places, gash veins of quartz

trending N-S are seen. They vary between 2 and 10 cm in

length and less than 1 cm across and have tapering ends.

These veins are traversed by a very prominent set of

quartz veins trending N230o. They vary in width from 5-

30 cm. The veins pinch and swell both along the strike

and dip (Plate II Photo 1). The intersections of these

veins with those of the second generation are invariably

occupied by sulphides. At places, along intersections of

veins crescent shaped, unsupported country rock fragments

are seen within milky quartz. At places, augen shaped

fragments of country rock are found enclosed in loops of

vein quartz. Along the contacts of the veins the country rocks are discoloured in comparison with the unaltered rock which is dark grey to pale greyish in colour. The width of discoloured zone varies depending upon the thickness of the quartz vein. In general, vein with an average width of about 2 cm shows a discolouration zone of the same width. The veins also exhibit a thin zone of sericite and propyllite along the contact. In the immediate vicinity of the veins the proportion of sericite increases. Away from the vein contact the wall rock alteration assemblage is represented by epidote, sphene and calcite. The thicker veins of quartz (4-6) cm show banding and crustification which is marked by alternate bands of calcite and quartz. The quartz-rich bands are generally thicker than those of calcite. At places, vugs and cavities are lined by idiomorphic crystals of quartz and calcite. The veins also show well developed crystals of quartz grown from opposite side of the vein wall.

The area is predominantly covered by metasediments with interlayered metavolcanics which belong to the Barcem Formation. The various lithological units exposed in the area are shown in the geological sketch map (Fig. 2.1)
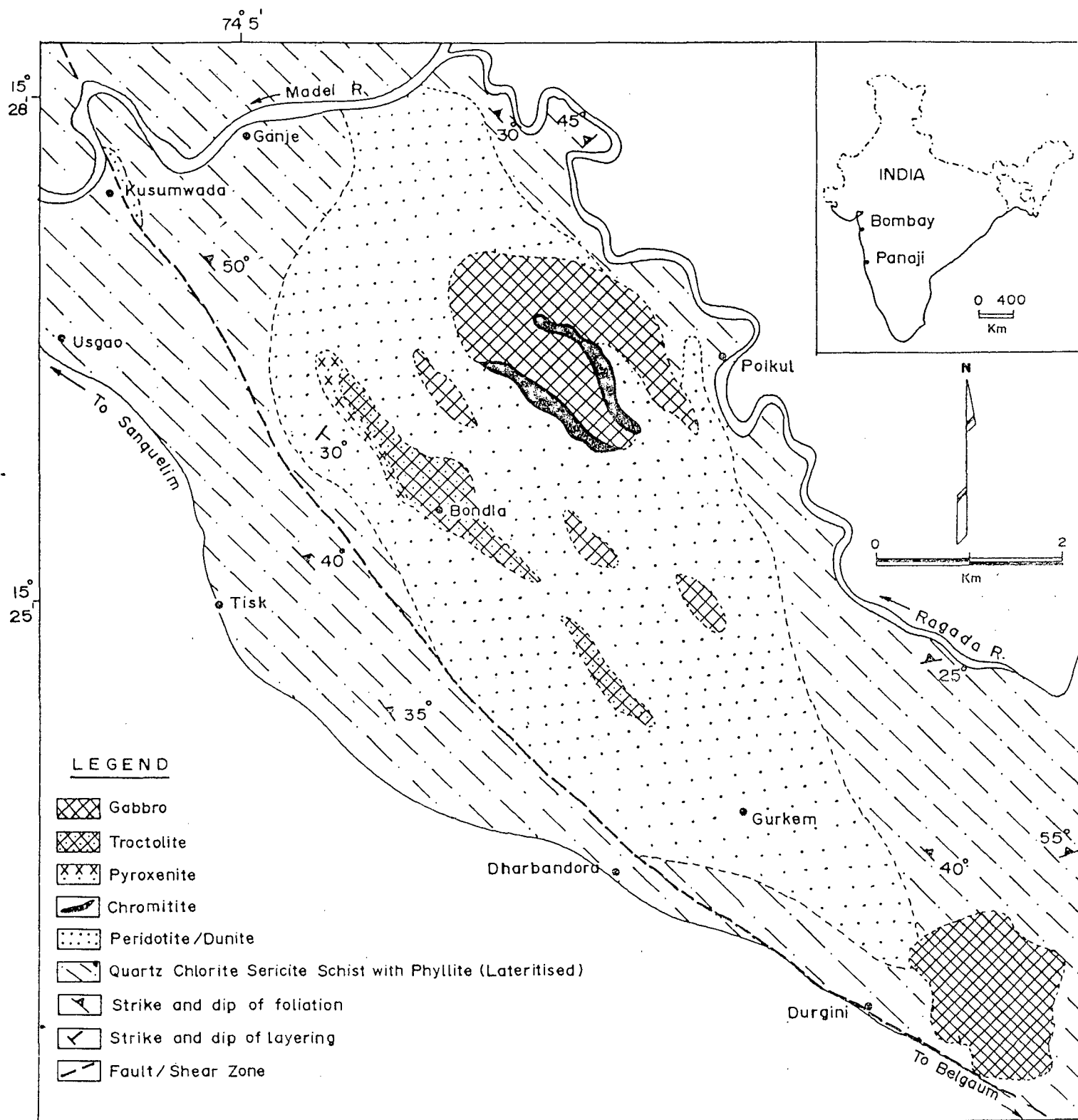
Fig. 2.1   Geological sketch map of the Bondla mafic-ultramafic
complex (modified after Gokul, _et al._,   1985 and
Balakrishnan _et al._, 1992)

which is compiled based on field observations, study of
the aerial photographs and information from the litera-
ture. The metasediments consist of quartz - chlorite-
sericite-schists and phyllites with banded iron-formations
which outcrop mainly to the north of the area. The quartz-
chlorite-sericite-schists are exposed to the west of
Usgaon-Tisk (Mollem) road. They are extensively lateri-
tised. Isolated exposures are found along the road cut-
tings. The rocks are well foliated. The foliation is
marked by parallel arrangement of flaky chlorite and
sericite. The foliation strikes N305o and dips 35-
40o due N45o. At places, intercalations of pink- ferrugi-
nous phyllite can be seen. The chlorite schists along the
strike are gradational into sericite schists. The
quartz-chlorite-sericite-schists are underlained by
phyllites. The latter constitute the most dominant hori-
zon in the stratigraphic sequence. Isolated exposures of
phyllite are found from Usgaon in the north to Durgini in
the south, however, rarely they are fresh. The phyl-
lites are extensively and almost completely lateritised
except in places where they are more arenaceous. Along
the strike, the phyllites which are normally pale grey in
colour, become ferruginous and grade into pink phyllites.

27

They have intercalations of haematite-quartzite. The phyllites strike N10o and dip 40-50o due N50o. To the north of Usgaon, they ~~ares~~ are intercalated with metabasalts which are exposed in the Madai river. The metabasalts are non-vesicular and exhibit weak schistosity.

The metasediments are intruded by an almost elliptical N-S trending mafic-ultramafic complex. A composite schematic stratigraphic section (not to scale) is shown in Fig.2.2. The complex occupies the core of the NW-SE trending fold (Dessai, 1985a; Dessai and Peshwa, 1982) discernable on aerial photograph. The western contact of the complex is sheared and mylonitised. The shear zone trends NW-SE. The complex comprises mafic and ultramafic rocks. The latter are represented by dunites and peridotites which are exposed towards the northern and central part of the area. Those towards the north are exposed at Ganje about 2.5 km east of Usgaon. In the central part the exposures are found about 2 km east of Tisk. Good exposures of peridotites are also found to the east of the Usgaon- Bondla road. The ultramafites are represented by serpentinised and talcose peridotites and dunites. They are pale greyish green in colour when fresh. Along the
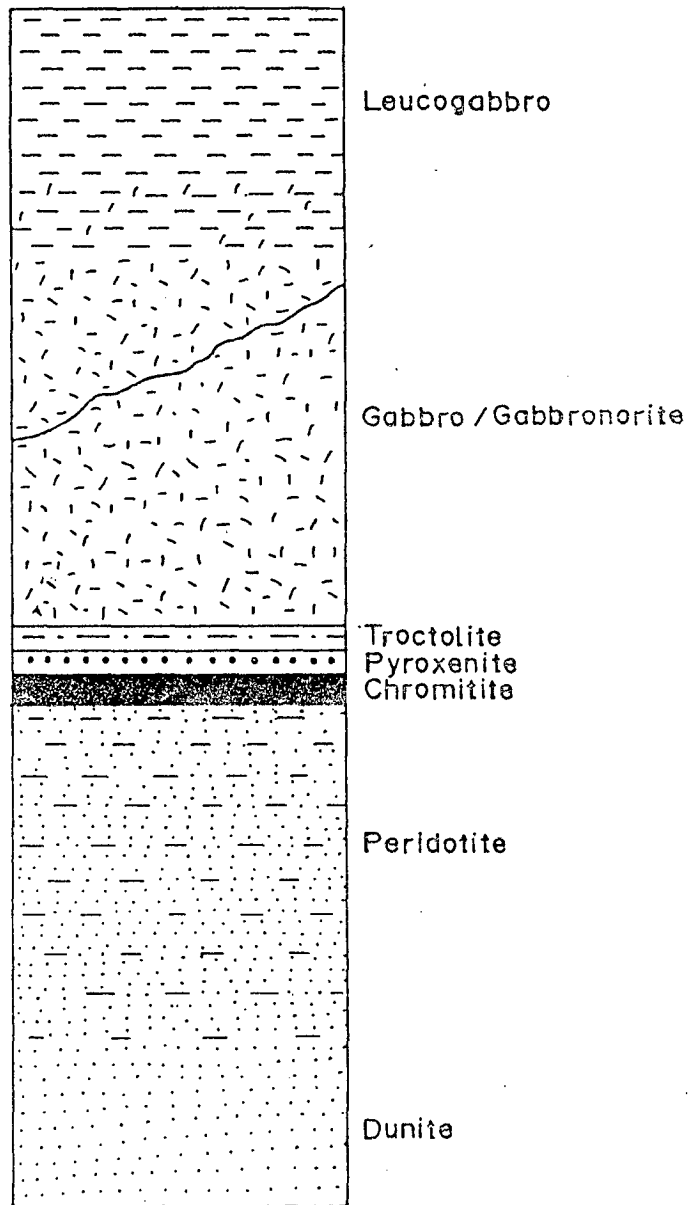
Fig.2.2   A schematic stratigraphic column (not to scale) of the
Bondla mafic-ultramafic complex.

shear zone they exhibit a foliation parallel to that of the enclosing metasediments. The ultramafites in general extend over a length of 6 km. The width of the outcrop is more than 3 km. Along the shear zone they exhibit fracturing, crushing and development of slickensided surfaces. The fractures trend N100o and dip 25o towards N350o, and N65o and dip 55o towards N335o. Along the fractures, veins of amphibole asbestos and chlorite are seen. The veins vary in width from 3 cm to over 40 cm and they are mainly of cross - fibre type.

The peridotites are also exposed at Kusumwada. The contact of the peridotites with metasediments is sheared. Along the shear zone, the peridotites are rendered talcose. They pinch out laterally. The ultramafites at lower levels are coarse grained. The grain size decreases at higher elevation. This variation is best seen along the road from Usgaon to Bondla. The peridotites in the field show banded appearance due to alternating light and dark coloured layers. The dark bands are made up predominantly of coarse grained chromite. These layers stand out (Plate II Photo 2) and alternate with those of greyish green coloured olivine. The latter vary in thickness

from 3 to 10 cm. This type of banding was originally described as pseudo stratification (Hall, 1932 in Wager and Brown, 1967). Such-sheet like structures were later described as layering in the Bay of Island intrusion, Newfoundland (Ingerson, 1935 in Wager and Brown, 1967) and the Stillwater Complex, Montanna (Peoples, 1936 in Wager and Brown, 1967). The term layering was also adopted by Wager and Brown (1967) for similar features in Skaergaard intrusion, East Greenland. Following Wager and Brown (1967) the banding shown by the ultramafic rocks of Bondla has been referred to as `layering'. This type of layering which is due to variation in proportion of chief minerals was referred to as rhythmic layering (Wager and Deer, 1939). Buddington (1936) refers to this type of layering as gravity stratification. For the thickness of layered rocks developed while a specific cumulus mineral or assemblage of cumulus minerals was forming , the term `Zone' is used (Wager and Brown, 1967). The same terminology is followed in this work. ·

The chromite layers vary in thickness from 1 cm to more than 10 cm. The layers thicken and thin and pinch out laterally. The layers trend N50o and dip 30 to 35o

towards N130⁰. Along the shear fractures the chromites are remobilised and they give an appearance of a thin network of chromite veins which occur at an angle to the layering. Such veins vary in thickness from 1 to 3 cm. The layering and the remobilised chromite veins thus give an appearance of a network of chromite. Along the remobilised chromite veins, fibrous green chlorite is invariably developed perpendicular to the vein wall.

A thick chromitite layer occurs at the top of the ultramafic zone and is exposed to the west of Poikul. It extends laterally over a distance of 1 to 1.5 km and has a width of outcrop of about 300 m. The rock is massive, dark grey in colour and very fine grained.

The troctolites are exposed at the Bondla recreation park. These are underlained by a thin horizon of pyroxenites.

Gabbroic rocks are exposed along the Madai river 2 km NE of Ganje. The contacts of the gabbros with the metasediments are fine grained due to shearing. Quartz veins are intruded along the shear zone. Veins of epidote

have developed along the shear fractures. They can be traced intermittently upto Bondla along the eastern slopes of the Bondla ridge. Those in the Madai river are coarse grained and exhibit uniform layering (Wager, 1968). The bottom of the layers is generally coarse grained than the top which is gradational. The layers are generally distinguishable by virtue of their texture and grain size. The grain size at the bottom of the layer varies between 1 and 2 cm and it decreases towards the top.

Excellent exposures of gabbro are found to the east of Durgini along the Mollem-Panaji highway. The gabbro rise to a height of 396 m above M.S.L. The western contact is fine grained, sheared and fractured. The contact zone is more melanocratic than the rest of the body. The gabbros exhibit uniform layering (Wager, 1968). The bottom of the layer is coarser and more melanocratic than the top. The top of the layer is gradational due to increasing proportion of plagioclase.

CHAPTER III

PETROGRAPHY AND GEOCHEMISTRY

CHAPTER III

PETROGRAPHY AND GEOCHEMISTRY

In this chapter, it is proposed to deal with the petrography and geochemistry of the mafic and ultramafic rocks and the associated metasedimentary lithological types occurring in the area. The chapter is divided into two parts. In the first part the petrographical characters of the various rocks are described. The second part deals with the whole rock geochemistry and the mineral chemistry of the mafic and ultramafic rocks.

PART I - PETROGRAPHY

This part describes the petrographic characters of the different rocks from the Bondla area.

33

Quartz-chlorite-sericite-schist

Megascopic Characters: The rock is pale grey in colour, fine grained, and schistose. At places it shows intercalations of quartzite and quartz-chlorite-schist. The schistosity is defined by parallel arrangement of sericite and chlorite. The schistosity also shows crenulations.

Microscopic Characters: The rock exhibits schistose structure defined by sericite and chlorite. It is composed of quartz, sericite, chlorite, biotite with small amounts of epidote, zoisite and ilmenite. The predominant minerals are quartz and sericite. Sericite occurs as flakes of varying sizes concentrated in bands which alternate with quartz-rich bands. Sericte encircles quartz which shows strain shadows. Little chlorite is also present alongwith sericite. At places, biotite has developed at the expense of chlorite. Epidote, zoisite and ilmenite make up the accessories. The rocks along the shear zone are pulverised to submicroscopic size (Plate III Photo 1). The rock is traversed by criss-cross veins of quartz.

34

The quartzites and quartz-chlorite-schist exhibit quartz belonging to two generations. Quartz I occurs as porphyroclasts which is lenticular and shows strain shadows. Quartz II is undeformed and is recrystallized along with sericite forming bands which swerve around quartz porphyroclast. The rocks in the vicinity of the shear zone are crushed and pulverized and show banding. The alternate bands are made up of quartz plus calcite and quartz, calcite plus sericite (Plate III Photo 2). The bands are formed due to crushing and crystallization.

Phyllite

Megascopic Characters: Phyllite is hard and compact, fine grained and grey in colour when fresh. When altered, it is usually soft and friable and shows variety of shades of red depending on the degree of alteration. Phyllitic structure is seen in fresh rock. It is predominantly made up of sericite and quartz. Sericite - and quartz - rich bands impart a crude foliation to the rock.

Microscopic Characters: The rock is mainly composed of sericite, quartz, chlorite with some biotite, epidote and

35

zoisite. Ilmenite, sphene and calcite occur as accessories. Sericite is the most abundant constituent. It is very fine grained. Quartz is next in the order of abundance. It is fine grained, crushed and shows strain shadows. At places, quartz-rich bands alternate with sericite-rich bands. Chlorite is represented by penninite. Biotite has developed at the expense of chlorite. Tiny grains of epidote and zoisite are scattered in the matrix. Ilmenite and sphene occur as accesories. Sphene invariably forms rims around ilmenite.

The Mafic-Ultramafic Complex

The mafic-ultramafic complex at Bondla extends in general NNW-SSE direction. It was systematically sampled from SE to NW along two parallel traverses, one in the north and the other in the south of the area to study the textural, structural, minerological and lithological variation within the complex. Wager and Brown (1967) in their study of the Skaergaard intrusion of Greenland defined a zone as a thickness of layered rocks formed while a specific cumulus mineral was forming. Using the same principle the Bondla complex is divided into two

zones - The Lower Zone and The Upper Zone with a thin
horizon of pyroxenite and troctolite in between which also
serves as a marker to separate these two zones. Although
the complex is layered, it was not always possible to
correlate the sequence of layered rocks with a regular
cryptic variarion in the cumulus mineral composition of
successive layers. Hence the textural and minerological
characters have not been described from the base to the
top of the intrusion but as per the rock type variation
(Wager and Brown, 1967).

The Lower Zone

The Lower Zone of the intrusion is made up of
ultramafic cumulates. The cumulates are made up of olivine
and chromite. The olivine-chromite cumulates are litholog-
ically represented by dunite, peridotite, chromitite and
pyroxenite as per the standard modal classification. The
pyroxenite marks the top of this zone and separates the
olivine-chromite cumulates below it from the plagioclase
cumulates above. The cumulates of this zone in general are
medium to coase grained and greyish to olive green in
colour. They are generally massive when fresh. However, at

37

places where they are altered and deformed, show schistose structure and are represented by serpentine-talc-tremolite-shist. All the cumulates of this zone are invariably converted to serpentinites. However, here they will be described as per their minerological composition before alteration. This is possible as in majority of cases relict minerals can be recognised in thin sections.

The Upper Zone

The pyroxenites of the Lower Zone are followed stratigraphically higher up by troctolites wherein the plagioclase feldspar makes its first appearance as a cumulus phase. From troctolite upwards plagioclase occurs throughout as a cumulus phase alongwith pyroxene in the gabbros, the gabbro-norites and the leucogabbros.

In the following paragraphs the megascopic and microscopic characters of the various lithological types from the above two zones are described. For this purpose the cumulate terminology developed by Wager *et al.*, (1960) and Wager and Brown (1967) for describing the rocks of the Skaergaard intrusion has been followed. This nomenclature

together with contributions by Jackson (1967) is well established and is widely used. Irvine (1982) has also encouraged the continuation of cumulate nomenclature with appropriate provisions. This nomenclature with various provisions is followed in this work.

Dunite (olivine cumulate)

Megascopic Characters: It is greyish to greyish green in colour, coarse to medium grained, hard and compact rock with equigranular texture. At places, specially in the vicinity of the shear zone it has developed a foliation. Thin layers of chromite are at places seen. Green chlorite is invariably developed perpendicular to chromite layers. Veins of asbestos have developed with fibres at right angles to the walls of the fractures in sheared dunites.

Microscopic characters : The rock exhibits a cumulate texture (Wager et al., 1960) made up of subhedral crystals of olivine which make up the framework of the rock. The interstices between olivines are occupied by clinopyroxene which is intercumulus. The modal proportions of the minerals are shown in Table No. 3.1. The rock is a mesocu-

Table No. 3.1 Modal proportions of Mafic and Ultramafic rocks from Bondla

Sample	Plagioclase	Orthopyroxene (Ca-poor pyroxene)	Clinopyroxene (Ca-rich pyroxene)	Olivine	Biotite	Chromite/ Opaques	Total
B19B	42.29	12.91	1.06	43.48	----	0.23	99.97
BT1	45.37	7.32	5.41	41.36	----	0.52	99.98
BT2	60.75	4.43	1.20	33.19	----	0.42	99.97
GB1	48.18	18.29	28.43	3.92	0.27	0.98	100.07
GB2	55.21	16.06	25.64	0.34	0.68	2.05	99.98
S35	56.84	16.96	19.27	3.15	1.81	1.93	99.96
S40	63.94	13.00	13.84	5.29	0.92	2.97	99.96
S41	58.48	13.83	23.02	2.09	0.58	1.97	99.97
GS23	53.56	29.14	16.18	----	0.10	1.00	99.99
GD12	48.89	16.26	29.21	3.31	0.80	1.50	99.97
S36	54.16	15.62	26.04	3.00	0.34	0.81	99.97
S39	66.35	10.44	16.24	64.64	0.46	1.85	99.98
S33	58.00	9.00	30.00	----	----	3.00	100.00
N44A	56.60	23.00	9.00	----	----	11.00	99.60
U1	58.50	1.50	21.70	----	15.00	3.20	99.90
D15	58.00	22.60	12.30	----	-----	7.00	99.90
S9	54.30	22.60	18.30	----	-----	4.60	99.80
D12	56.00	30.60	10.00	----	-----	3.30	99.90
DS	48.00	31.30	13.60	----	-----	7.00	99.90
S22	58.32	22.54	13.76	3.53	-----	1.80	99.95
S10	55.14	32.42	9.70	2.33	-----	0.38	99.97
S11	41.99	20.15	29.19	7.34	-----	1.20	99.87
D12/5	50.11	17.52	27.86	----	-----	4.49	99.98
DA/A1	64.20	-----	20.50	12.50	-----	2.70	99.90
G49	49.00	23.50	8.50	-----	-----	18.00	99.00
B3	86.00	3.00	3.00	-----	-----	8.00	100.00
B4	3.6	----	84.60	-----	-----	11.30	99.50
B14	24.50	----	73.00	-----	-----	2.00	99.50
B19A	----	----	11.20	72.20	-----	16.50	99.90
N1	----	1.39	16.15	77.29	-----	5.15	99.98
B22	----	2.96	-----	79.80	-----	17.24	100.00
B23	----	----	28.80	66.60	-----	4.60	100.00
DA/B1	----	18.00	30.30	45.00	-----	6.60	99.90
T5	-----		23.00	66.70	-----	10.00	99.90
B15	-----	-----	------	25.70	-----	74.20	99.90
B15A	-----	-----	------	20.80	-----	79.20	100.00

B19A, BT1 & BT2 – Troctolites   GB1, GB2, S35, S40, S41, GS23, GD12, S36, S39, S33, N44A, U1, D15, S9,
D12, D8, S22, S10, S11, D12/5, DA/A1, G49, B3 – Gabbros   B4 & B14 – Pyroxenites
B19A, N1, B22, B23, DA/B1 & G49 – Peridotites   B15, B15A – Chromitites

mulate (Plate IV Photo 1). Olivine is completely replaced by serpentine which forms pseudomorphs after it. The former can however, be recognised by its relict form and at places, by canal - like fractures characteristic of olivine. No relict of olivine is preserved. Serpentine shows low order grey interference colours. However, at places, high order colours than those of serpentine can be recognised in the fibrous aggregates. This could be due to antigorite.

Orthopyroxene occurs as intercumulus mineral interstitial to olivine and chromite. It is pale brown, faintly pleochroic and shows inclined extinction. C $\hat{}$ Z varies between 20 to 30o. It has very large 2V and is biaxial positive. It is represented by bronzite. It is rarely fresh. Invariably, it is altered to turbid bastite. Pyroxene is also replaced by chlorite which is penninite with deep blue interference colours. Chlorite has developed invariably around opaques. The latter is represented by chromite. Chromite wherever present occurs either as euhedral to subhedral skeletal crystals and rarely seen to form chains.

Peridotite (olivine-chromite cumulate)

Megascopic Characters: The rock is greyish in colour,
medium to coarse grained, hard and compact with equigranu-
lar texture. Thin layers of chromite varying between 0.5
to 2 cm alternate with olivine-rich layers (Plate IV Photo
2). Generally the olivine-rich layers are two to three
times the thickness of chromite layers. The top contact of
the chromite and olivine layer is generally gradational,
whereas the bottom contact is sharp.

Microscopic Characters : The rock consists of olivine
(pseudomorphed by serpentine), chromite and chlorite. It
exhibits cumulate texture. The cumulate minerals are
olivine and chromite. Olivine is subhedral and is pseudo-
morphed by serpentine. However, the former can be made out
by its relict form. No fresh olivine is preserved.

Chromite occurs as euhedral to subhedral crystals
which form mosaic within which rounded olivines give the
appearance of ring texture. The modal proportions are
shown in Table No.3.1. It is seen from the table that the
cumulates form about 90% of the rock. The remainder being

made up of intercumulus clinopyroxene which occurs inter-granular to olivine and chromite. Clinopyroxene is invariably bastitised. The rock can therefore, be categorised as a mesocumulate and has olivine layers alternating with chromite layers. Olivine shows preferred alignment of its longer axis within the plane of layering (Plate V Photo 1) giving fissility to the rock. This feature has been referred to as igneous lamination (Wager and Brown,1967).

At places the rock exhibits heteradcumulate texure - large irregular amoeboid oikocrysts of orthopyroxene poikilitically enclose a number of irregular to rounded olivine and chromite crystals (Plate V Photo 2). Chromite occurs as a cumulus phase forming layers which alternate with olivine layers. Chromite is subhedral and smaller in size as compared to olivine.

Chromitite (chromite-olivine cumulate)

Megascopic Characters : The rock is very fine grained, dark grey in colour, hard and massive. Rare altered silicates can be seen at places.

<u>Microscopic Characters</u> : The rock is constituted dominantly of chromite which makes up about 75% of the rock. The remainder being altered silicates. The proportion of chromite to silicate vary considerably in different samples of chromitites as seen in Table No. 3.1. It shows a heteradcumulate texture made up of large irregular chromite crystals which appear to have grown by mutual attraction between adjacent chromite crystals. Chromite grains poikilitically enclose vermicular silicates represented by pseudomorphs of serpentine after olivine (Plate VI Photo 1). Serpentine mineral is fibrous antigorite. At places, anhedral to subhedral grains of chromite occur forming a mosaic and at places, showing rounded silicates in between, giving rise to ring texture (Plate VI Photo 2). The detailed textural and petrographical characters of the chromitite are described in the next chapter.

Pyroxenite (clinopyroxene cumulate)

<u>Megascopic Characters</u> : The rock is melanocratic, coarse grained, hard and compact. It shows equigranular texture made up of well developed crystals of pyroxene which are dark green in colour.

43

<u>Microscopic Characters</u> : The rock is almost entirely made up of clinopyroxene with a small proportion of opaques and intercumulus plagioclase. The modal proportions of the minerals are shown in Table No.3.1. Clinopyroxene makes up about 84% of the rock. The remainder being made up of opaques and plagioclase. It exhibits an adcumulate texture. Clinopyroxene occurs as subhedral crystals. It is non-pleochroic, pale green in colour, shows inclined extinction. C ^ Z varies between 30 and 40o. It is biaxial positive with 2V varying between 50 and 60o. Clinopyroxene is studded with minute exsolutions of rutile (Plate VII Photo 1) which are either concentrated towards the center of the crystal or form a zonal arrangement. The peripheries of the crystal are invariably free from exsolutions. Under high magnification the exsolutions are brown in colour and are aligned at an angle to the cleavage of the clinopyroxene (Plate VII Photo 2).

Opaques occur as cumulus crystals alongwith clinopyroxenes. Plagioclase is intercumulus.

Troctolite

Megascopic Characters: It is coarse grained, hard and compact, melanocratic and equigranular rock. It is composed of well developed crystals of plagioclase which vary in size between 1 mm and 9 mm and olivine which measures from 0.9 mm to 3 mm.

Microscopic Characters: The rock exhibits an orthocumulate texture made up of cumulus plagioclase, olivines and opaques. The modal proportions of the minerals are shown in Table No.3.1. The cumulus minerals vary in size from 0.9 to 2.3 mm. Whereas, the intercumulus plagioclase are much smaller. The cumulus plagioclase has irregular core of uniform composition and normally zoned borders (Plate VIII Photo 1) which have grown at the expense of the intercumulus liquid. The An content of the core of the cumulus plagioclase varies between $An_{87.5}$ – $An_{87.9}$ and it decreases towards the borders.

Olivines occur as well developed crystals. It is quite fresh and unaltered. The olivine has very restricted range of composition which on an average varies between

45

Fo85 and Fo86. However, in some grains, it may go upto Fo89 [86·2]. It is subhedral and traversed by canal-like fractures typical of olivine. At places, along cracks, olivine is altered to serpentine with release of iron-oxide which forms vermicular intergrowth with antigorite.

Opaques occur as skeletal crystals making up about 0.5% of the rock. They are represented by chromite. The Cr_2O_3 percentage varies between 38 and 41 wt.%. The chromites are ferriferous and the percentage of total iron varies between 33.00 to 37.50 wt.%.

Gabbro

The gabbroic rocks constitute the Upper Zone of the complex. They vary between gabbros, olivine gabbros, gabbronorites and leucogabbros. The petrographical characteristics of all these lithological types are described together.

Megascopic Characters: The rock is coarse grained, hard and compact, melanocratic with equigranular texture. The gabbros in the vicinity of the contact zone are fine

grained mainly because of crushing. They show uniform layering which is discernible due to size and colour variation of the constituent minerals. However, in some specimens the layering is marked by variations in proportion of cumulus minerals. The constituent minerals are represented by plagioclase and pyroxene. Plagioclase is dirty greyish in colour and varies in size between 4 mm to 1 cm. The pyroxene is dark grey and ranges in diameter from 5 mm to over 1 cm.

Microscopic Characters: In micro-section the rock consists of plagioclase which makes up 40-58% of the rock. It is followed in order of abundance (between 10- 30%) by clinopyroxene and Ca-poor pyroxene (orthopyroxene) which also varies from 10-30%. The modal proportions of the minerals of the different rock types are presented in Table No. 3.1. A triangular plot of plagioclase, pyroxene and olivine (Streckeisen, 1974) is shown in Fig. 3.1a. It is seen that the majority of the gabbroic rocks plot in the gabbronorite field. However, some samples plot in the field of olivine-gabbros, gabbronorites and luecogabbros. The modal data have also been plotted in the plagioclase, orthopyroxene and clinopyroxene triangular diagram

47
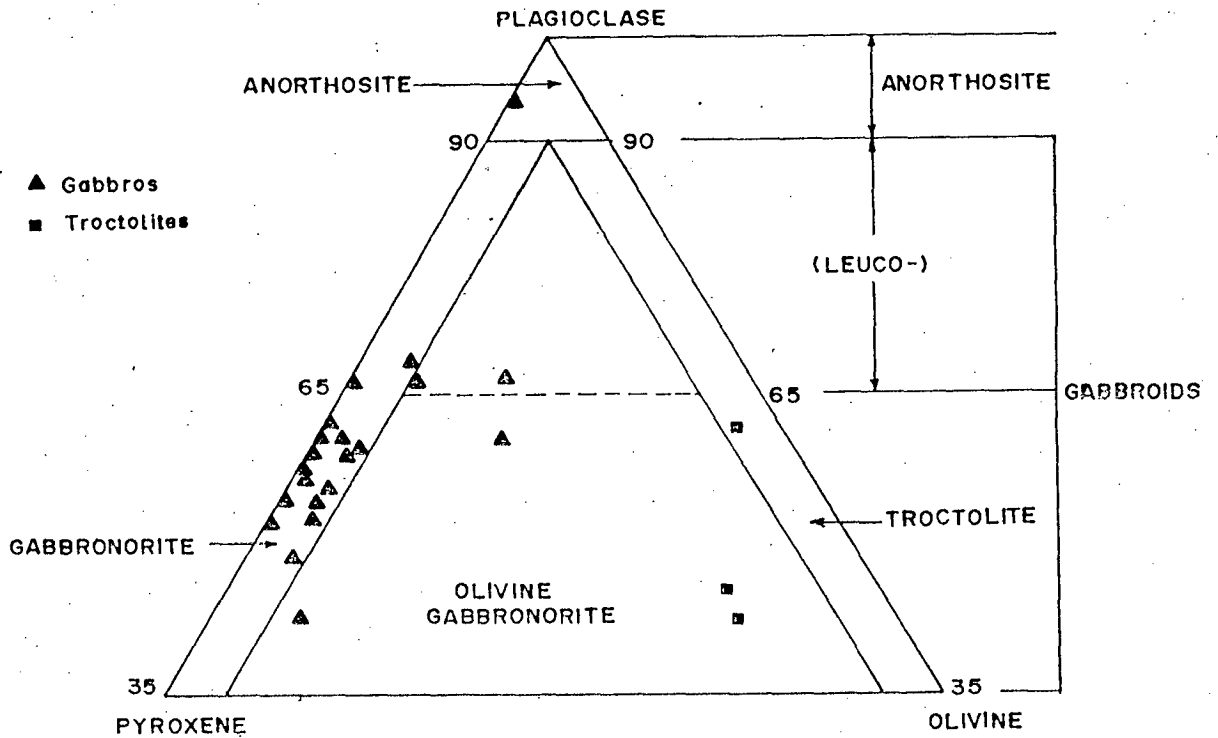
Fig.3.1a   Plots   of   Bondla   gabbros   in   plagioclase-
          pyroxene-olivine   triangular   diagram   (after
          Streckeisen,1974).
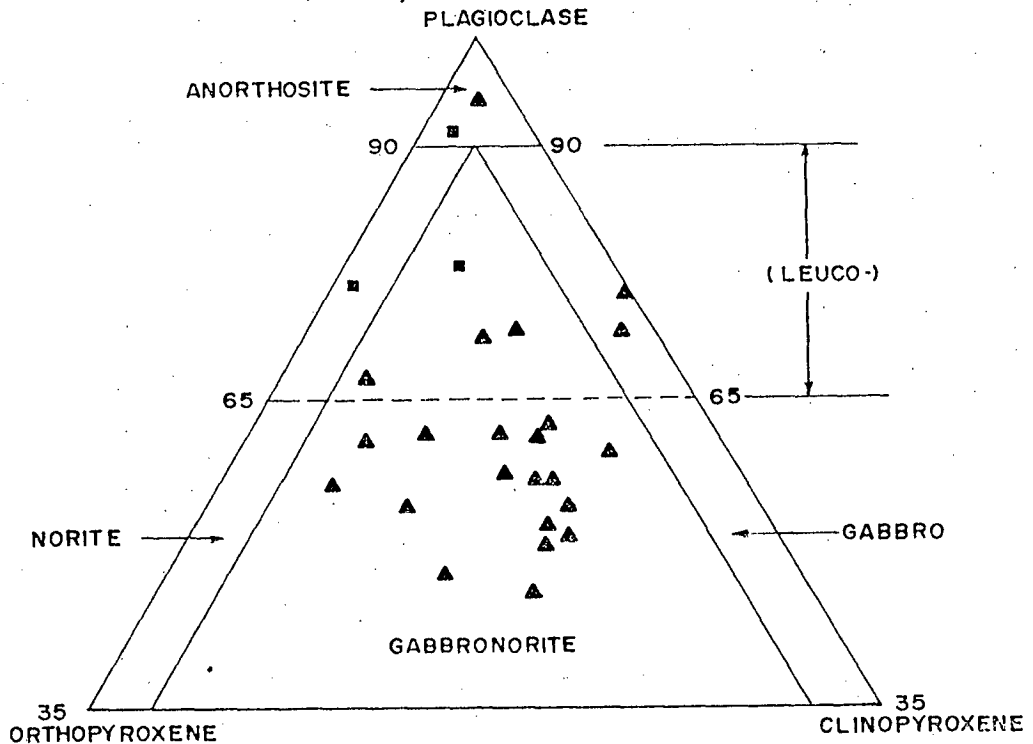
Fig.3.1b   Plots   of   Bondla   gabbros   in   plagioclase-
          orthopyroxene-clinopyroxene   triangular   diagram
          (after Streckeisen, 1974).

Fig.3.1b (after Streckeisen, 1974). In this diagram, majority of the gabbroic rocks occupy the gabbronorite field. The remaining samples plot in leucogabbro and anorthosite fields. In general the samples from horizons nearer the base of the zone plot in the gabbronorite field whereas, the rocks from the top of the section occupy the field of leucogabbros due to higher proportion of plagioclase in comparison with both the pyroxenes taken together. Similarly, the troctolites also plot in the leucogabbro field as olivine is not represented in this diagram.

A typical gabbronorite exhibits a mesocumulate texture. The cumulus plagioclase are lath shaped with irregular and resorbed core which show marginal zoning due to post-cumulus growth (Plate VIII Photo 2). The cores are uniform in composition as seen both from their extinction and microprobe chemical data. The marginal zones vary in composition considerably. The An content of the core of cumulus crystals varies between An_{63} and An_{78}. The An content decreases towards the margin. The intercumulus plagioclase occurs as smaller laths in between, with An content varying between An_{25} and An_{50}. Further details are described under mineral chemistry.

Cumulus pyroxene is represented by Ca-poor pyroxene and clinopyroxene . The former is inverted pigeonite which occurs as subhedral crystals varying in size between 1.5 and 3.8 mm. It is faintly pleochroic in shades of pink to pale brown. It shows exsolution blebs of clinopyroxene parallel to (001) and fine exsolution lamellae parallel to (100) (Plate IX Photo 1). It varies in composition from $Ca_{3.8}Mg_{84.0}Fe_{12.1}$ to $Ca_{3.3}$ $Mg_{58.3}Fe_{38.2}$. The Mg # (Mg/Mg + Fe^{+2}) varies between 0.60 and 0.86. The intercumulus Ca-poor pyroxene is represented by ferrian pigeonite varying in composition between $Ca_{15.1}Mg_{15.4}Fe_{69.4}$ and $Ca_{14.4}Mg_{15.3}Fe_{70.2}$ with Mg #s ranging from 0.17 to 0.18.

The cumulus clinopyroxene occurs as subhedral to anhedral crystals which vary in size between 0.9 and 3.5 mm. It is pale brown in colour and non-pleochroic. It contains exsolution blebs of pigeonite parallel to (001) and fine exsolution lamellae of orthopyroxene (hypersthene) parallel to (100) (Plate IX Photo 2). Compositionally, the pyroxene varies between $Ca_{34.8}Mg_{51.5}Fe_{13.6}$ and $Ca_{35.10}Mg_{43.5}Fe_{21.7}$. Therefore, mineralogically, the pyroxene is between augite to sub- calcic augite and

49

ferro-augite. The Mg # shows a variation between 0.66 and 0.79. The intercumulus clinopyroxene varies in composition between $Ca_{33.3}$ $Mg_{19.8}Fe_{46.7}$ and $Ca_{22.7}Mg_{38.5}Fe_{38.6}$. The Mg #s for these vary between 0.29 and 0.49.

Olivine occurs as subhedral crystals with typical canal-like fractures and varies in proportion from 2-5%. It is biaxial positive with a large 2V. Biotite occurs as intercumulus mineral, strongly pleochroic in shades of brown, shows straight extinction, is biaxial negative and occurs to the extent of less than 2% by volume. Opaques are represented by Fe-Ti oxides..

A typical leucogabbro exhibits an orthocumulate texture. It is dominated by plagioclase and clinopyroxene with Fe-Ti oxides and biotite forming the accessories. The An content of cumulus plagiocalse varies between An_{22} and An_{42}. Clinopyroxene varies in composition between sub-calcic augite and ferroaugite.

PART II - GEOCHEMISTRY

This section deals with geochemistry of the peridotites, the gabbroic rocks and the associated metabasalts. Representative rocks have been chemically analysed for the major, trace and rare earth element abundances.

The chemical data have been plotted in variation diagrams to determine the nature of the parent magma, the magma type and the course of crystallization.

The petrochemistry is followed by mineral chemistry of peridotites and gabbros. The different mineral phases from selected rocks have been analysed by electronprobe microanalyser for the major and some trace element composition. Various parameters have been computed from these data to bring out their characteristic features.

Whole-rock   Chemistry

Representative rock samples of peridotites, gabbros and metabasalts were chemically analysed to determine

51

their major element content by the rapid analysis method of Shapiro and Brannock (1962) using USGS silicate rock standards (Flannagan, 1967). All major elements were determined by Atomic Absorption Spectroscopy except Si, Al and FeO. Si and Al were determined by colourimetry. Total iron was analysed as FeO. The ferric iron was standardised following Le Maitre (1976). Repeat analyses of some selected samples were carried out by X-Ray flourescence spectroscopy on fused glass discs at C.S.I.R.O., Australia and N.G.R.I., Hyderabad. Analytical precision was controlled by standard natural samples and synthetic standards. The trace and rare earth elements were analysed by instrumental neutron activation analysis (INAA) at C.S.I.R.O., Australia. Additional samples were analysed at N.G.R.I., Hyderabad by inductively coupled plasma spectroscopy (ICP-MS).

Twenty four representative major oxide analyses of the mafic and ultramafic rocks with mean and standard deviation are presented in Table No. 3.2. Out of these, three analyses are of peridotite (serpentinite), two of troctolite and fourteen of gabbroic rocks. Five analyses of associated metabasalts (greenstones) are also present-

ide	B15	B19A	G11	N1	Mean (S.D.)	BT1	BT2	Mean (S.D.)	GB1	GB2	GS23	GD12	S35	S36	S39	S40	S41	S33
iO$_2$		43.35	44.56	42.77	43.56(0.91)	51.65	50.74	51.19(0.64)	51.41	49.61	50.37	49.28	52.27	51.81	52.95	51.88	52.28	51.51
l$_2$O$_3$		2.59	2.82	2.80	2.73(0.12)	20.42	20.98	20.70(0.39)	19.00	18.82	19.31	17.86	16.43	17.96	16.19	17.13	17.19	17.58
iO$_2$		0.03	0.11	0.14	0.09(0.05)	0.82	0.77	0.79(0.03)	0.72	0.64	0.63	0.64	0.70	0.65	0.68	0.68	0.70	0.46
$_2$O$_3$		1.57	1.66	1.64	1.62(0.04)	2.48	2.42	2.45(0.04)	2.44	2.26	2.22	2.25	2.44	2.36	2.37	2.43	2.51	2.27
eO		9.38	10.85	13.89	11.37(2.30)	1.28	1.32	1.30(0.02)	1.08	2.17	2.78	3.97	2.36	3.13	3.04	2.66	2.54	5.41
nO		0.25	0.13	0.27	0.2 (0.05)	0.07	0.07	0.07(0.00)	0.08	0.11	0.23	0.15	0.12	0.12	0.12	0.12	0.12	0.16
gO		40.46	38.89	36.47	38.60(2.01)	12.56	12.53	12.54(0.02)	9.05	9.84	9.43	11.08	9.80	9.66	9.29	9.62	9.52	8.94
aO		2.25	0.82	1.24	1.43(0.73)	9.87	10.13	10.00(0.18)	14.87	15.19	13.86	13.54	14.46	12.96	14.06	14.12	13.82	11.96
a$_2$O		0.01	0.01	0.02	0.01(0.005)	0.69	0.55	0.62(0.09)	1.00	0.99	0.85	0.92	1.06	1.01	0.98	0.98	0.96	1.21
O		0.03	0.06	0.01	0.03(0.02)	0.05	0.38	0.21(0.23)	0.22	0.23	0.19	0.18	0.22	0.21	0.20	0.23	0.23	0.39
O$_5$		0.05	0.05	0.05	0.05(0.00)	0.07	0.07	0.07(0.00)	0.08	0.08	0.08	0.08	0.08	0.08	0.07	0.08	0.72	0.08
otal		99.97	99.96	99.30		99.96	99.96		99.95	99.94	99.95	99.95	99.94	99.95	99.95	99.93	99.96	99.97

CIPW Norms

	B15	B19A	G11	N1		BT1	BT2		GB1	GB2	GS23	GD12	S35	S36	S39	S40	S41	S33
		---	---	---		---	---		0.34	---	0.34	---	---	---	---	---	1.68	---
		---	0.15	0.30		1.52	1.52		1.37	1.22	1.22	1.22	1.37	1.22	1.37	1.37	0.15	0.91
		2.09	1.37	2.32		2.09	2.09		---	3.25	3.25	3.25	3.48	3.48	3.48	3.48	3.71	3.25
		---	---	---		1.12	0.96		2.40	---	---	---	---	---	---	---	---	---
		---	---	---		0.56	2.22		1.11	1.11	1.11	1.11	1.11	1.11	1.11	1.11	1.11	2.22
		---	---	---		5.76	4.72		8.38	8.38	7.34	7.86	8.91	8.38	8.38	8.38	7.86	10.48
		4.17	4.17	6.12		48.93	50.32		46.70	46.43	48.09	43.92	39.48	43.92	39.30	41.70	42.26	41.98
		3.3	---	---		---	---		20.74	22.29	16.39	18.00	24.78	15.53	23.83	21.40	17.47	13.56
		21.10	45.26	30.04		31.40	31.30		13.00	16.78	18.68	23.83	14.39	19.71	14.65	16.09	18.25	23.44
		68.43	48.68	61.04		---	---		---	---	---	---	---	---	---	---	---	---
rr		---	1.33	0.50		1.12	1.12		---	---	---	---	---	---	---	---	---	---
		---	---	---		7.38	5.58		4.98	1.02	3.96	0.54	6.18	6.36	7.92	6.06	7.62	4.26
otal		99.09	100.9	100.3		99.98	99.73		99.02	100.4	100.3	99.73	99.70	99.70	100.0	99.58	100.1	100.0
#		74.41	70.95	64.80		73.56	73.56		68.29	64.52	60.48	58.95	62.60	58.78	58.27	60.73	60.67	48.25

A, G11, N1 – Ultramafics BT1, BT2 – Troctolites GB1, GB2, GS23, GD12, S35, S36, S39, S40, S41, S33 – Gabbros

Table No. 3:2 (continued)

des	S37	N22	N44H	N44A	Mean (S.D.)	N46H	N26H	N26A	RBKH	N48A	Mean (S.D.)	9	14	22	3	21	8	4
O2	52.11	52.82	47.56	48.50	51.05(1.68)	46.77	49.39	52.84	44.83	49.73	48.71(3.05)	38.60	40.10	48.78	41.52	41.40	41.94	49.20
2O3	17.08	15.66	11.84	13.99	16.86(2.01)	13.50	13.09	15.88	12.44	14.63	13.90(1.36)	5.28	16.12	2.46	18.82	17.12	19.10	14.73
O2	0.37	0.57	1.67	1.57	0.76(0.37)	0.58	0.51	0.56	1.63	1.39	0.93(0.53)	0.11	0.07	0.04	0.11	0.08	0.07	0.54
2O3	2.16	2.11	3.21	3.17	2.44(0.33)	2.08	2.03	2.12	3.20	2.91	2.46(0.54)	1.61	1.57	1.54	1.61	1.58	1.57	2.04
O	7.31	6.91	18.00	16.04	5.52(5.19)	11.11	10.06	7.16	20.33	14.66	12.66(5.05)	8.89	5.06	7.25	4.41	4.03	3.27	8.38
O	0.17	0.17	0.27	0.28	0.15(0.06)	0.22	0.19	0.16	0.33	0.28	0.23(0.06)	0.15	0.11	0.20	0.10	0.10	0.09	0.16
O	8.17	7.40	7.23	5.77	8.91(1.35)	16.02	13.83	9.06	7.83	5.55	10.45(4.33)	33.03	20.01	25.80	10.83	19.27	16.32	10.83
O	10.17	9.55	7.40	7.59	12.39(2.64)	5.64	7.19	8.57	7.12	7.54	7.21(1.05)	3.26	9.50	8.63	10.89	9.70	11.05	9.30
2O	1.33	3.00	2.55	2.79	1.40(0.76)	2.21	3.51	3.49	2.09	3.03	2.86(0.68)	0.30	----	---	0.18	0.24	0.16	1.49
O	0.46	1.62	0.12	0.14	0.33(0.38)	1.61	0.09	0.11	0.02	1.00	0.38(0.68)	----	0.02	0.03	0.05	0.01	0.02	0.57
O5	0.08	0.14	0.10	0.09	0.13(0.17)	0.06	0.07	0.06	0.14	0.13	0.09(0.03)	---	---	---	---	---	---	0.12
tal	99.94	99.95	99.95	99.93		99.80	99.96	100.0	99.96	99.95		100.0	100.0	99.96	98.76	99.98	99.01	99.94

CIPW Norms

des	S37	N22	N44H	N44A		N46H	N26H	N26A	RBKH	N48A		9	14	22	3	21	8	4
	0.34	0.34	0.34	0.34		---	---	---	0.34	0.34								
	0.76	1.06	3.19	3.04		1.06	0.91	1.06	3.04	2.58								
	3.02	3.02	4.64	4.64		3.02	3.02	3.02	4.64	4.18								
	---	---	---	---		---	---	---	---	---								
	2.22	9.45	0.56	0.56		9.45	0.56	0.56	---	0.56								
	11.00	25.15	21.48	23.58		18.86	29.87	29.34	17.82	25.68								
	39.30	24.74	20.57	25.30		21.96	19.46	27.80	24.46	25.85								
	10.60	17.80	12.84	9.84		4.70	12.84	11.89	8.42	9.81								
	26.61	13.58	27.03	28.68		0.76	2.82	22.86	21.52	29.22								
	---	4.78	9.35	4.05		39.72	30.28	3.42	19.51	1.92								
IT	---	---	---	---		---	---	---	---	---			---	---	---	---	---	---
	5.64	---	---	---		---	---	---	---	---			---	---	---	---	---	---
tal	99.48	99.92	100.0	100.0		99.53	99.76	99.95	99.75	100.1								
#	40.62	39.46	21.00	18.86		48.93	47.49	43.72	20.74	19.92		71.20	70.56	69.86	58.89	73.27	71.16	45.10

S37, N22, N44H, N44A - Gabbros   N46H, N26H, N26A, RBKH, N48A - Metabasalts
4, 22, 3 - Ultramafics (Balakrishnan *et al.*, 1992) 21, 8, 4 - Gabbros (Balakrishnan *et al.*, 1992).

and Rare earth elements

B15	B19A	G11	N1	Mean (S.D.)	BT1	BT2	Mean (S.D.)	GB1	GB2	GS23	GD12	S35	S36	S39	S40	S41	S33
0.08			8.3			556			274.8	241	249	249					
0.61			25.77			420			2040	1800	1680	1980					
648			166.7			128			169.7	197.5	156.7	159.0					
11426			1227			372.2			188.5	244.4	172	261					
217			373			129.2			96.5	90.54	82.90	---					
11.36			105.0			27.77			132.8	106.3	104.8	72.00					
21.88			6.65			10.00			19.01	18.55	17.77	14.00					
6.51			2.15			15.18			11.65	10.08	8.54	6.00					
3.45			14.85			99.65			274.8	237.7	225.1	218.0					
1.99			4.91			2.59			11.78	11.74	10.61	11.00					
3.72			4.32			6.12			28.64	26.57	26.02	33.00					
0.51			0.99			0.68			2.40	1.86	2.10	---					
11.06			14.42			34.84			34.76	34.92	36.74	81.00					
1.64			1.64			2.52			3.18	2.68	3.22	4.26					
0.94			2.42			0.92			2.83	3.42	2.25	---					
0.20			0.52			0.28			1.28	0.60	0.82	---					
0.99			1.48			1.59			4.95	4.99	5.79	12.00					
1.64			2.43			1.96			4.85	5.35	5.14	---					
2.13			2.88			2.03			3.14	2.96	2.93	1.53					
0.42			0.88			0.53			1.47	1.00	1.13	0.56					
1.13			2.71			1.65			3.62	3.13	3.48	---					
---			---			---			---	---	---	0.29					
0.88			1.95			0.82			4.04	3.14	2.48	---					
0.70			1.47			0.94			1.96	2.54	1.57	---					
0.62			1.19			0.75			2.89	3.00	2.04	0.88					
0.20			0.52			0.24			1.01	0.89	0.52	0.12					
0.44			0.28			0.36			0.33	0.40	0.40	---					
0.28			0.36			0.29			0.26	0.26	0.35	---					

B15 - Chromitite   N1 - Ultramafic   BT2 - Troctolite   GB2, GS23, GD12, S35 - Gabbros

and Rare Earth Elements (ppm).

S37	N22	N44H	N44A	Mean (S.D.)	N46H	N26H	N26A	RBKH	N48A	Mean (S.D.)	9	14	22	3	21	S	4
---	1345	116	100		1337	75.0	91.0	17.0	83.0								
---	3420	9420	10002		3480	3060	3360	9780	8340								
---	172	623	470		223	146	225	258	370								
---	378	9.00	25.6		404	256	315	62.3	37								
---	---	38	---		55	34	---	25	---								
---	51	140	122		36	39	28	54	118								
---	17	20	22		18.3	12.3	13.0	18.8	22								
---	32	4.0	6.74		54.44	3.56	---	---	---								
---	408	56	76.2		101.7	87.1	101	40.3	45								
---	17	28	29		15	30	21	21	35								
---	90	66	26		28	21.8	46	20.4	88								
---	2.00	---	4.23		2.59	2.12	---	5.22	---								
---	611	34	25.3		199	37.6	36	20	19								
---	18.6	4.96	3.77		1.70	3.77	3.19	6.21	6.50								
---	---	---	1.71		2.20	1.46	---	1.19	---								
---	---	---	0.8		0.85	0.38	---	0.94	---								
---	37	16	8.56		3.05	14.7	9.00	80	17.0								
---	---	---	6.24		4.01	5.56	5.63	11.12	11.8								
---	3.6	2.85	3.81		3.13	2.07	1.77	4.30	3.66								
---	1.12	1.13	0.78		0.80	0.73	0.56	1.01	0.85								
---	---	---	4.75		3.55	2.58	---	5.85	---								
---	0.50	0.70	---		---	---	0.46	---	0.84								
	---	---	4.19		3.33	4.17	---	4.39	---								
---	---	---	2.80		2.18	1.91	---	3.15	---								
---	1.40	3.02	3.48		2.02	2.01	2.11	3.39	3.72								
---	0.18	0.44	0.67		1.02	2.01	2.11	3.39	3.72								
---	---	---	0.53		0.38	0.61	---	1.02	---								
---	---	---	0.40		0.22	0.52	---	0.57	---								

N44H, N44A - Gabbros   N426H, N26H, N26A, RBKH, N48A - Metabasalts

ed. Seven analyses of mafic and ultramafic rocks from the same area (Balakrishnan et al.,1992) are taken for comparison. All analysis were processed on anhydrous basis. It is seen from the table that the analyses of peridotites (serpentinites) show limited variation in major oxides. The SiO_2 of the peridotites varies from 42.7 to 44.5 wt.%. Total iron (as FeO) varies from 11.6 to 17.0 wt.%. The alkalies are very low (less than 1 wt.%), Al_2O_3 is low (less than 3.0 wt.%). The SiO_2 of the gabbros ranges from 47.5 to 52.9 wt.%, total iron (FeO) is between 3.5 and 22.0 wt.%, Al_2O_3 varies from 11.0 to 20.0 wt.% and MgO is between 5.7 and 12.5 wt.%. The TiO_2 varies between 0.3 and 1.6 wt.%. The iron enrichment is moderate, with Mg # [Mg/(Mg + Fe +2)] decreasing from 0.68 to 0.39 except in two smples N44H and N44A where it is about 0.21 and 0.18.

The chemical data has been recast into CIPW normative minerals (Table No.3.2). It is seen from the table that the majority of the gabbroic rocks are quartz-normative except N22, N44H, and N44G which are olivine-normative. Thus broadly the gabbroic rocks vary between olivine - and quartz - tholeiitic in character.

53

The major element oxide percentages are plotted against Mg # to understand the evolutionary trend (Fig. 3.2) It is observed that MgO, CaO and Al_2O_3 decrease with increasing differentiation. TiO_2 however, behaves differently. It shows an increasing trend in early differentiates (ultramafics) and shows a decrease in the gabbros. The latter trend is typical of tholeiitic differentiation. SiO_2 does not show a well defined trend. This could be partly related to alteration. A crude negative correlation with Mg # is, however, consistent with crystal fractionation of a gabbroic assemblage involving pyroxene, plagioclase and olivine (Cox, 1980). The trends shown by Na_2O, K_2O and P_2O_5 are not very clear cut and show a scatter of points with wt.% values very low as well as high but largely show an increasing trend. These scatters are due to the compositional heterogeneity which can be ascribed to the mobility of these elements during regional alteration or metamorphism.

It is seen that though several elements show smooth systematic trends in the various diagrams reflecting primary magmatic history, these trends can be ascribed to progressive differentiation by fractional crystallisation.
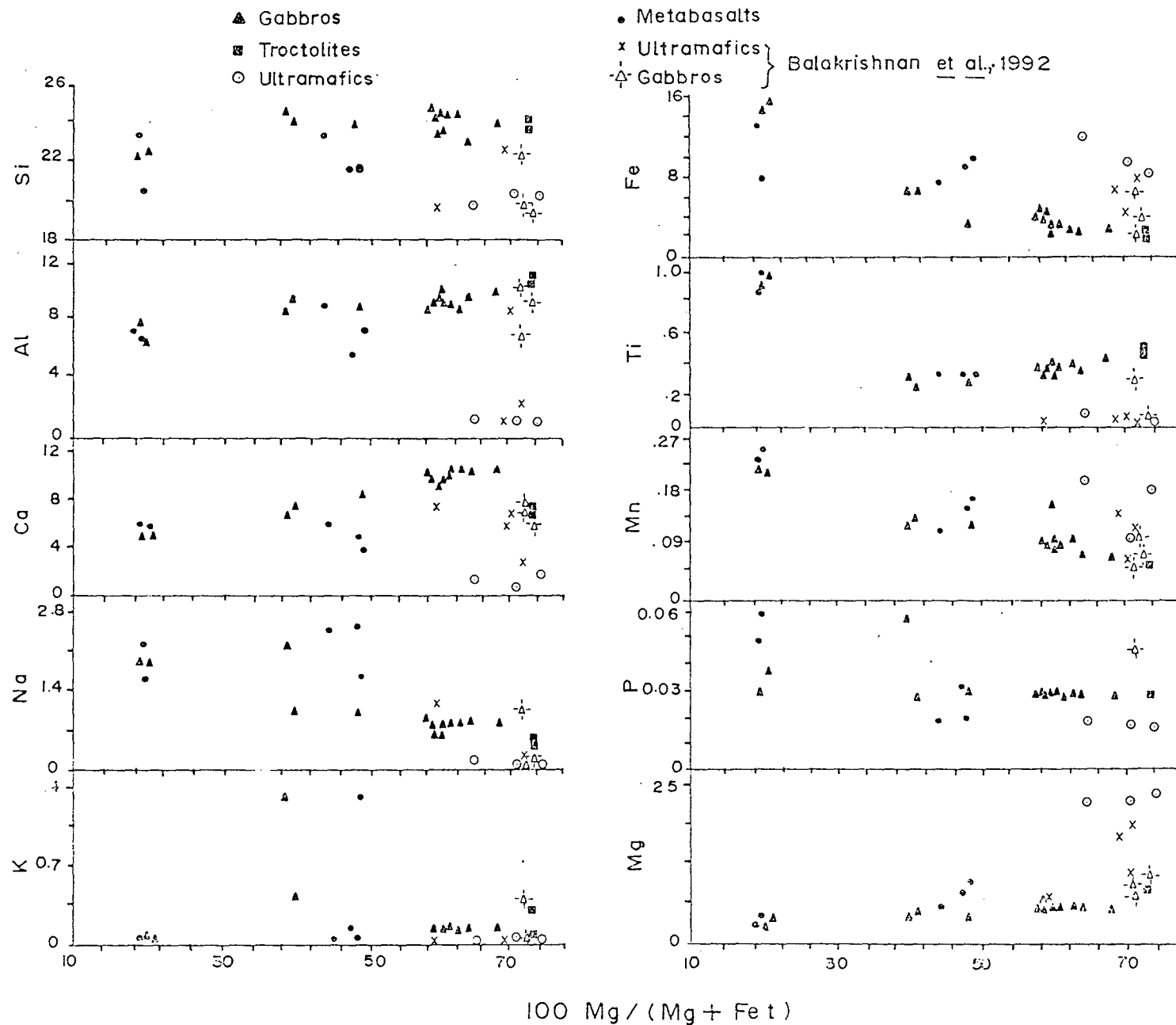
Fig. 3.2   Major element wt.% vs Mg # diagram showing plots of Bonala rocks.

Although a majority of the samples are cumulates, they probably approach liquid compositions as discussed later. Evidences in support are (i) non cumulate modal mineralogy particularly in some of the gabbroic rocks (ii) whole-rock major and trace element compositions that are similar to MORB or arc - basalts (iii) mineral differentiation trends (discussed later under mineral chemistry) are comparable to whole rock differentiation trends and (iv) the presence of intercumulus minerals indicating considerable volume of trapped melt.

In an attempt to understand the magma type, its nature and the differentiation trend the chemical data have been plotted in various discrimination diagrams. In the TAS (total alkalis versus SiO_2) diagram (Irvine and Baragar, 1971), all analyses plot in the sub- alkaline field (Fig.3.3a). The sub-alkaline rocks can be subdivided into calc-alkaline and low-K tholeiitic series. The data were therefore, plotted in Alkali Index versus Al_2O_3 diagram (Middlemost, 1975). Majority of rocks plot in the low-K tholeiitic basalt field (Fig. 3.3b) with few analyses occupying the calc-alkali basalt field obviously due to higher proportion of calcic plagioclase. The rocks
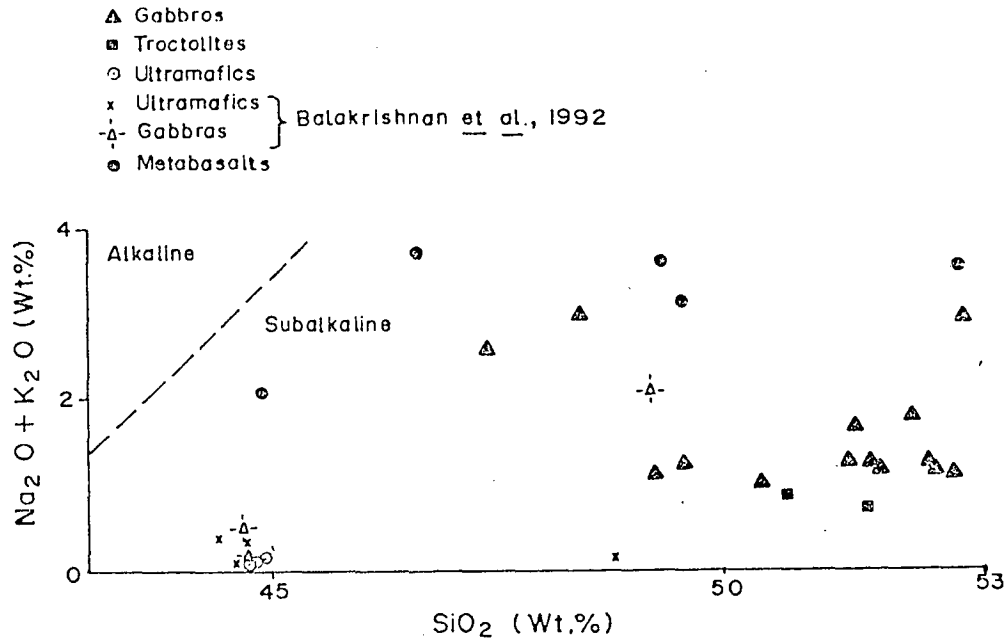
Fig.3.3a Total alkalis wt.% vs SiO2 wt.% diagram
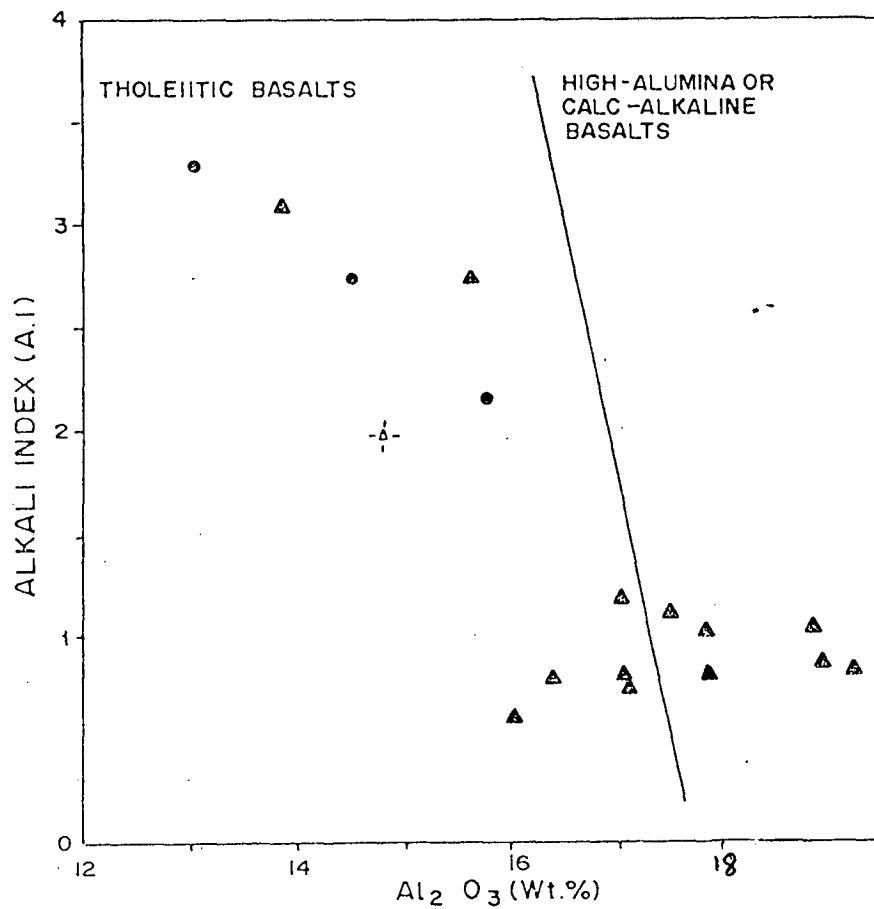(after Irvine and Baragar, 1977) showing plots of
Bondla rocks.

Fig.3.3b Alkali index vs Al2O3 wt.% diagram (after
Middlemost, 1975) showing plots of Bondla rocks.

belonging to the subalkaline and low-K series can be differentiated on the basis of their trend on the AFM diagram (Irvine and Baragar, 1971). Majority of the samples plot in the field of tholeiitic basalts (Fig. 3.4a) and show an iron enrichmemt trend. It has some points of similarity with Karoo tholeiitic series but it strongly resembles the trend of Vourinon, Greece (Brunn, 1956), the Maryland-Pennsylvania (Hopson, 1964), gabbroic rocks of alpine mafic suite and the Precambrian Thessaloniki gabbros, Greece (Sapountzis, 1979).

Serri (1981) has identified different tectonic settings for the origin of gabbroic rocks on the basis of major element chemistry. This approach was adopted by him because the gabbroic rocks are generally less altered during metamorphism with most elements except Na_2O, K_2O and CaO well preserved (Serri, 1981). As the gabbros from Bondla are least metamorphosed, the major element compositions could be used to decipher the tectonic environments. In the TiO_2 versus Mafic Index [FeO/(FeO+MgO)], diagram Serri, 1981), majority of the gabbros from Bondla plot in the field of low-Ti gabbros (Fig.3.4b). However, as pointed out by Serri (1981), rocks with Mafic Index less than
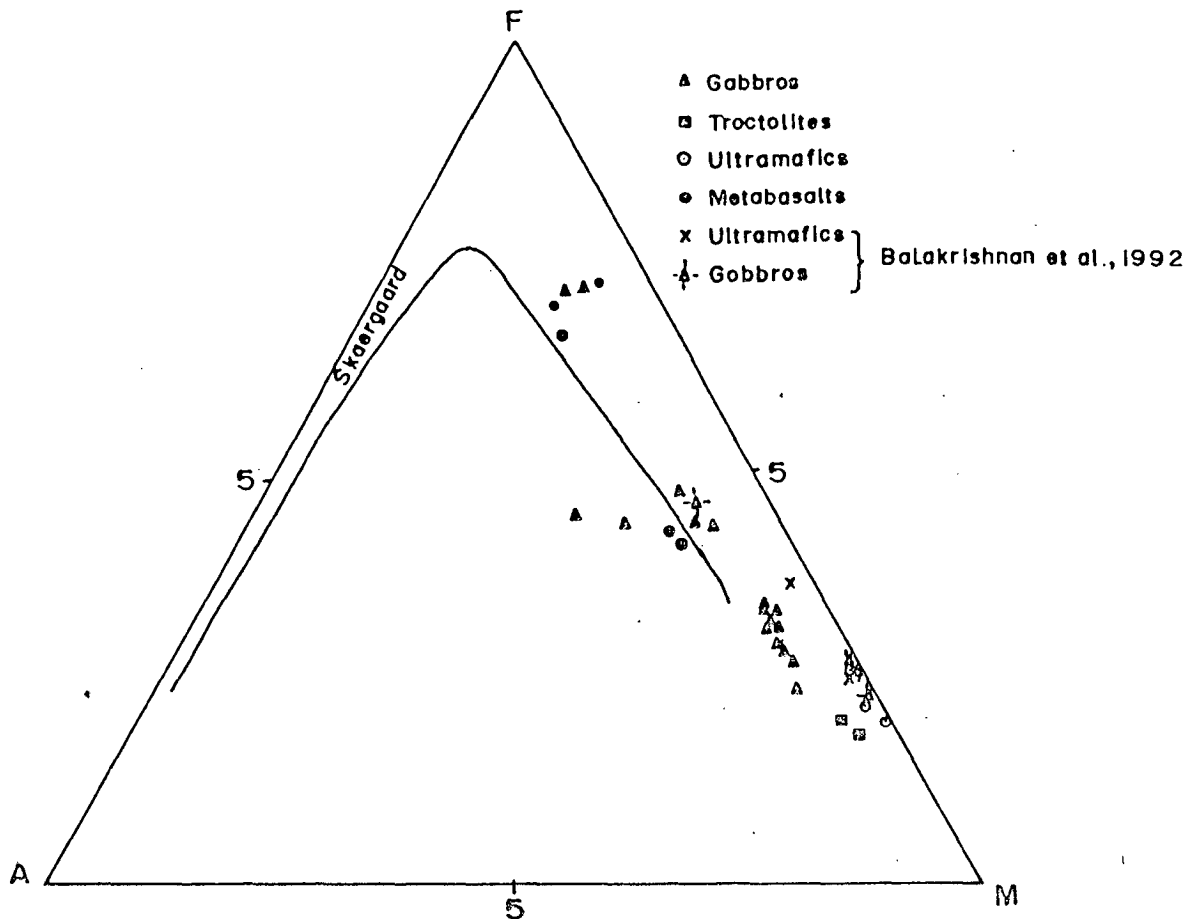
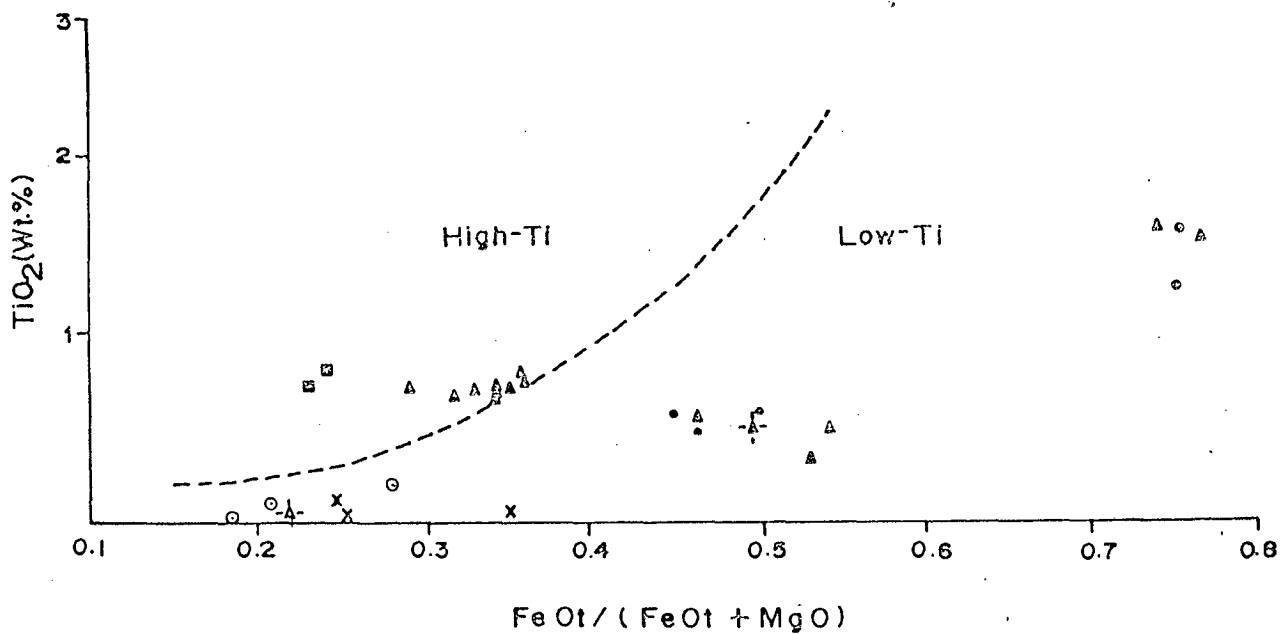Fig.3.4a   AFM diagram showing plots of Bondla rocks.

Fig.3.4b   TiO2   wt.%   vs   Mafic   Index   diagram   (after
           Serri, 1981) showing plots of Bondla rocks.

0.35 show an overlapping trend because majority of high-Ti cumulate rocks with TiO$_2$ less than 0.15 wt.% consist largely of TiO$_2$-free phases such as olivine and plagioclase. The decrease in TiO$_2$ with differentiation can be ascribed to the decrease of modal Fe-Ti oxide phases. In the upper gabbros TiO$_2$ concentration decreases.

Trace Elements

Trace element abundances of 15 samples are presented in Table No. 3.2. It is seen from the table that the compatible elements eg. Ni and Cr show high abundances in ultramafic rocks. Cr varies between 11426 -1227 ppm, Ni is between 217 to 373. These high abundances could indicate cumulate crystallization process. Both these elements show congruently decreasing trend through the rock series with increasing differentiation indicating olivine, clinopyroxene and spinel dominated fractionation. This is also corroborated by the modal compositions of the rocks.

The large-ion-lithophile (LIL) elements eg. Rb, Ba, Th, Y, Nb, Ta, Hf, Zr and light rare earth elements (La and Ce) of the gabbroic rocks are plotted against Mg #

(Fig. 3.5). It is seen that all the elements show a distinctive enrichment trend that parallels the variation trend shown by major elements such as FeO and MnO. Sr content shows a progressive increase in the melt during the crystallisation of the Lower Zone and reaches maximum value in the troctolites. With further differentiation the Sr content progressively decreases in the gabbroic rocks of the Upper Zone. The increase in Sr content in the early stages can be attributed to crystallization of olivine, spinel and pyroxene in which Sr is incompatible. The decrease in Sr content in gabbroic rocks may reflect plagioclase crystallization during differentiation. The Rb/Sr values also show a decrease, with selective partitioning of Sr over Rb into plagioclase. To a first approximation the data are compatible with preferential partioning of the elements into anorthitic plagioclase in which Sr generally is more compatible than Rb. Enrichment of other highly incompatible elements such as Nb, Ta, Th with differentiation also supports dominant role of plagioclase in differentiation.

The plots of chondrite normalised trace element abundance profiles (spidergrams) (Thompson, 1982) for
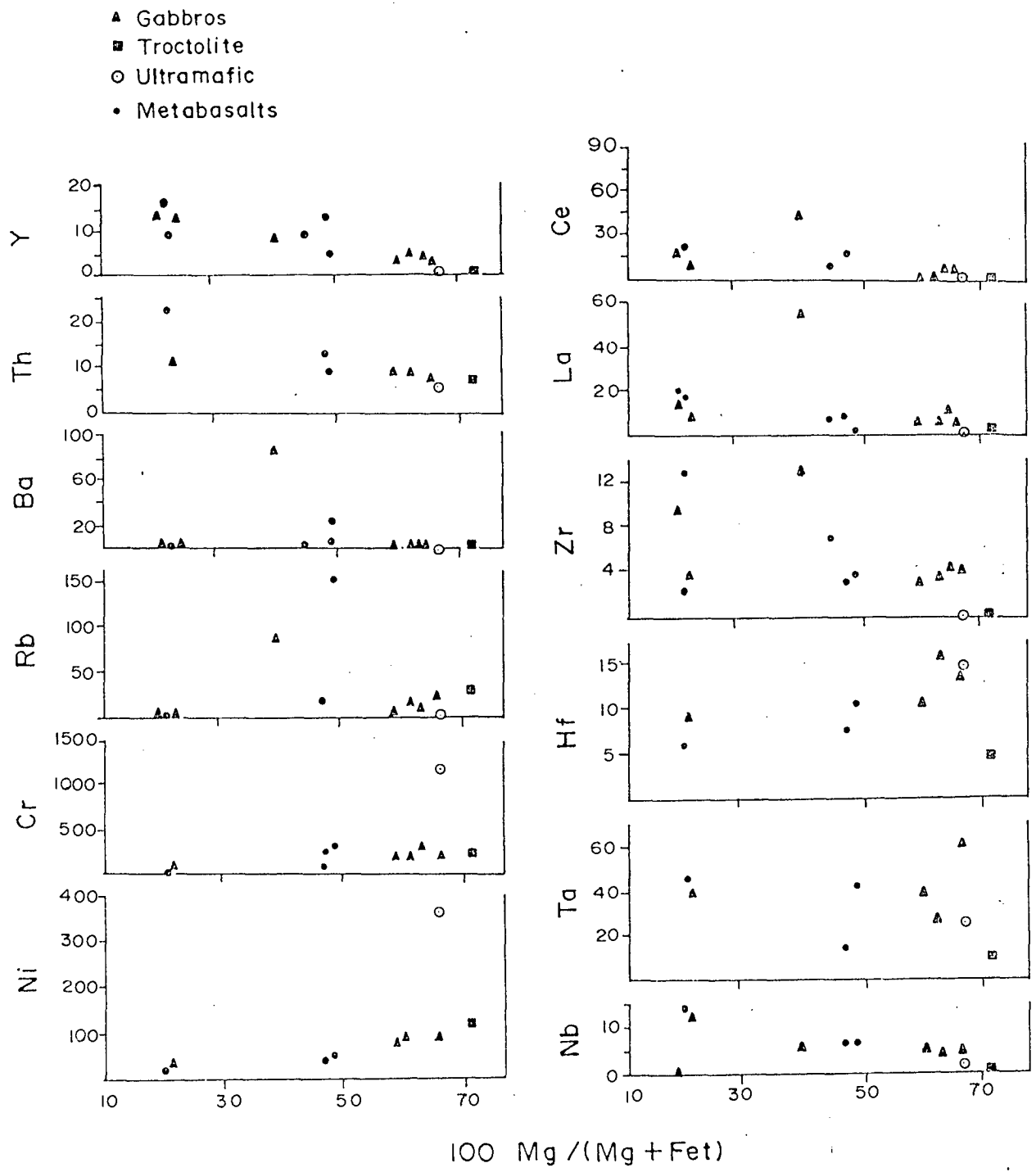
Fig.3.5   Trace   element   concentrations   (ppm)   vs   Mg   #
diagram showing plots of Bondla rocks.

ultramafic rocks, gabbros and metabasalts are shown in Fig.3.6, 3.7 and 3.8 respectively (Thompson, 1982). The rocks of the Bondla complex show internally consistent patterns that are characterised by a prominent trough shown by Sr in ultramafic rocks and a peak in gabbroic rocks. The trough shows its incompatibility in the former and the peak can be attributed to its concentration of An-rich plagioclase (eg. BT2 GB2, GD12). This is also seen from Table No. 3.1 wherein most of the rocks contain more than 50% modal plagioclase.

The patterns also show strong trough at Ti which can be attributed to the early fractionation of spinel into which Ti has a higher distribution coefficient. Strong trough at Nb and Zr indicates their incompatibility during differentiation. Correspondence of increasing Nb with Ti and Fe indicates that crystallization of Fe-Ti oxides was not important during the differentiation of most of the gabbroic rocks. Over all, low abundances of Nb relative to other trace elements, however, may also reflect unusually low concentrations in the initial magma composition.

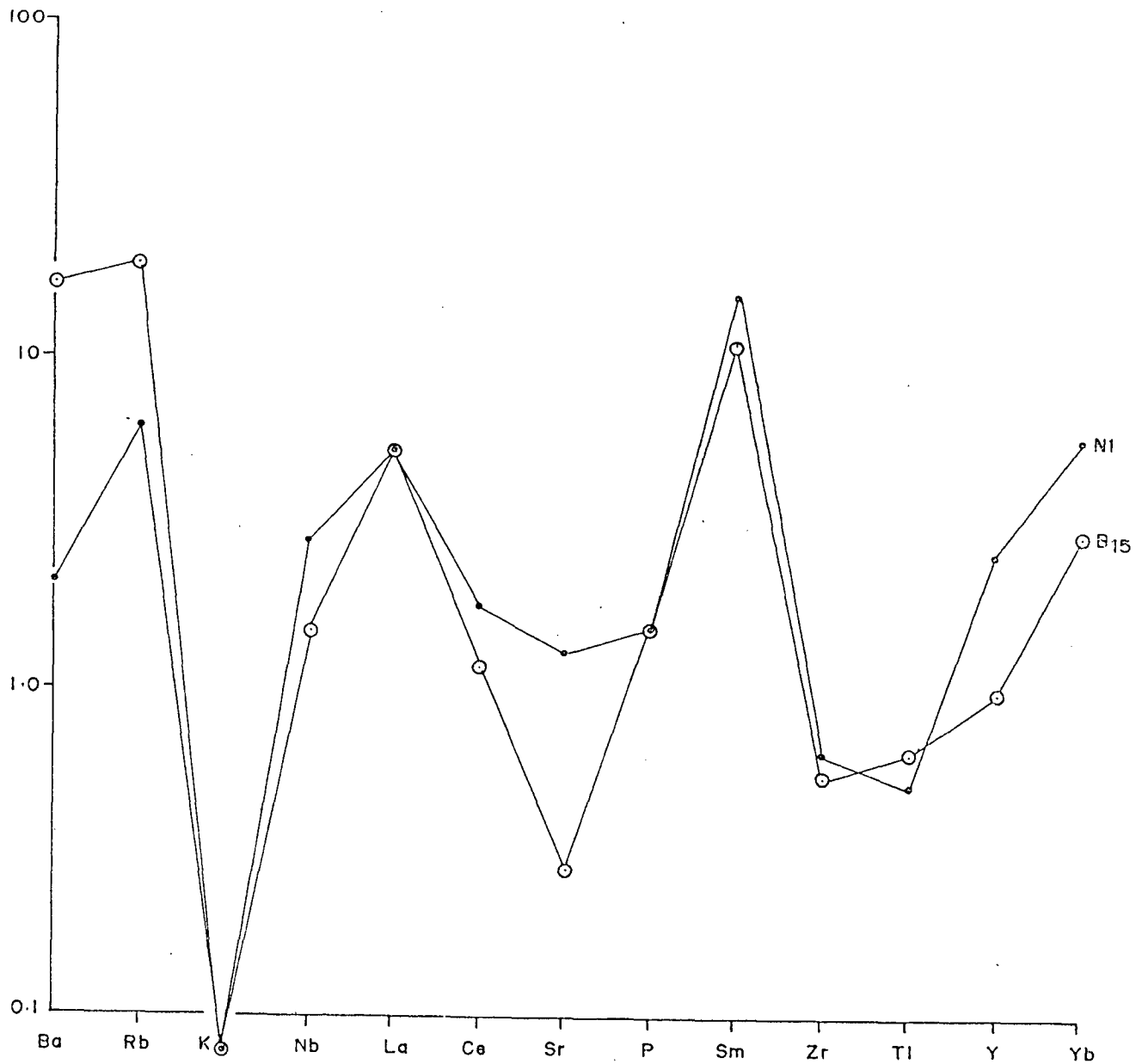Fig.3.6   Chondrite   normalised   trace   element   patterns
           of   ultramafic   rocks   from   Bondla.   Element
           order   and   normalising   values   after   Thompson
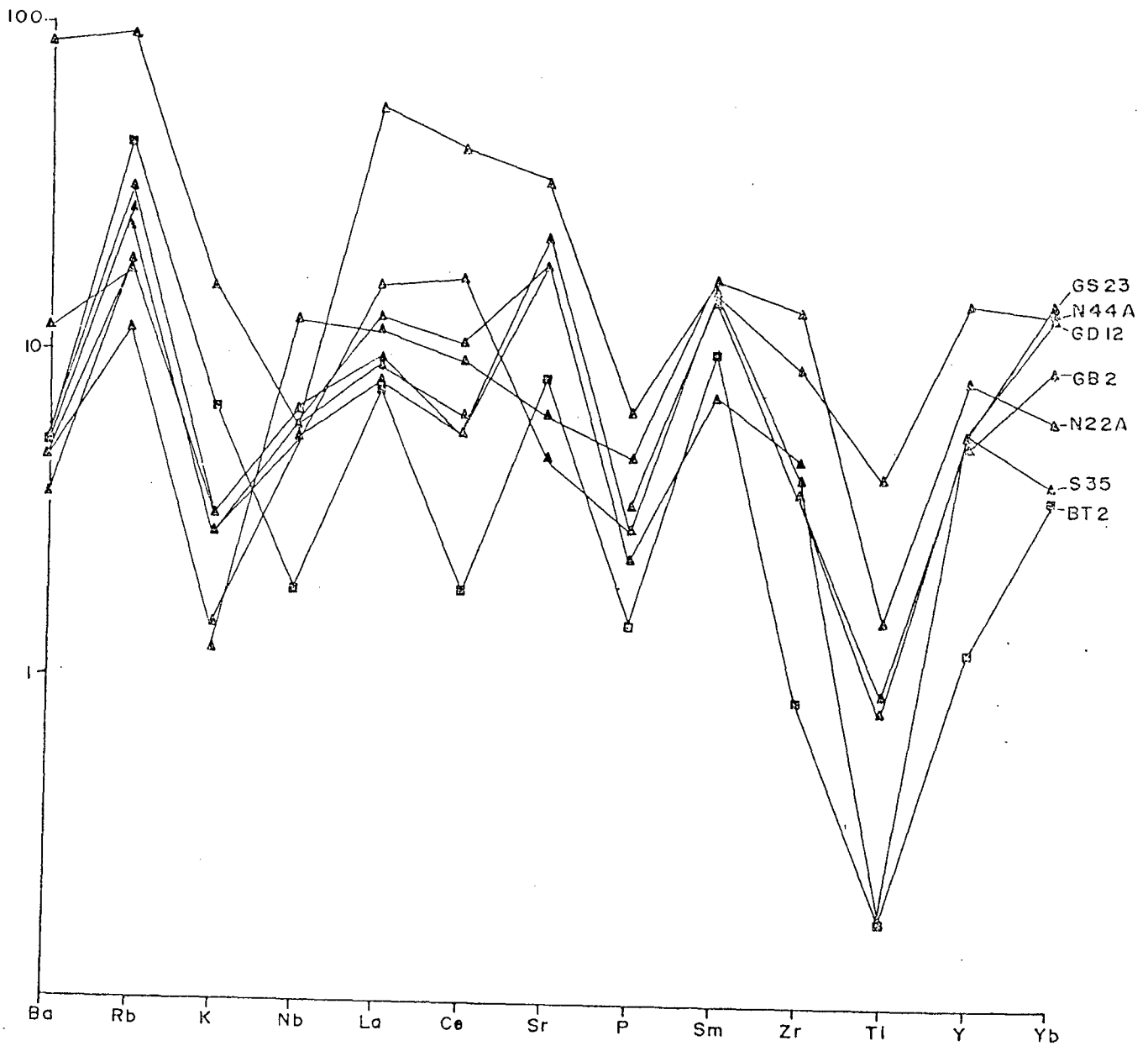   (1982).

Fig.3.7   Chondrite   normalised   trace   element   patterns
of   gabbros   from   Bondla.   Element   order   and
normalising values after Thompson (1982).
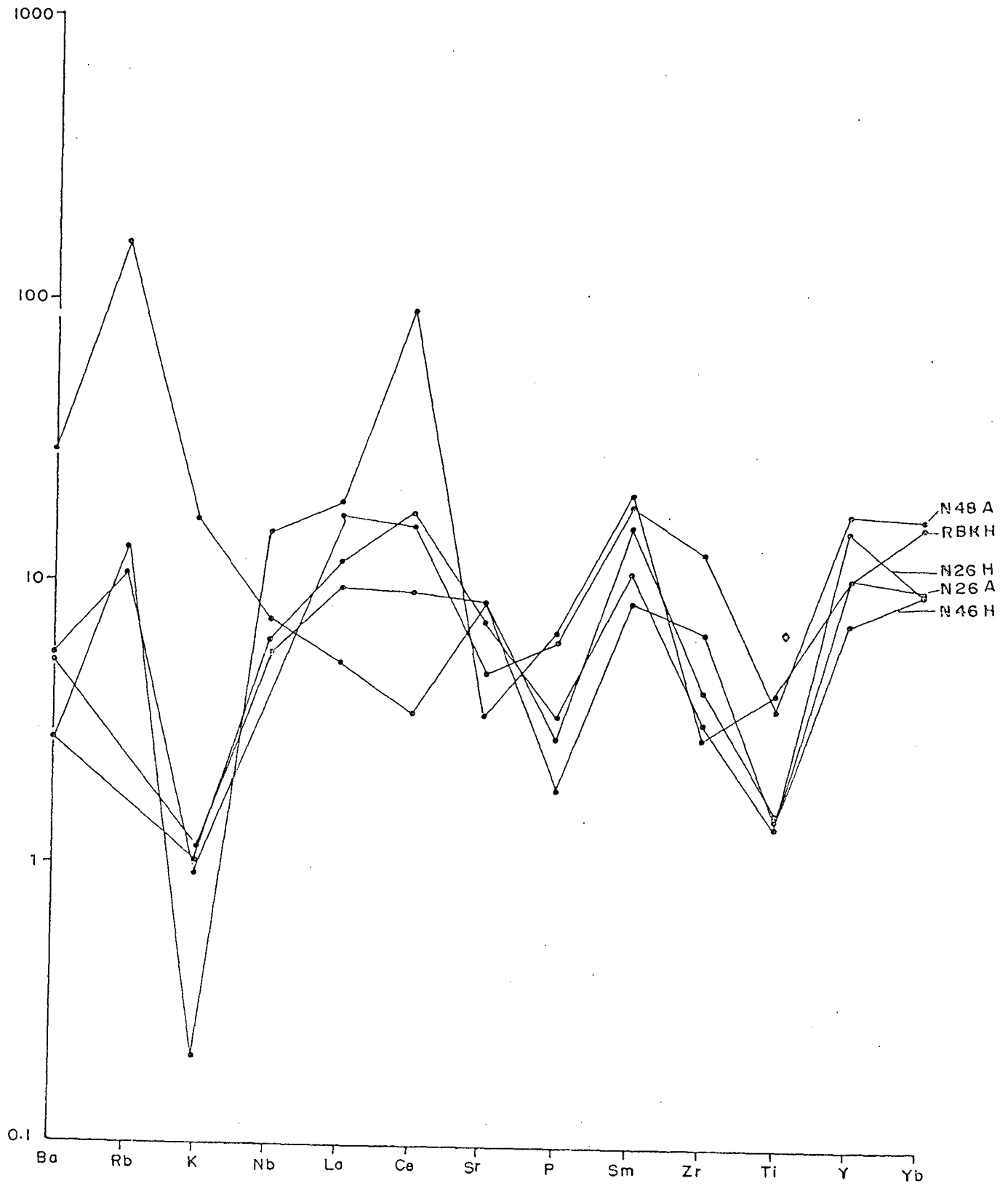
Fig.3.8   Chondrite   normalised   trace   element   patterns
of   metabasalts   from   Bondla.   Element   order
and normalising values after Thompson (1982).

The Zr/Nb ratio for ultramafic rocks varies between 4 and 7 and for the gabbroic rocks between 9 and 14. The values are lower than those typical of MORB (i.e. 730). The Zr/TiO2 ratios in general decrease with differentiation whereas, Nb/Y shows a very restricted variation; in most samples it is almost constant at 0.2. The values of La/Nb ratio ranges between 0.8 to 9.0 which according to Thompson *et al.,* (1984) could indicate crustal contamination.

The Ti/V ratio of the gabbros is generally low, (less than 10) except in GB2, GD12, S35 and N22A where they are between 10 and 20. Those of metabasalts are higher i.e. between 16 and 50. Ti/V ratio of igneous rocks reflect the oxygen fugacity of the magma (Shervais, 1982). The Y/Zr ratio shows a very restricted variation and in all the gabbros except N44H, it is almost constant at around 0.4. This indicates that these elements are inherited from the parent magma.

The spidergrams of the metabasalts (Fig. 3.8) are by and large identical to those of gabbros indicating that both are comagmatic.

Rare Earth Elements (REE)

The rare earth elements (REE) are a group of 15 elements (atomic number 57 to 71) fourteen of which occur naturally. They are particularly useful in petrogenetic studies because all the REE are geochemically similar (Wilson, 1989).

REE have received special attention (Condie, 1976a; Sun and Nesbitt, 1977) because their behaviour can be interpreted in terms of partial melting and fractional crystallisation process. In particular, they can be used to explore the REE abundance patterns of the source rocks, the residual mineralogy after partial melting and the effect of fractional crystallisation (Gast, 1968).

Chrondrite normalised REE patterns of the ultramafic rocks, the gabbroic rocks and the metabasalts are presented in Figs.3.9a, 3.9b and 3.10 respectively. Visual inspection reveals that there are no major differences amongst the patterns. Subtle differences could be due to the variation in mineralogy accentuated by the coarse grain size of the rocks. The patterns in general are flat
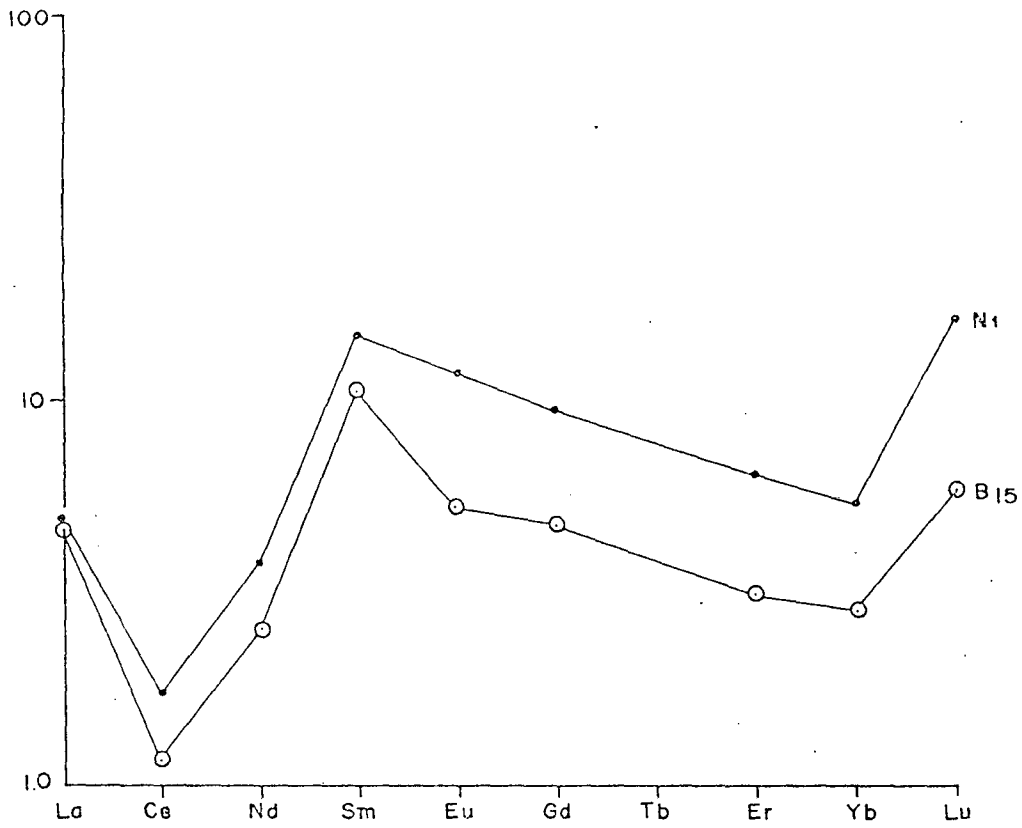
Fig.3.9a   Chondrite   normalised REE patterns of   ultramafic
            rocks from Bondla.
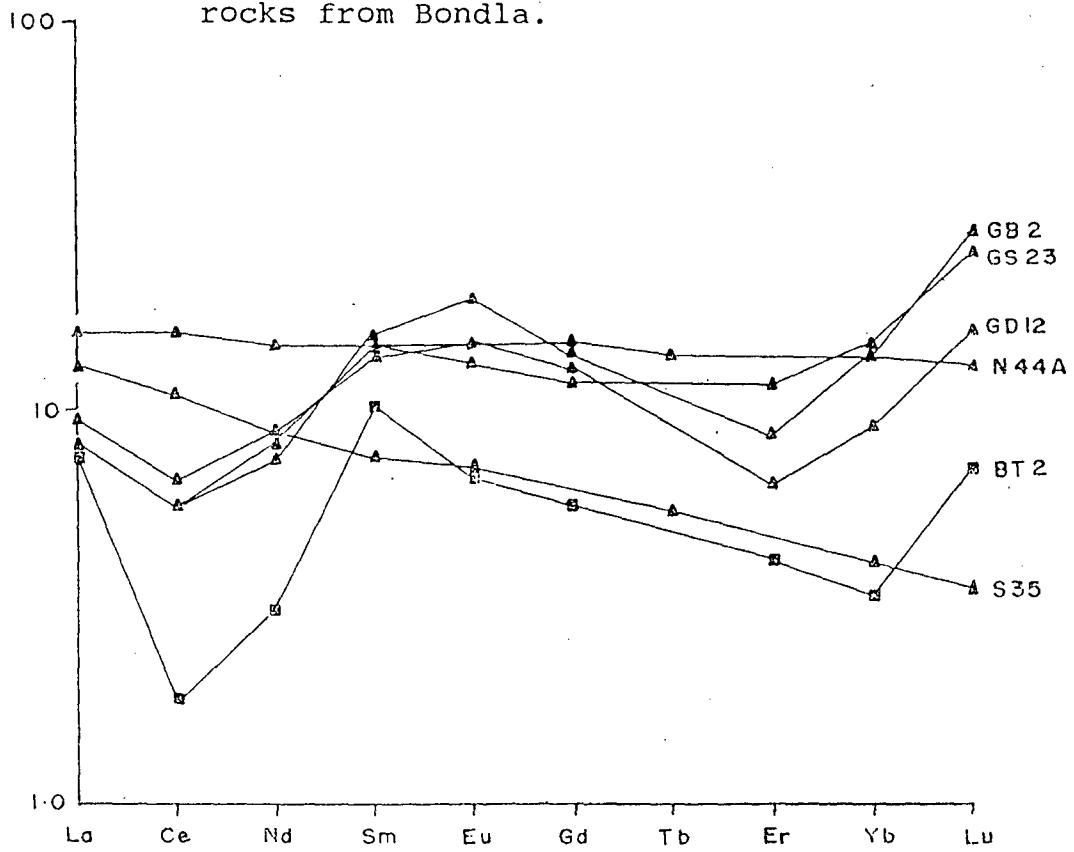

Fig.3.9b   Chondrite   normalised   REE   patterns   of   gabbros
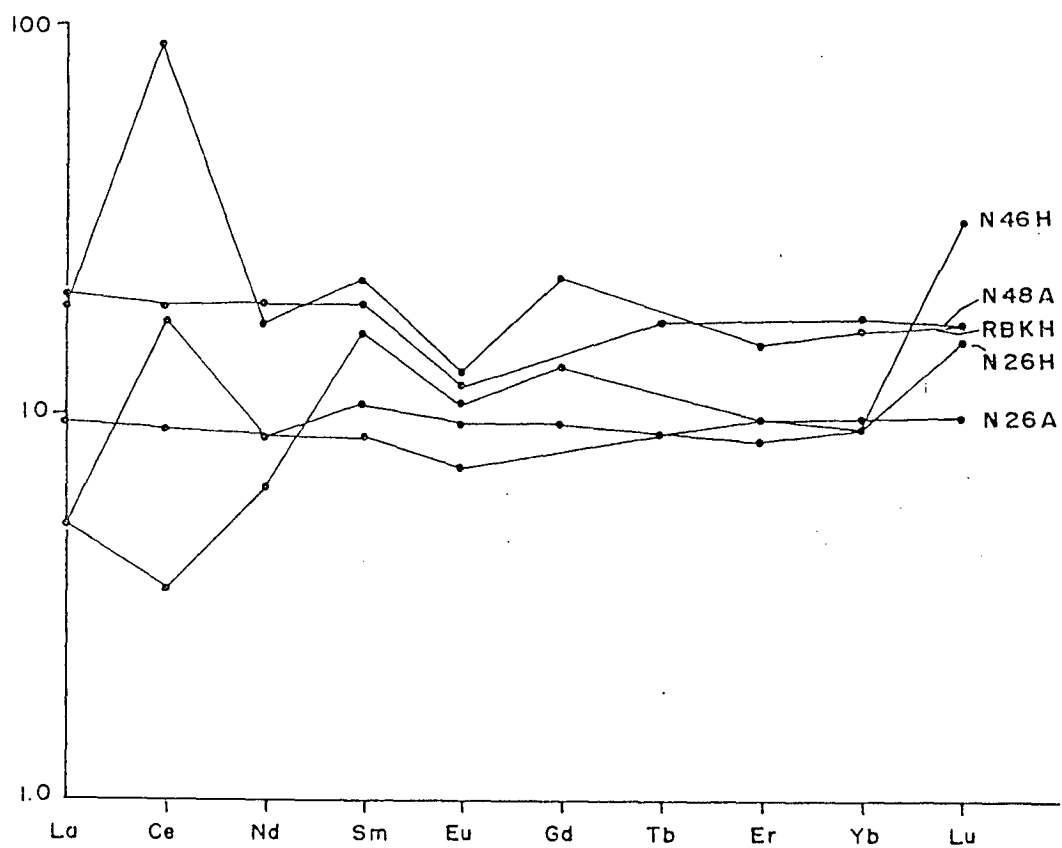   from Bondla.

Fig.3.10   Chondrite normalised REE patterns of metabasalts
           from Bondla.

with slight LREE enrichment as compared to the HREE. The La/Yb ratio varies from 1-13. The general smooth change in the shape of the patterns as total concentration increases is consistent with these rocks being related to partial melting of a common source or crystal fractionation. The patterns are, however, more consistent with the effects of crystal fractionation. The parallel patterns as well as the range of compositions may have been produced by crystallisation of a relatively constant mineral assemblage as corroborated from Table No.3.1. The negative Ce anomaly shown by peridotites could be ascribed to olivine and pyroxene controlled differentiation. REE distribution coefficients are higher for clinopyroxene than any other phase (De Bari, 1994).

The gabbroic rocks (GB2, GD12) show a small positive Eu anomaly which can be attributed to fractionation of Eu^{+2} in plagioclase, but the amount must be small as the MgO content is quite high. The Eu anomaly correlates with a positive Sr peak which is supported by higher Al_2O_3 and LILE concentration in general than the starting composition such as that shown by BT2. Similarly a negative Eu anomaly (GS23, N44A) could be ascribed to differentiation

62

involving An-rich plagioclase. Another factor responsible for the change in the Eu anomaly could be the decrease in plagioclase and consequent increase in clinopyroxene and opaques which account for rising levels of trivalent REE excepting Eu.

The LREE abundances of the gabbroic rocks in general share a single trend which increases with increasing differentiation as seen in Fig.3.5. The Ce/Yb ratio ranges from 1.5 to 26.4 and increases with increasing differentiation. The trend of increasing bulk REE abundance and Ce/Yb ratio with increasing differentiation fits favourably with the crystal fractionation process. Slight departure of this increasing trend of Ce/Yb ratio in the middle differentiates could be ascribed to the depletion of LREE as a result of apatite crystallisation.

The REE patterns of metabasalts mimic those of the gabbros supporting the earlier contension that both are comagmatic.

Mineral Chemistry

The mineral phases from selected rocks such as peridotites, pyroxenites, troctolites and gabbros were analysed with electronprobe microanalyser under standard conditions at CSIRO, Australia. An accelerating voltage of 15kv and specimen current of 3nA on cobalt were used. A range of natural and synthetic standards were used. At least three spot analyses were carried out per grain to know the intragrain compositonal variation. Average composition of a phase was determined from at least three spot analyses . At least four grains were analysed in each sample to know the intergrain variation.

Olivine, Ca-poor pyroxene, Ca-rich pyroxene, plagioclase, and chrome-spinels were analysed. In the present work six analyses of olivine, fourteen analyses of Ca-poor pyroxene, thirty-six analyses of Ca-rich pyroxene, thirty-one analyses of plagioclase and fourteen analyses of chromite are included. The details of the analyses of chromites are discussed in Chapter - IV.

Olivine

The olivine in dunites and peridotites from the Lower Zone occur as euhedral to subhedral serpentine pseudo-morphs and hence its composition could not be obtained by electronprobe. It varies in size between 0.5 and 4 mm. Average size is about 1.5 mm.

Fresh olivines were available for analysis from troctolites and gabbroic rocks. The olivines from troctolites (BT1) are euhedral to subhedral and vary in size between 0.9 to 3 mm. Chemical composition and atomic proportions are presented in Table No.3.3. All analysed grains contain about 40 wt.% SiO_2, MgO content is almost constant between 45 and 46 wt.%. The Fo content varies between 85 and 86.

The olivines are zoned, the Fo content decreases towards the rim, however, in some grains a reverse behaviour is observed. The latter could be due to alteration of olivine.

Table No. 3.3 Electronprobe Microanalysis of Olivines

in Troctolite from Bondla

Oxides	BT1 1	BT1 2	BT1 3	BT1 4	BT1 5	BT1 6
SiO_2	40.37	40.08	40.07	40.40	40.53	40.39
TiO_2	0.02	0.01	0.01	-----	0.01	-----
Al_2O_3	------	0.03	0.01	-----	0.01	------
Cr_2O_3	0.06	----	0.02	----	0.02	0.03
FeO	13.46	13.37	13.43	13.13	13.25	13.25
MgO	45.75	46.16	46.09	46.13	45.83	45.97
CaO	0.12	0.11	0.13	0.10	0.12	0.14
MnO	0.17	0.18	0.18	0.16	0.17	0.15

Cations recalculated on the basis of 4 oxygens

Si	1.004	0.9954	0.9975	1.0033	1.0067	1.0037
Ti	0.0002	0.0001	0.0001	-----	0.0001	-----
Al	------	0.0007	0.0001	-----	0.0001	-----
Cr	0.001	------	0.0003	-----	0.0002	0.0004
Fe^{+2}	0.2809	0.2860	0.2805	0.2736	0.2762	0.2763
Mg	1.7017	1.7146	1.7164	1.7134	1.7025	1.7085
Mn	0.0034	0.0037	0.0037	0.0032	0.0035	0.0031
Mg #	0.858	0.857	0.859	0.862	0.86	0.86

BT1 - Troctolite

Ca-poor Pyroxene

It is third in order of abundance in ultramafic rocks and most abundant mafic phase in gabbros. In some gabbros however, Ca-rich pyroxene is dominant over the former. The analyses of pyroxenes and their structural formulae are presented in Table No.3.4. The analyses are not corrected for exsolutions.

Ca-poor pyroxenes in dunite is very subordinate and is intercumulus. It occurs as pseudomorphs of bastite. Brown relicts of bronzite are seen at places. It is anhedral and poikilitically encloses olivine forming heteradcumulates. Individual crystals reach upto 8 mm in size. It contains exsolutions of clinopyroxene parallel to (100). It is invariably altered to serpentine and its presence could be made out from relicts in serpentine. It has not been analysed by microprobe.

In the gabbroic rocks Ca-poor pyroxene occurs as subhedral crystals 1.5 to 1.8 mm in size. It is faintly pleochroic in shades of pale pink to pale brown. It is represented by inverted pigeonite which shows blebs of

Table No.3.4 Electronprobe Microanalysis of Ca-poor Pyroxenes in Mafic and Ultramafic Rocks from Bondla

Oxides	BT1 1	BT1 2	BT1 3	BT1 4	GB1 5	GB1 6	GB1 7	GB1 8	GB1 9	GS23 10	GS23 11	GS23 12	GS23 13	GS23 14
SiO_2	56.40	56.43	55.77	56.23	56.46	55.50	47.84	47.92	47.91	53.60	52.62	53.00	52.92	52.56
TiO_2	0.43	0.10	0.13	0.12	0.17	0.11	0.47	0.44	0.38	0.12	0.33	0.28	0.30	0.29
Al_2O_3	0.70	1.21	1.25	1.40	1.48	1.38	0.71	0.71	0.80	1.97	0.93	1.04	0.93	0.70

clinopyroxene parallel to (100) and fine exsolution lamel-
lae parallel to (100).

Fresh Ca-poor pyroxene was analysed from trocto-
lites. The silica percentage has a very narrow range
between 55.7 and 56.4 wt.%. Al_2O_3 varies from 0.79 to 1.4
wt.% and Cr_2O_3 between 0.19 and 0.45 wt.%. TiO_2 is
present in small amounts (0.1-0.43 wt.%) as is common with
tholeiitic pyroxenes (Kushiro, 1960). MnO content is also
very low between 0.25 and 0.3 wt.%. The pyroxenes belong
to Quad (Ca-Mg-Fe) pyroxenes (IMA, 1988). Their composi-
tion may be expressed as $Ca_{2-4.5}$ $Mg_{82.5-85.4}$ $Fe_{12.5-13.1}$.
Chemical variation within the grain is insignificant. The
chemical data in the pyroxene quadrilateral (Fig. 3.11a)
plot in the enstatite field. The enstatites are rich in
Mg. Mg # varies between 0.86 and 0.87 and shows good
agreement with Mg #s reported for Ca-poor pyroxenes from
other layered intrusions.

The Ca-poor pyroxenes in the overlying gabbros (GB1
and GS23) has SiO_2 percentage varying between 46.8 and
53.6 wt.% which is less than those in troctolite (BT1).
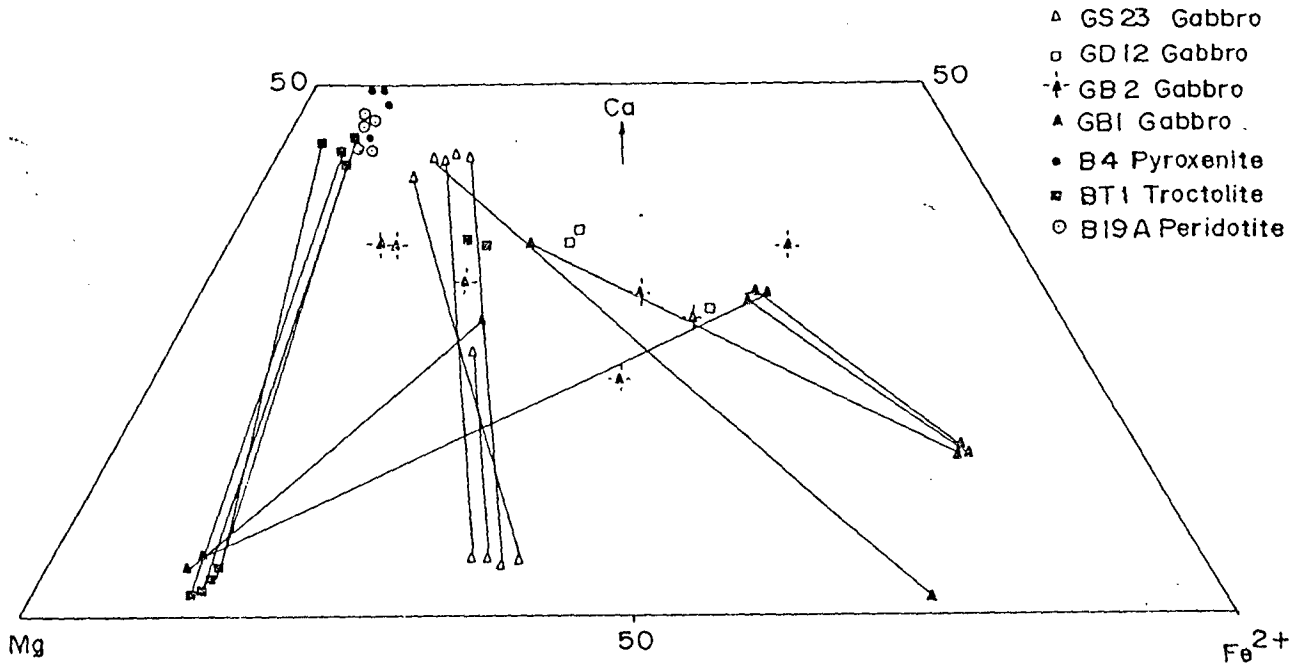They contain more Ti (between 0.11 and 0.47 wt.%) and Mn

Fig. 3.11a Plots of compositions of pyroxenes from Bondla rocks in the pyroxene quadrilateral.
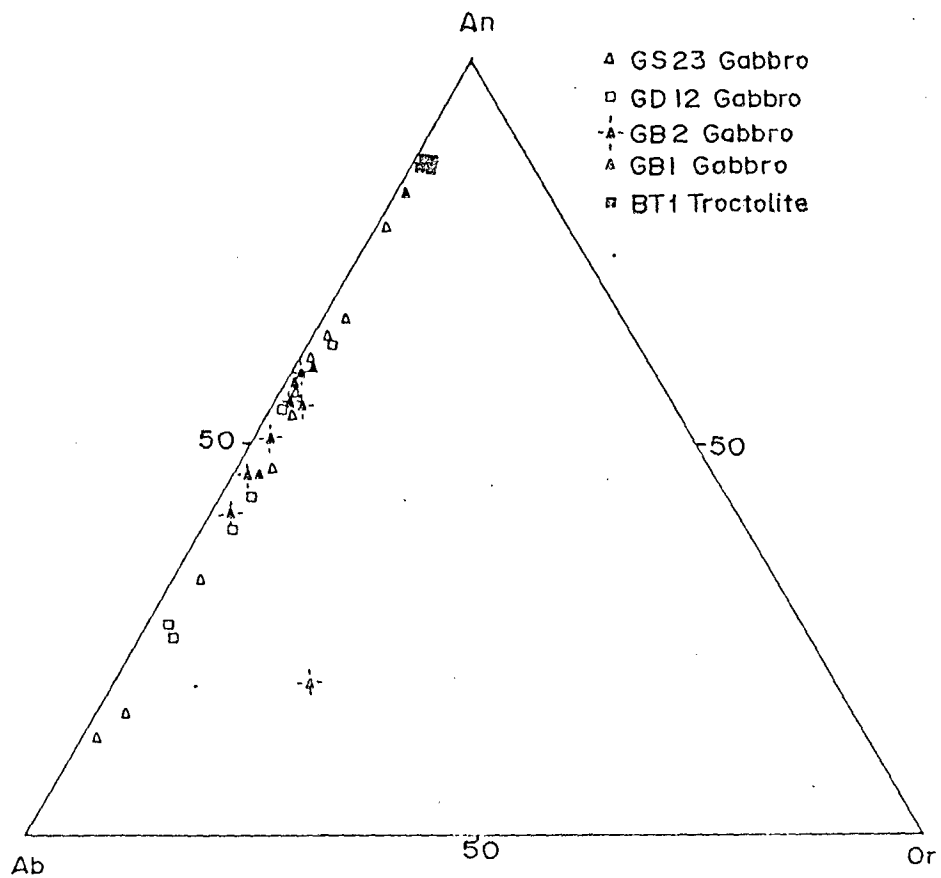

Fig. 3.11b Plots of compositions of plagioclase from Bondla rocks in Rb-Rn-Or traingular diagram.

(between 0.25 and 0.84 wt.%) than those in troctolite. Alumina content, however, is more in troctolite pyroxene (0.79-1.48 wt.%) than in pyroxenes from gabbros (0.70-1.38 wt.%) except in one analysis where it is 1.97 wt.%. They range in composition from $Ca_{3.8}Mg_{84.0}Fe_{12.1}$ to $Ca_{4.1}Mg_{82.7}Fe_{13.0}$. In the pyroxene quadrilateral, the pyroxenes from (GB1) plot in the pigeonite field with Mg # about 0.86. They co- exist with more ferrian pigeonites ($Ca_{15.1}Mg_{15.4}Fe_{69.4}$ to $Ca_{14.4}Mg_{15.3}Fe_{70.2}$) with Mg# varying between 0.17 and 0.18. These latter pyroxenes represent intercumulus phases. In the more fractionated gabbro (GS23) the cumulus pyroxene becomes progressively richer in iron. The composition varies between $Ca_{1.9}Mg_{73.9}Fe_{24.1}$ to $Ca_{3.3}Mg_{58.3}Fe_{38.2}$. The Mg # varies between 0.60 and 0.61.

Ca-rich Pyroxene

It occurs as an intercumulus mineral in peridotites poikilitically enclosing cumulus olivine and occurs to the extent of 20% by mode in the peridotites. It is the most dominant mineral in pyroxenites contributing 84% by volume of the rock.

Ca-rich pyroxene is the most abundant mafic mineral in the gabbroic rocks contributing about 10-30% by mode. It is generally fresh. Cumulus phases vary between 0.9-3.5 mm and are generally anhedral. It contains exsolution blebs of pigeonite parallel to (001) and fine exsolutions lamellae of orthopyroxene (hypersthene) parallel to (100). It was not possible to resolve the closely spaced exsolution lamellae under the electron microprobe. Hence, average bulk chemical analyses were obtained. The results of chemical analyses and the atomic proportions are presented in Table No.3.5.

It is seen from the table, that the clinopyroxenes from peridotite, pyroxenite and troctolite in general contain 53.2 to 55.2 wt.% SiO_2. Those in peridotite are more aluminous and contain 2.18-2.2 wt.% Al_2O_3. Al_2O_3 decreases in clinopyroxenes from troctolite (1.6-2.1 wt.%) and further decreases to (0.1-0.7 wt.%) in pyroxenite.

The SiO_2 percentage of the pyroxenes from gabbros varies from 48.9 to 52.6 wt.%. The Al_2O_3 content ranges from 1.39 to 3.13 wt%. They are richer in TiO_2 (0.41-0.87 wt.%) than those from ultramafic rocks wherein it is

Table No. 3.5 Electronprobe Microanalysis Of Ca-rich Pyroxenes in Mafic and Ultramafic Rocks from Bondla

des.	B19A 1	B19A 2	B19A 3	B19A 4	B19A 5	BT1 6	BT1 7	BT1 8	BT1 9	B4 10	B4 11	B4 12	B4 13	GB1 14	GB1 15	GB1 16	GB1 17
O_2	53.87	53.52	53.68	53.27	53.21	53.67	53.25	54.41	55.56	55.08	54.89	53.94	53.49	52.28	49.02	48.97	50.38
O_2	0.22	0.20	0.24	0.25	0.23	0.21	0.43	0.20	0.30	0.01	0.02	0.04	0.05	0.41	0.59	0.65	0.61
$_2O_3$	2.18	2.20	2.22	2.24	2.22	1.97	2.10	1.60	1.67	0.16	0.18	0.74	0.63	2.37	1.22	1.39	2.29
$_2O_3$	1.00	0.98	0.99	0.94	0.97	0.74	0.84	0.66	0.77	0.01	0.07	0.01	0.01	0.03	0.01	0.01	0.01
$_2O_3$	----	----	----	----	----	0.0526	0.1075	----	----	----	----	0.0003	0.079	0.2263	0.0242	----	----
O	4.07	3.88	3.95	4.32	4.28	3.9626	4.1133	3.77	0.37	2.90	3.21	4.3398	4.4668	15.386	27.06	26.49	15.92
O	16.83	16.91	16.81	17.25	17.12	18.10	17.78	17.77	18.43	16.35	16.51	17.66	16.85	17.96	7.53	8.07	13.81
O	21.41	21.62	21.67	21.27	21.61	21.73	21.64	21.91	22.45	25.04	25.25	22.37	24.04	10.76	13.79	13.58	15.76
$_2O$	0.23	0.25	0.26	0.26	0.24	0.19	0.22	0.21	0.22	----	0.01	0.21	0.01	0.14	0.16	0.01	0.27
O	----	----	0.01	----	----	----	0.01	0.01	0.01	----	----	----	----	----	0.01	----	----
O	0.15	0.14	0.09	0.14	0.09	0.13	0.18	0.17	0.17	----	0.16	0.15	0.14	0.33	0.57	0.56	0.37

Cations recalculated on the basis of 6 oxygens

	B19A 1	B19A 2	B19A 3	B19A 4	B19A 5	BT1 6	BT1 7	BT1 8	BT1 9	B4 10	B4 11	B4 12	B4 13	GB1 14	GB1 15	GB1 16	GB1 17
	1.9581	1.9517	1.9532	1.9419	1.934	1.9384	1.9139	1.9623	1.9793	2.0119	1.9974	1.9767	1.9813	1.8904	1.9592	1.9453	1.9222
	0.0059	0.0052	0.0063	0.0068	0.0061	0.0056	0.0114	0.0052	0.0079	0.0002	0.0004	0.0008	0.0013	0.0111	0.0175	0.0194	0.0174
	0.0933	0.0945	0.0952	0.0962	0.0951	0.0838	0.0888	0.0680	0.07	0.0068	0.0076	0.0318	0.0301	0.1009	0.0571	0.0651	0.1030
	0.0287	0.0281	0.0285	0.027	0.0276	0.0211	0.0024	0.0187	0.0216	0.0003	0.0019	----	----	0.0006	0.0002	0.0002	0.0002
$^{+3}$	----	----	----	----	----	0.0013	0.0028	----	----	----	----	0.0022	0.0002	0.0061	0.0007	----	----
$^{+2}$	0.124	0.1187	0.1204	0.1321	0.1304	0.12	0.1239	0.1139	0.0219	0.0887	0.0978	0.1334	0.1387	0.4668	0.9047	0.8829	0.5096
	0.9149	0.9198	0.9147	0.9404	0.963	0.9777	1.0014	0.9584	0.9818	0.8931	0.8984	0.9676	0.9335	0.9712	0.4485	0.4793	0.7879
	0.8366	0.8475	0.8476	0.8335	0.8282	0.8437	0.8362	0.8494	0.8598	0.9832	0.9877	0.8812	0.9571	0.5818	0.5873	0.5914	0.6462
	0.0081	0.0175	0.0182	0.0182	0.0168	0.0132	0.0151	0.0145	0.015	----	0.0006	0.0148	0.0006	0.0098	0.0122	0.0007	0.02
	----	----	0.0004	----	----	----	0.0004	0.0004	0.0004	----	----	----	----	----	0.0004	----	----
	0.0046	0.0041	0.0026	0.0041	0.0048	0.0039	0.0054	0.005	0.0049	----	0.0048	0.0041	0.0042	0.01	0.0192	0.0186	0.0119
#	0.88	0.885	0.883	0.876	0.880	0.890	0.889	0.893	0.978	0.903	0.901	0.878	0.870	0.675	0.331	0.351	0.607

B19A - Peridotite BT1 - Troctolite B4 - Pyroxenite GB1 - Gabbro

Table No. 3.5 (continued)

Oxides	GB1 18	GB2 19	GB2 20	GB2 21	GB2 22	GB2 23	GB2 24	GB2 25	GD12 26	GD12 27	GD12 28	GD12 29	GD12 30	GS23 31	GS23 32	GS23 33	GS23 34	GS23 35	GS23 36
SiO_2	49.17	52.64	49.78	52.69	49.98	51.87	50.44	51.03	51.15	53.05	52.04	52.13	50.68	51.87	51.50	51.41	53.74	52.24	52.42
TiO_2	0.58	0.27	0.71	0.29	0.52	0.48	0.61	0.12	0.80	0.87	0.56	0.58	0.87	0.31	0.39	0.55	0.37	0.28	0.46
Al_2O_3	1.19	3.13	2.00	2.58	1.44	2.49	1.66	0.99	1.80	1.56	2.08	2.05	1.79	2.50	2.63	1.93	2.91	2.65	1.90
Cr_2O_3	----	0.18	----	0.32	0.03	----	----	----	0.02	0.03	0.17	0.04	----	0.17	0.10	0.06	----	0.13	0.08
Fe_2O_3	1.029	-----	0.0234	0.0281	0.0277	0.0419	0.0149	----	0.0466	----	0.2013	0.0141	----	0.098	0.07	0.043	----	----	0.0329
FeO	27.161	8.41	21.809	8.0238	25.315	12.512	23.096	26.37	17.578	22.88	11.938	13.327	17.09	7.4118	9.127	9.0747	14.74	7.56	8.7404
MgO	7.98	17.93	10.75	18.54	9.64	16.49	12.93	6.29	12.45	8.74	15.37	14.98	12.09	15.59	15.22	14.18	16.21	16.23	14.87
CaO	13.53	16.76	14.25	17.14	13.07	15.55	10.60	14.68	16.43	12.39	17.10	16.81	16.83	21.51	19.80	20.47	10.84	20.22	20.87
Na_2O	0.20	0.27	0.21	0.18	0.20	0.24	0.20	0.16	0.33	0.13	0.25	0.25	0.02	0.29	0.31	0.31	0.60	0.29	0.30
K_2O	----	----	0.01	----	----	----	----	0.02	0.01	0.05	----	----	----	----	0.01	----	0.17	----	----
MnO	0.52	0.20	0.40	0.15	0.52	0.29	0.41	0.30	0.36	0.26	0.27	0.29	0.32	0.21	0.24	0.26	0.38	0.20	0.30

Cations recalculated on the basis of 6 oxygens

Si	1.9523	1.9304	1.9352	1.9279	1.9511	1.9299	1.9474	2.0179	1.9372	2.0453	1.9408	1.9434	1.9412	1.9205	1.9233	1.9365	1.9847	1.9284	1.9467
Ti	0.0172	0.0072	0.0205	0.0079	0.015	0.0132	0.0176	0.0033	0.0226	0.0251	0.0155	0.0164	0.0249	0.0084	0.0108	0.0154	0.0102	0.0075	0.0127
Al	0.0555	0.1352	0.0914	0.1112	0.0661	0.1092	0.0753	0.046	0.0803	0.0709	0.0915	0.0901	0.0808	0.1091	0.1157	0.0856	0.1264	0.1153	0.083
Cr	----	0.005	----	0.0092	0.0007	----	----	----	0.0004	0.0002	0.0494	0.0011	----	0.0049	0.0029	0.0015	----	0.0037	0.0022
Fe^{+3}	0.0019	----	0.0004	0.0011	0.007	0.0011	0.0004	----	0.0011	----	0.0056	0.0004	----	0.0026	0.0018	0.0011	----	----	0.0008
Fe^{+2}	0.9030	0.2587	0.7102	0.2462	0.8293	0.3906	0.7483	0.8751	0.5586	0.7207	0.3735	0.4167	0.5492	0.2302	0.286	0.3152	0.4567	0.2341	0.2723
Mg	0.4683	0.9779	0.6238	1.0145	0.5626	0.9175	0.7464	0.372	0.705	0.5038	0.8573	0.8351	0.6925	0.8632	0.8499	0.7986	0.8952	0.896	0.8257
Ca	0.5775	0.6607	0.5943	0.6741	0.5485	0.622	0.4398	0.624	0.6689	0.5133	0.6854	0.6735	0.6929	0.8560	0.795	0.8289	0.4302	0.8022	0.8330
Na	0.0153	0.0192	0.0156	0.0127	0.015	0.0172	0.0149	0.0121	0.0242	0.0095	0.0174	0.0179	0.0013	0.0207	0.0225	0.0227	0.0429	0.0207	0.0214
K	----	----	0.0004	----	----	----	----	0.0009	0.0004	0.0023	----	----	----	----	0.0004	----	0.008	----	----
Mn	0.0174	0.0061	0.0131	0.0046	0.0171	0.0089	0.0132	0.01	0.0114	0.0083	0.0085	0.0089	0.0103	0.0064	0.0074	0.0081	0.0118	0.0062	0.0094
Mg #	0.341	0.790	0.467	0.804	0.404	0.701	0.499	0.298	0.557	0.411	0.696	0.667	0.557	0.789	0.748	0.717	0.662	0.792	0.752

GB2, GD12, GS23 - Gabbros

generally less than 0.2 wt.%. Cr_2O_3 is generally less than
0.2 wt.% and may rarely exceed this value. As against
these, the pyroxenes from peridotite and troctolite
(B19A, BT1) contain between 0.6 and 1.0 wt.% Cr_2O_3.

The pyroxenes from ultramafic rocks generally
contain less than 0.2 wt.% MnO, whereas, those in gabbro-
ic rocks have slightly higher values.

Compositionally, the ultramafic rock pyroxenes
vary between $Ca_{43.0}Mg_{50.1}Fe_{6.7}$ to $Ca_{50.0}Mg_{45.4}Fe_{4.5}$.
Their Mg # varies between 0.87 to 0.97. On an average the
Mg # is 0.88 which is shared by most grains of peridotite,
pyroxenite and troctolite. In comparison with these, the
pyroxenes from gabbroic rocks have composition varying
between $Ca_{28.8}Mg_{48.0}Fe_{23.1}$ and $Ca_{43.8}Mg_{44.1}Fe_{11.9}$. The
Mg # shows a very wide range from 0.33 to 0.79. The
intercumulus pyroxene has low Mg #s (0.33) and the compo-
sition represented by $Ca_{30.2}Mg_{23.1}Fe_{46.6}$.

The pyroxenes from gabbros show strong composition-
al zoning. The cumulus pyroxene cores from lower gabbros
(GB2) have Mg # varying between 0.70 and 0.79 and it

70

decreases towards the rims to 0.40 to 0.46.

The intercumulus pyroxene has core Mg # 0.5 and rim Mg # 0.4. In the overlying gabbros (GD12) the cumulus pyroxene has core Mg # 0.55 and rim Mg # 0.41.

In the pyroxene quadrilateral majority of Ca-rich pyroxenes can be classified as augites and few as sub-calcic augites. The ones from peridotite (B19A) and troc-tolite (BT1) co-exist with enstatite as shown by tie-lines (Fig.3.11a). The ones from gabbro (GS23) occur alongside inverted pigeonites and those from GB1 (ferro -augites) are found to co-exist with ferrian pigeonite. The evolu-tionary trend shown by the pyroxenes is depicted in Fig.3.11a.

Plagioclase

Plagioclase is the most dominant constituent in the gabbroic rocks making up between 41 and 66% of the modal composition. It occurs both as cumulus and intercumulus phases. The cumulus-crystals are subhedral, lath shaped and vary in length between 0.19 and 4 mm and measure 0.6

to 1.6 mm across. The intercumulus plagioclase is anhe-
dral and measure between 0.5 and 2 mm. along longer dimen-
sion and between 0.2 and 0.8 mm across. The ones from
troctolite are unzoned and form adcumulates whereas,
those from the other gabbroic rocks show marginal zoning
forming ortho and meso cumulates.

Cumulus plagioclase makes its first appearance in
the troctolite. The An content has a very restricted
range from $An_{87.5}$-$An_{87.9}$ (Table No.3.6). In the gabbros
which are stratigraphically higher eg. GB1 the cumulus
plagioclase varies in composition from $An_{84.0}$ to $An_{60.0}$.
The intercumulus plagioclase shows a much wider variation
from $An_{46.0}$ to $An_{15.0}$. Still higher in the section eg.
GS23 the An content of cumulus plagioclase is between
$An_{60.0}$ and $An_{78.0}$. The intercumulus plagioclase is more
sodic with An varying between $An_{32.0}$ and $An_{55.0}$. The
compositional variation shown by all feldspar analyses
from Bondla mafic rocks is depicted in Fig.3.11b.

Table No.3.6 Electronprobe Microanalysis of Plagioclase in Mafic Rocks from Bondla

es	BT1 1	BT1 2	BT1 3	BT1 4	GB1 5	GB1 6	GB1 7	GB1 8	GB1 9	GB1 10	GB2 11	GB2 12	GB2 13	GB2 14	GB2 15	GB2 16	GB2 17
)	46.78	46.81	46.98	46.86	55.73	65.82	47.44	64.31	53.40	57.72	54.49	59.24	54.63	57.34	56.06	56.20	59.97
)	0.04	0.02	0.01	0.02	0.05	----	----	0.02	0.06	0.06	0.03	0.04	0.07	0.05	0.05	0.04	----
)3	33.58	33.54	33.21	33.40	27.29	21.67	32.95	22.90	28.29	26.28	28.06	25.58	27.47	26.26	26.78	27.89	22.76
	0.39	0.34	0.41	0.40	0.80	0.10	0.40	0.09	0.69	0.64	0.80	0.66	0.78	0.64	0.83	0.80	----
	0.07	0.10	0.09	0.08	0.17	0.01	0.13	0.02	0.10	0.05	0.12	0.01	0.11	0.04	0.08	0.11	0.06
	17.85	17.66	17.63	17.54	11.39	2.44	17.21	3.00	12.19	9.52	12.15	8.27	11.34	9.29	10.67	11.50	4.51
0	1.35	1.38	1.36	1.35	4.50	9.62	1.77	8.97	4.19	5.72	4.47	6.28	4.76	5.79	5.24	4.95	8.09
	0.01	0.02	0.03	0.02	0.30	0.30	0.06	0.67	0.26	0.38	0.21	0.41	0.24	0.33	0.34	0.31	4.51
	0.02	----	----	----	0.01	0.02	0.02	----	0.04	0.01	0.01	0.05	0.01	0.06	0.02	0.11	0.06

Cations recalculated on the basis of 8 oxygens

	BT1 1	BT1 2	BT1 3	BT1 4	GB1 5	GB1 6	GB1 7	GB1 8	GB1 9	GB1 10	GB2 11	GB2 12	GB2 13	GB2 14	GB2 15	GB2 16	GB2 17
	2.1506	2.1541	2.1658	2.1608	2.5024	2.8889	2.1791	2.8323	2.4402	2.5872	2.4617	2.6378	2.4863	2.5815	2.5307	2.4969	2.7265
	0.0011	0.0005	0.0002	0.0005	0.0016	----	----	0.0005	0.0019	0.0018	0.0008	0.001	0.0021	0.0016	0.0016	0.0008	----
	1.8218	1.8213	1.8067	1.8174	1.4589	1.1222	1.786	1.19	1.5256	1.3898	1.4959	1.3438	1.4752	1.3948	1.4265	1.462	1.2211
2	0.0149	0.0130	0.0158	0.0152	0.0303	0.0034	0.0152	0.0031	0.0264	0.024	0.0302	0.0244	0.0296	0.0241	0.0313	0.0294	----
	0.0047	0.0066	0.0061	0.0052	0.0114	0.0005	0.0088	0.001	0.0066	0.0032	0.0079	0.0005	0.0074	0.0024	0.0051	0.0065	0.0038
	0.8822	0.8736	0.8737	0.8694	0.5546	0.1151	0.8498	0.1418	0.5988	0.5486	0.5901	0.3957	0.5546	0.4495	0.5178	0.5491	0.2204
	0.1206	0.1234	0.1217	0.1209	0.3964	0.8213	0.1578	0.7682	0.3723	0.4986	0.3925	0.5437	0.4212	0.5068	0.46	0.427	0.7152
	0.0005	0.0011	0.0016	0.0011	0.0084	0.0166	0.0033	0.0377	0.0151	0.0216	0.0119	0.0233	0.0137	0.019	0.0196	0.0172	0.2623
	0.0005	----	----	----	0.0002	0.0005	0.0077	----	0.0013	0.0002	0.0002	0.0018	0.0002	0.0021	0.0005	0.0038	0.0021
	87.92	87.52	87.63	87.69	57.80	12.07	84.06	14.96	60.71	46.85	59.33	41.10	56.04	46.08	51.91	55.28	18.39

BT1 - Troctolite   GB1 & GB2 - Gabbros

Table No. 3.6 (continued)

ides	GD12 1	GD12 2	GD12 3	GD12 4	GD12 5	GD12 6	GS23 7	GS23 8	GS23 9	GS23 10	GS23 11	GS23 12	GS23 13	GS23 14
iO_2	58.13	58.28	55.01	62.12	57.35	62.72	56.96	51.87	52.04	54.77	53.53	52.84	54.42	60.89
iO_2	0.09	0.04	0.07	0.06	0.09	0.06	0.04	0.03	0.06	0.06	0.05	0.05	0.04	0.01
l_2O_3	25.65	25.26	27.53	22.92	26.15	22.90	26.76	30.24	29.89	28.39	28.73	29.32	28.19	24.34
$:O$	0.56	0.61	0.61	0.42	0.50	0.44	0.40	0.46	0.49	0.31	0.58	0.43	0.28	0.31
gO	0.07	0.03	0.08	0.02	0.08	0.01	0.02	0.04	0.03	0.02	0.05	0.03	0.03	0.02
aO	8.91	8.09	11.26	5.25	9.44	5.17	9.53	13.53	13.34	11.13	12.44	12.89	11.20	6.58
l_2O	5.99	6.29	4.85	7.81	5.59	8.07	5.56	3.57	3.85	4.91	4.29	3.91	4.79	7.33
$_2O$	0.57	0.65	0.35	0.72	0.47	0.54	0.62	0.24	0.27	0.38	0.30	0.31	0.32	0.47
iO	0.01	----	----	----	0.05	0.02	0.08	----	----	----	----	0.01	0.01	0.02

Cations recalculated on the basis of 8 oxygens

	GD12 1	GD12 2	GD12 3	GD12 4	GD12 5	GD12 6	GS23 7	GS23 8	GS23 9	GS23 10	GS23 11	GS23 12	GS23 13	GS23 14
i	2.6127	2.6326	1.8697	2.7768	2.5835	2.7844	2.5627	2.3587	2.3677	2.4733	2.4295	2.4256	2.474	2.7111
i	0.0029	0.001	0.0016	0.0018	0.0029	0.0018	0.001	0.0008	0.0019	0.0019	0.0016	0.0016	0.001	0.0002
l	1.3597	1.3464	1.1041	1.209	1.3901	1.1996	1.4205	1.6226	1.6047	1.5128	1.5386	1.5882	1.5122	1.2789
e^{+2}	0.0208	0.0228	0.0172	0.0156	0.0187	0.0163	0.0149	0.0175	0.0186	0.0117	0.0218	0.0163	0.0104	0.0115
g	0.0046	0.0019	0.0038	0.001	0.0051	0.0005	0.001	0.0024	0.0019	0.001	0.0032	0.0019	0.0019	0.001
a	0.4249	0.3927	0.4111	0.252	0.4572	0.2465	0.4609	0.6614	0.6524	0.5403	0.6067	0.6361	0.5472	0.3149
a	0.5236	0.5524	0.3205	0.679	0.2447	0.6968	0.4864	0.3156	0.1701	0.4311	0.3785	0.349	0.4235	0.6347
	0.0327	0.0375	0.0151	0.0204	0.0133	0.0305	0.0355	0.0137	0.0104	0.0217	0.0172	0.0179	0.0183	0.0265
n	0.0002	----	----	----	0.0019	0.0005	0.0029	----	----	----	----	0.0005	0.0002	0.0005
n	43.30	39.96	55.06	26.48	63.92	25.31	46.89	66.76	78.32	54.40	60.52	63.41	55.32	32.26

GD12 & GS23 — Gabbro

CHAPTER IV

CHROMITE MINERALISATION

Chapter IV

Chromite Mineralisation

The chapter deals with field characters, structures and textures, ore petrography and mineral chemistry of chromites associated with the mafic- ultramafic rocks. On the basis of these characteristics, the chromites have been classified.

The chromite ores are confined to the Lower Zone which consists of dunite-peridotite associatiion (olivine-chromite cumulate and olivine-pyroxene- chromite). Mineralisation is well exposed at two localities namely Nanus - NW of Bondla and at Bondla, mainly between Bondla and Poikul. Chromite at Nanus occurs as thin layers 1-3 cm thick which alternate with layers of dunite. The latter vary in thickness from 4-10 cm. The chromite layers strike N40o and dip 30o-35o towards N130o. The peridotites are sheared and fractured. The fractures trend (i) N65o and dip 50o towards N335o and (ii) N110o and dip 25otowards N350o. Along these fractures, the layered chromites are remobilised and the layers appear to form a

criss-cross pattern of veins. The original layering is still discernible at places. Along the shear fractures fibrous actinolite and chlorite have developed perpendicular to the layering. These veins vary in width from 2.0 cm to 1.0 m.

The chromites at Bondla can be traced intermittently over a distance of about one kilometre. In the lower part of the peridotites they occur as thin layers 1 cm to approximately 10 cm thick. Such layers alternate with thicker layers of peridotite. The chromite layers invariably exhibit a sharp lower contact with a gradational top. Individual layers at places pinch out along the strike. At places, the layers bifurcate, giving the appearance of veins. Such a pattern of veins could be the result of `unconformities' formed during deposition (Wager, 1968). Stratigraphically higher in the section, the chromite layers become thicker. In the vicinity of Poikul, a massive chromitite layer is exposed which extends over an outcrop width of more than 300 m. The layer is of chromitite and consists of 75% fine grained chromite with about 25% silicates. The chromitite grades into a chromite-olivine cumulate with progressive increase

of olivine. In some chromite-olivine layers the chromite to silicate ratio is low, thus making the chromite appear as dissemination in silicates.

Ore Petrography

The section on ore petrography describes the structures and textures exhibited by chromites in hand specimen and in thin - and polished - sections.

Structures of Ores

The term structure is here meant to include the forms and shapes assumed by ore minerals and their aggregates as seen by unaided eye in hand specimen.

Some of the important structures observed include layered and disseminated structure, occluded-silicate structure, chromite-net (reticulate) structure, compact and massive ores and schlieren of chromite.

Layered and Disseminated Structure

The term `layer' is here used in preference to `band' because the former has a genetic connotation. The layered structure is made up of alternating dark and light coloured layers. The dark layers consist of chromite. These alternate with light coloured layers made up of serpentinised olivine. The layers are repetitive in nature. Individual chromite layers vary in thickness from 1 cm to as much as 3 cm. Invariably, the olivine-rich layers are many times thicker than the chromite layers. At places, the chromite layers pinch out laterally. Individual layers may be composed entirely of chromite giving rise to massive chromite layers. Invariably, however, little interstitial silicate is always present. The chromite layers exhibit a sharp lower contact and a gradational upper contact with the olivine-rich layers. At places, chromite is interstitial in olivine-rich layers giving rise to disseminated structure.

Occluded Silicate Structure

The structure is exhibited by massive ore layers

which contain little silicates in them. It is observed that olivine either singly or as an aggregate of crystals is enclosed within chromite forming spherical, rounded or elliptical islands of olivine in chromite. At places, olivine is elongated forming lenticles and streaks within chromite.

Chromite-Net (Reticulate) Structure

The structure is generally shown by chromite layers which contain considerable proportion of interstitial silicates. In this case subhedral grains or grain aggregates of chromite have interstitial olivine so that chromite forms a network with olivine grains in between (Plate X Photo 1).

Massive Structure

Massive structure is shown by thicker layers of chromite. The layer in this case is made up of fine grained chromite with very little interstitial silicates. Majority of the chromite grains are subhedral and tightly packed.

Schlieren of Chromite

The thin veinlets of chromite 1-2 cm thick are seen at places at an angle to the general layering of the rock. Some of them are a couple of cm long with tapering ends. Such ore forms are included under streaks and are also referred to as schlieren.

Chromite Petrography

Chromite has been studied both in transmitted light and incident light. In microsections the chromite from chromitite is typically dark brown in colour. Individual grains are subhedral to anhedral. The grains join each other and form aggregates with irregular, cuniform interstices in between filled by serpentinised olivine (Plate X Photo 2) forming myrmekitic intergrowth with gangue. Chromites from peridotite are dark brown in colour, typically subhedral and join each other forming chains of chromite.

Under incident light, the chromite is greyish-white in colour and has pitted surface (Plate XI Photo 1).

The reflectivity of a grain in general is moderate. Between cross nicols it is faintly anisotropic. However, careful examination shows that the borders of grains have higher reflectivity than the central part. Such high reflecting borders are made up of ferrit-chromit (Spangenberg, 1943). It is the result of alteration of chromite during which magnetite replaces the former. Well developed grains of chromite show exsolutions of ilmenite parallel to (111) (Plate XI Photo 2). Similar exsolutions have been described from certain Fe-rich chromites from Bushveld. Exsolution bodies of ilmenites in Fe-poor chromites have also been described from the Bastetal and from the Monche Tundra, Cola (Ramdohr, 1980). In oil, the chromite shows brown- internal reflection. At places, especially along thin layers and veins, it is replaced by fibrous chlorite which has developed perpendicular to the layer or vein in question (Plate XII Photo 1).

Textures of Chromites

Under textures, are described, the inter- relationship between chromite and silicate minerals as seen under the microscope. Some of the important textures observed

are layered texture, micro-reticulate texture, chain texture, occluded silicate texture, disseminated texture and myrmekitic texture.

Layered Texture

The most commonly observed texture is layered texture. It is made up of alternate layers of chromite and serpentinised olivine. The chromites are subhedral and are arranged into layers that alternate with olivine rich layers. In chromite layers serpentinised olivine occurs interstitially.

Micro-reticulate Texture

The texture is commonly exhibited by layered chromites. In this case subhedral to rounded grains of chromite form a framework. The interstices between chromites are occupied by olivine giving the appearance of a chromite network. At places, rounded, elliptical or irregular islands of serpentinised olivine are found within a ring of chromite grains (Plate XII Photo 2). Such a texture is referred to as ring texture (Chang Chung, 1969).

80

Chain Texture

The texture is common in layered chromites and chromite veins. Polygonal crystals of chromite join each other to form continuous chains.

Occluded Silicate Texture

The texture is exhibited both by massive chromites and layered chromites. It is made up of rounded, elliptical or irregular grains of silicates that are poikilitically enclosed within chromite (Plate   XII Photo 2).

Disseminated Texture

The texture is exhibited by chromites from olivine-rich layers. Euhedral to subhedral layers of chromite occur in between olivine crystals.

Myrmekitic Texture

The texture is typically observed in massive chromite ores. Elongated or cuniform silicates are surround-

ed by anhedral aggregates of chromites. Such a texture is described as myrmekitic texture by Ramdohr (1980). The silicates are poikilitically enclosed in a cumulate of chromite forming a heteradcumulate.

Mineral Chemistry

Mineral chemistry of chromite has been investigated with an electronprobe microanalyser. Representative polished thin sections of chromite from chromitite, peridotite and troctolite were analysed for major element composition. Three samples of chromite bearing rocks were selected for study. A minimum of three spot analyses were carried out per grain and average composition was determined. At least four grains were analysed in each sample to know the variation amongst the grains. The chromites were analysed from core to rim to know the variation in composition within a grain. In all fourteen micro-chemical analyses are presented in Table No. 4.1. Total iron was determined as FeO. Fe_2O_3 was calculated from total FeO on the basis of spinel stoichiometry. The major element oxide percentages were recalculated to cations per formula unit for 24 cations.

Table No.4.1 Electronprobe Microanalysis of Chromites from Bondla

Oxides	B19A 1	B19A 2	B19A 3	B19A 4	B15 5	B15 6	B15 7	B15 8	B15 9	B15 10	BT1 11	BT1 12	BT1 13	BT1 14
TiO_2	0.72	0.72	0.75	0.78	0.81	0.51	0.70	0.72	0.71	0.70	3.35	3.41	3.37	3.45
Al_2O_3	17.02	17.30	17.15	17.17	7.63	1.58	7.97	1.36	7.01	1.38	13.26	13.12	13.25	12.87
Cr_2O_3	45.17	45.26	45.19	45.19	51.65	54.92	51.25	52.05	51.49	54.25	41.10	38.16	39.59	38.01
Fe_2O_3	8.99	8.54	8.99	8.54	8.99	12.45	8.99	15.29	8.99	13.04	14.39	17.79	16.19	17.79
FeO	17.32	17.35	17.12	17.46	27.10	27.09	27.33	27.20	28.21	27.45	20.10	19.77	19.20	20.74
MgO	10.41	10.51	10.46	10.52	1.99	1.43	1.97	1.45	1.85	1.09	7.25	7.21	7.89	6.66
MnO	0.33	0.28	0.30	0.30	1.78	1.98	1.75	1.91	1.70	2.06	0.51	0.50	0.47	0.44

Cations recalculated on the basis of 32 oxygens

	B19A 1	B19A 2	B19A 3	B19A 4	B15 5	B15 6	B15 7	B15 8	B15 9	B15 10	BT1 11	BT1 12	BT1 13	BT1 14
Ti	0.1367	0.1365	0.1426	0.1489	0.1715	0.1109	0.1476	0.1571	0.1504	0.1536	0.6618	0.6861	0.6627	0.6852
Al	5.1176	5.1931	5.1489	5.1595	2.534	0.5444	2.6444	0.4696	2.3444	0.4769	4.1017	4.144	4.0901	4.0127
Cr	9.1318	9.1386	9.1226	9.1305	11.542	12.729	11.443	12.090	11.5838	12.6092	8.5617	7.7134	8.2196	7.9681
Fe^{+3}	1.7304	1.6420	1.7275	1.6430	1.9124	2.6792	1.9111	3.3809	1.9255	2.8846	2.8533	3.4547	3.2001	3.5521
Fe^{+2}	3.7037	3.7061	3.6561	3.7314	6.4064	6.6409	6.4566	6.6842	6.7136	6.7497	4.4304	4.4411	4.2163	4.5991
Mg	3.9665	3.9992	3.9798	4.0063	0.8373	0.6235	0.8291	0.6338	0.7831	0.4769	2.847	2.8864	3.0865	2.631
Mn	0.0706	0.0597	0.0644	0.0644	0.4280	0.4914	0.4187	0.4572	0.4086	0.5122	0.1124	0.1130	0.1041	0.0988
Cr #	0.64	0.637	0.639	0.638	0.819	0.958	0.812	0.962	0.831	0.963	0.676	0.69	0.667	0.665
Fe^{+3} #	0.108	0.102	0.107	0.103	0.119	0.167	0.119	0.212	0.121	0.18	0.183	0.225	0.206	0.228
Al #	0.320	0.325	0.321	0.323	0.158	0.034	0.165	0.029	0.147	0.0298	0.264	0.27	0.263	0.258
Mg #	0.517	0.519	0.521	0.517	0.115	0.085	0.113	0.086	0.104	0.065	0.391	0.393	0.422	0.363

B19A – Peridotite   B15 – Chromitite   BT1 – Troctolite

From the microprobe chemical data (Table No.4.1) it is seen that majority of the grains show chemical zoning. There is an increase in Cr_2O_3 from core to rim as seen from analysis 5-10 (Table No. 4.1). The Cr # (Cr/Cr+Al) varies between 0.81 to 0.83 for the core and it is between 0.95 and 0.96 for the rims. Fe^{+3} # [Fe^{+3}/Cr+Al+Fe^{+3}] also shows an increase from core to rim whereas, Mg # [Mg/Mg+Fe^{+2}] shows a progressive decrease rimward. This compositional variation can be attributed to secondary alteration and development of ferrit-chromit (Spangenberg, 1943) along the borders of chromite crystals. The chromites from the chromitites in general (chromite cumulate - B15) are very rich in Cr_2O_3 and have high Cr # [Cr/(Cr+Al)]. Cr_2O_3 varies between 54-51 wt.% and Cr # between 0.81 and 0.96. Cr_2O_3 content (45 wt.%) and Cr # (0.63-0.64) decrease in peridotite chromite (olivine-chromite cumulate - B19A). Cr_2O_3 decreases further to about 39 wt.% with Cr # 0.66 in disseminated chromite from troctolite (BT1). Thus overall there is a progressive decrease in Cr_2O_3 from chromitite chromite (B15) to peridotite chromite (B19A) to troctolite chromite (BT1). It may be noted though that the composition of accessory chromites (from BT1) may show considerable

variation due to sub-solidus re-equilibration with associated phases (Irvine, 1967; Dickey and Yoder, 1972) and due to alteration (Jan et al., 1984; 1985). The accessory chromites are impoverished in Mg # [$Mg/(Mg+Fe^{+2})$] and Cr # compared to unaltered chromites, possibly due to substantial Mg-Fe exchange with silicates-olivines and pyroxenes during sub-solidus re-equilibration. The altered chromites generally show enrichment in Cr and Fe^{+2} compared to unaltered parts of the grain. Cr_2O_3 content varies with modal mineralogy. Higher wt.% Cr_2O_3 is observed with increasing modal percentage of chromite. Such an increase is common (Cameron, 1975; Wilson, 1982).

Cr_2O_3 and Al_2O_3 show an inverse relationship. Total Fe (as FeO) in chromites is very high varying between 24 and 40 wt.%. Cr_2O_3 exhibits a negative correlation with $FeO(t)$ within samples specially of chromitites. The latter is almost constant within a sample whereas, amongst samples it shows considerable variation between 24 and 40 wt.%. A typical feature of chromites from chromitite (B15) is their high Cr_2O_3 which is more than 51 wt.% and more than 35 wt.% $FeO(t)$. Whereas, in peridotite chromites (B19A) Cr_2O_3 decreases to about 45 wt.% and FeO

84

to 25 wt.%. This behaviour of Cr_2O_3 and FeO is character-
istic of layered chromites.

In general TiO_2 in all samples is more than 0.5
wt.% - a feature typical of stratiform chromites. Dickey
(1975) suggests 0.3 wt.% TiO_2 as the dividing line between
podiform and stratiform chromites. The TiO_2 in accessory
chromites (BT1) in particular is much higher, more than
3.0 wt.%. Herbert (1982) showed that in cumulate rocks,
TiO_2 varies from 0.1 to 2.0 wt.%. This is so because of
geochemical behaviour of Ti^{+4} which is enriched in the
melt relative to solid phases during crystallization
(Burns, 1973). Cameron (1979) reported 0.3-2.5 wt.% TiO_2
in chromites from Eastern Bushveld. Wilson (1982) noted
0.23-2.24 wt.% TiO_2 in the chromites from Great Dyke.
Chromites from other layered - and SE Alaskan-type com-
plexes generally contain more than 0.3 wt.% TiO_2 (Dickey,
1975; Bird and Clark, 1976). Evans and Wright (1972) and
Hill and Roeder (1974) showed that in more fractionated
basalts the chrome-spinels are richer in TiO_2. TiO_2 from
Bondla chromites do not show any significant correlation
with any of the major elements (Thayer 1964; Dickey,1975;
Greenbaum; 1977).

All chromite analyses contains very low wt.% MgO unlike podiform chromites. Similarly they contain higher wt.% Al_2O_3 over MgO unlike the podiform chromites which show a reverse relationship. The (Cr+Al) variation in chromites is very small (11.5-14.5). The Cr/Al ratio however, shows a wide variation from 1.5 to 25 which according to Dickey (1975) is the result of either bulk chemistry or temperature of crystallisation. A positive correlation is observed between Cr/(Cr+ Al) and Fe^{+2}/(Mg +Fe^{+2}). The Mg # shows a much broader range. It varies from 0.06 (in chromitite chromite - B15) to 0.52 (in peridotite chromite - B19A). The variation in the oxidation ratio [$2Fe_2O_3$/($2Fe_2O_3$+Feo)] is very small (0.39-1.11). The Fe^{+2}/Mg ratios are higher and have a broad range from 0.9 to 14 (in comparison with podiform chromites) which according to Dickey (1975) is indicative of fractional crystallization.

The MnO content of the chromites show a positive correlation with FeO. It is lower in peridotite chromites (about 0.3 wt%) and it increases in chromitite chromites (more than 1.7 wt %). The chromites from chromitite and peridotite are more ferriferous and contain more than 16

wt.% total iron (FeO) when Cr_2O_3 percentage is about 45 wt.% - a feature typically observed in some of the stratiform chromites from Bushveld complex. Various mechanisms have been suggested for this variation: (i) reaction with the magma (Henderson, 1975), (ii) post cumulus changes under variable oxygen fugacity (Cameron, 1975), (iii) exchange of Mg-Fe with the silicate minerals during sub-solidus re-equilibration (Irvine, 1967), (iv) alteration attendant to changing fo_2 and fH_2O during chloritization and serpentinization (Ahmed and Hall, 1981; Jan et al., 1985) and (v) increase in Fe^{+2} during metamorphism (Evans and Frost, 1974; Bliss and MacLean, 1975; Hoffman and Walker, 1978).

Cr # exhibits a reciprocal behaviour with Al # $[Al/(Al+Cr+Fe^{+3})]$ implying that Cr is preferentially incorporated in Al-spinel lattice. A comparison of this relationship with Fe^{+3} # $[Fe^{+3}/(Cr+Al+Fe^{+3})]$ indicates that Al is incorporated preferentially into the chromite lattice and that the gradual upward increase in the Fe^{+3} content (increasing Fe^{+3} from peridotite chromite upwards in the section) seems to be at the expense of both Al and Cr. The chromites from the chromitite (B15) and perido-

87

tite (B19A) have Fe^{+3} # in the range of 0.10- 0.18.
These values are higher than those observed in podiform
chromites (Jan and Windley, 1990). The accessory chro-
mites (BT1) show still higher values. Jan and Windley
(1990) suggest that ferric iron shows a considerable
increase in the altered and/or ∧ga-equilibrated grains.
Several workers have also shown that composition and
stability of chrome-spinels depend not only on tempera-
ture, pressure and bulk chemistry but also depends on
oxygen fugacity (fo_2) (Rivalenti et al., 1981). With
increasing fo_2 chrome-spinel becomes enriched in Fe^{+3} and
impoverished in Mg.

The Mg # of accessory chromites (BT1) varies
sympathetically with Mg # of co-existing olivine and Ca
-poor pyroxenes. A slight decrease in Mg # (except for one
analysis) is shown by accessory chromites. The associated
Ca-poor pyroxenes also show a slight decrease whereas,
the olivines have almost constant composition. The fluc-
tuations in these ratios may be affected by several fac-
tors including changing temperature and fO_2 conditions
with differentiation. Fisk and Bence (1980) ascribed the
decrease of Mg # in chromites to decreasing temperature.

The decrease in Mg # observed in the present case may probably reflect a decrease in Mg content in the melt due to crystallization of Mg rich silicates, however, in this case the decrease could be due to loss of Mg and enrichment of Fe^{+3} during metamorphic alteration and serpentinisation (Stowe, 1994).

In order to bring out the characteristic features of the chromites, the chemical data have been plotted in different variation diagrams. In the $Cr-Al-F^{+3}+2Ti$ ternary diagram (Irvine, 1967; Dickey, 1975; Bird and Clark, 1976; Eales and Marsh, 1983). The chromites from peridotite (B19A) occupy the overlapping fields of residual peridotites (ophiolite peridotites) and stratiform chromites. The accessory chromites from troctolite (BT1) occupy overlapping fields of stratiform -and SE Alaskan-type complexes. The chromitite chromites (B15) however, due to their high Cr and low Al content plot far removed from fields normally occupied by chromites from the three main type of complexes - namely, podiform -, stratiform - and SE Alaskan-type (Fig. 4.1a).
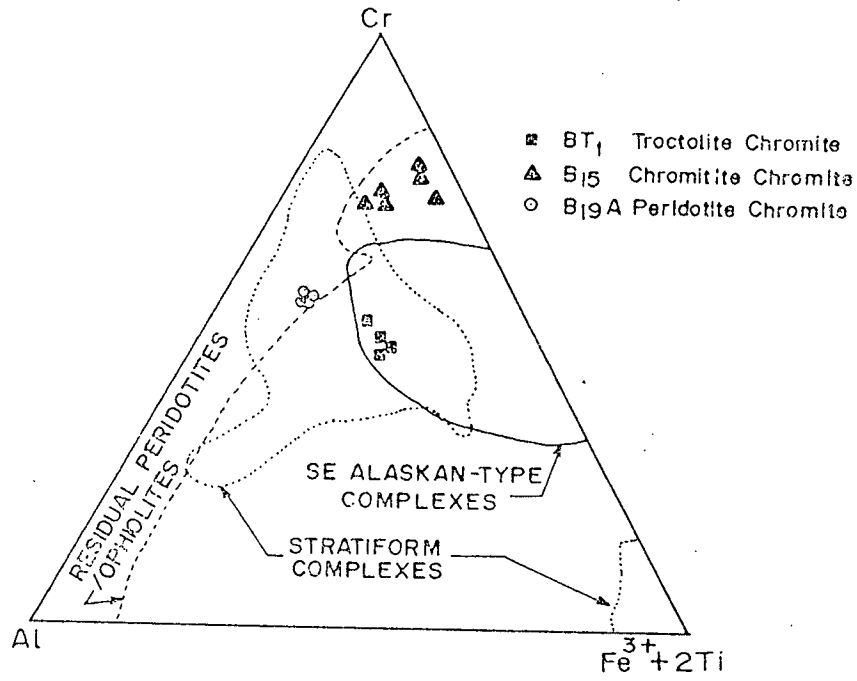
Fig.4.1a Cr-(Fe3++2Ti)-Al plot for chromites from Bondla
[based on Irvine (1967), Dickey (1975), Bird and
Clark (1976) and Eales and Marsh (1988)].
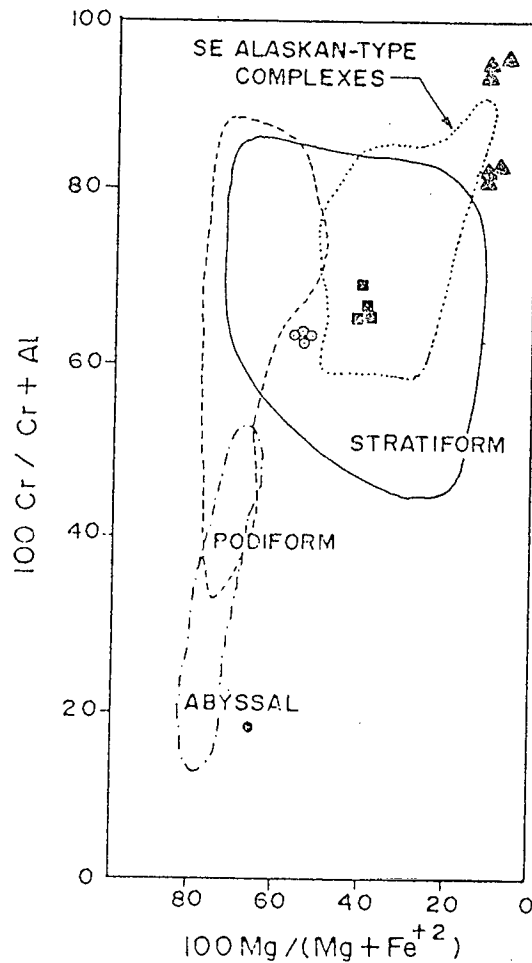
Fig.4.1b Mg # vs Cr # plot for chromites from Bondla.
[based on Irvine (1967), Leblanc et al., (1980).
Dick and Bullen (1984)].

In the Mg # vs Cr # face of the spinel prism
(Irvine, 1967; Leblanc et al., 1980) the peridotite
chromites (B19A) and the accessory chromites (BT1) strad-
dle the fields of stratiform and SE Alaskan-type complex-
es, whereas, the chromitite chromites (B15) plot outside
these fields due to their high Cr # and low Mg # (Fig.
4.1b). Such chromites have been reported from Kenticha
Hill (Bonavia, et al., 1993) and from the ultramafic
rocks of the Jijal complex, NW Pakistan (Jan and Windley,
1990). However, the behaviour of Mg # is opposite to that
shown by Jijal chromites. The chromites from chromitite
(B15) have low Mg # than the chromites from peridotite
(B19A) and troctolite (BT1).

The variation in Cr # are similar to $Cr/(Fe^{+2}+Fe^{+3})$
ratio which largely depends on the availability of
Cr^{+3} in the magma. Fisk and Bence (1980) demonstrated that
Cr # of chromite co-precipitating with olivine decreases
with falling temperature and that this trend may be relat-
ed to a decrease in Cr^{+3} in the magma with continued
spinel crystallisation. The Cr # of Bondla chromites
increases from peridotite chromites (B19A) to chromitite
chromites (B15) and then decreases further upwards. This

90

could be related to enrichment of Cr^{+3} in the magma brought about by replenishment in the magma chamber.

In the Mg # vs Fe^{+3} # face of the spinel prism, the peridotite chromites (B19A) plot in the field of stratiform chromites, the accessory chromites (BT1) occupy the overlapping fields of stratiform - and SE Alaskan-type complexes and chromitite chromites (B15) due to their low Mg # plot outside these fields. The perido-tite chromites (B19A) have low Fe^{+3} # (about 0.10), the accessory chromites (BT1) have between 0.18- 0.22 where-as, the chromitite chromites (B15) show Fe^{+3} # varying between 0.12-0.21. Fe^{+3} # of chromitites varies inversely with Mg #. Such a relationship could be ascribed to a drop in temperature at constant fo_2. Overall increase in Fe^{+3} content of the spinels from the chromitite layer upwards could be caused by gradual depletion of chromium in the crystallizing magma (Fig.4.2a).

A plot of Cr_2O_3 vs FeO + Fe_2O_3 is depicted in Fig.4.2b. In this diagram the peridotite (B19A) and accessory chromites (BT1) plot in the field of stratiform chromites. The chromitite chromites (B15), however, plot

91
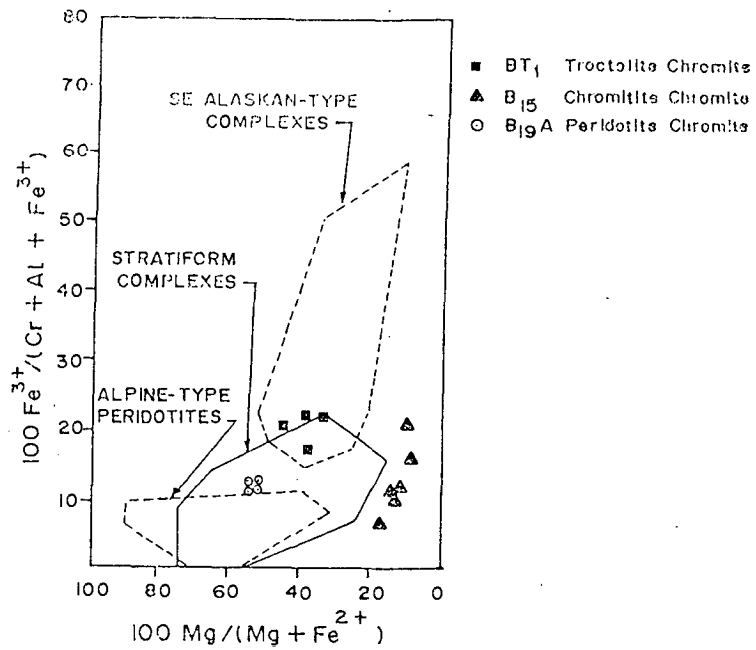
Fig.4.2a   Fe3+ # vs Mg # plot of chromites from Bondla
           [based on Irvine (1967) and Dick and Bullen (1984)].
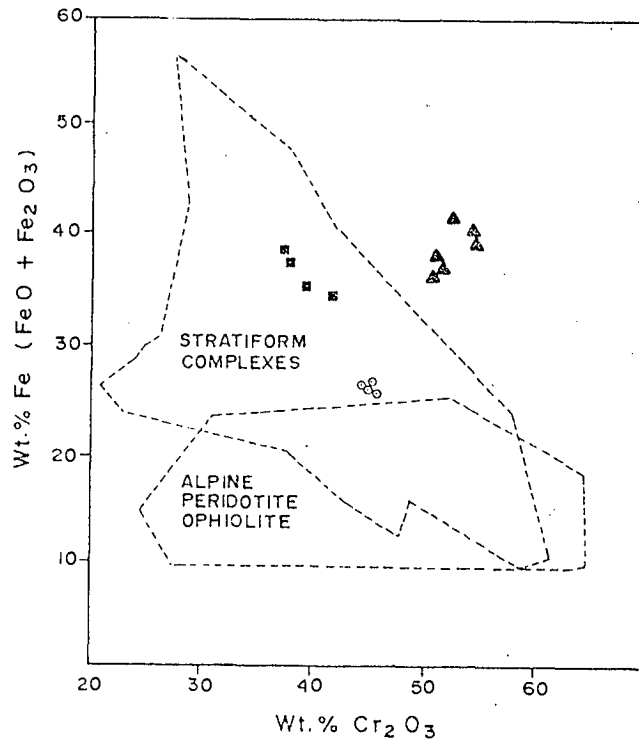
Fig.4.2b   FeO wt.% vs Cr2O3 wt.% plot for chromites
           from Bondla [based on Thayer (1970), Cameron (1975),
           Henderson (1975), Wilson (1982), Hatton and Gruene-
           waldt (1987), Agata (1988), Bilgrami (1969), Rodg-
           ers (1973), Greenbaum (1977), Ahmed (1984), Jan et
           al., (1984b;1985), Auge (1987), Malpas and Robinson
           (1987) and Rammlmair et al., (1987).

outside the field of stratiform chromites due to their higher Cr_2O_3 and $FeO_x(t)$.

In the TiO_2 vs Cr_2O_3 variation diagram (Fig.4.3a) the peridotite chromites (B19A) occupy the field of oceanic cumulates near the boundary of the field of SE Alaskan-type complexes. The accessory chromites (BT1) and the chromitite chromites (B15) lie outside these fields due to their higher TiO_2 and Cr_2O_3 respectively.

In the TiO_2 vs Al_2O_3 diagram (Fig.4.3b) the peridotite (B19A) and accessory chromites (BT1) lie in the field of stratiform chromites forming two separate clusters due to their variation in TiO_2 content. The chromitite chromites (B15), however, fall far removed from any of the fields due to their low content of Al_2O_3.

The TiO_2 content of chromites can provide information on the degree of differentiation. The TiO_2 content of the Bondla chromites in general increases from chromitite chromites (B15) into troctolite chromites (BT1). Evans and Wright (1972) and Hill and Roeder (1974) have shown that TiO_2 content of chrome spinels increases with
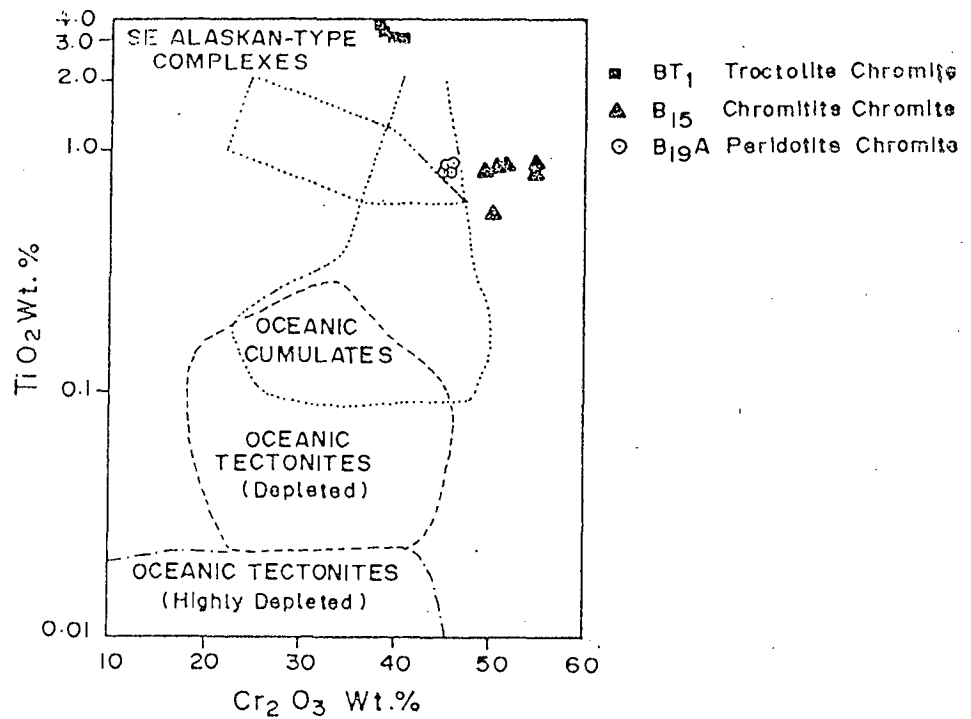
Fig.4.3a   TiO2   wt.% vs   Cr2O3 wt.% plot   of   chromites
from Bondla [based on Herbert(1982),Irvine (1967),
Bird and Clark (1976)].
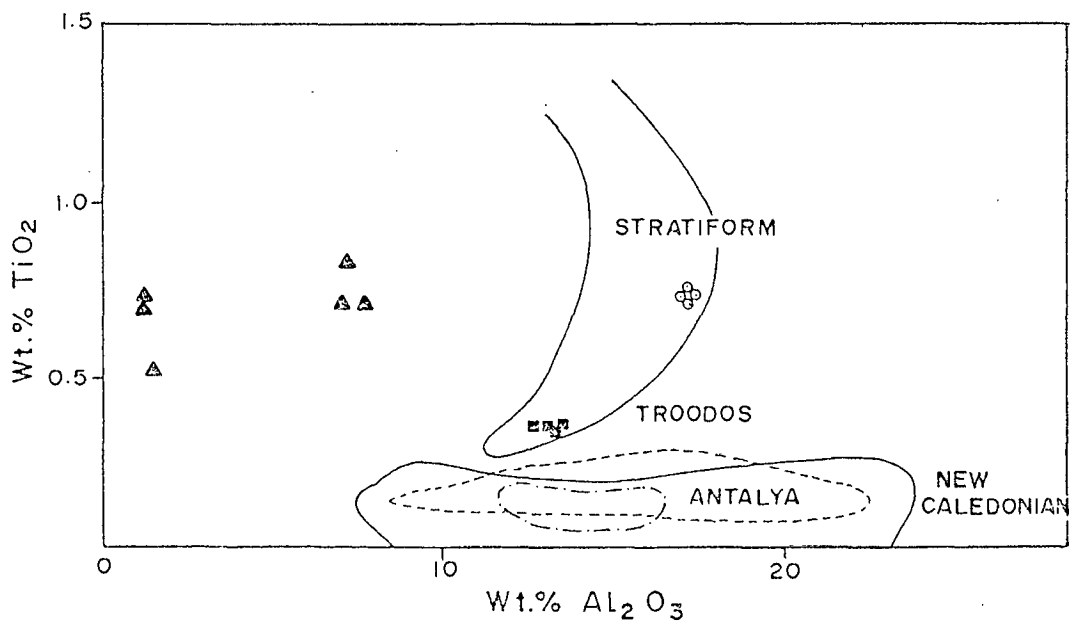
Fig.4.3b   TiO2   wt.% vs   Al2O3   wt.% plot for   chromites
from Bondla.

progressive fractionation of the basaltic magma. Ti by virtue of its lower distribution coefficient gets enriched in the melt relative to solid phases during fractionation (Eales and Reynolds, 1981). It is natural therefore, that stratigraphically higher chromites are derived from more fractionated liquid.

A number of workers have shown that the stability of chrome-spinels depends not only on the bulk composition, temperature and pressure but also on oxygen fugacity (Irvine, 1965; 1967; Ulmer 1969; Hill and Roeder, 1974; Fisk and Bence, 1980; Rivalenti et al., 1981). Hill and Roeder (1974) and Fisk and Bence (1980) observed that with increasing fo_2 the chrome- spinel is enriched in Fe^{+3} and is impoverished in Mg. In order to evaluate the effect of fo_2 on the composition of chromites, the analytical data were plotted in the Cr - and Al - free face of the spinel prism (Fig. 4.4) contoured with a set of surfaces representing the possible compositions for different fo_2 at constant pressure and temperature (Irvine, 1965). The intersection of three surfaces (fo_2 isobars) with the Cr and Al free faces of the spinel compositional prism are shown in (Fig.4.4) alongwith the
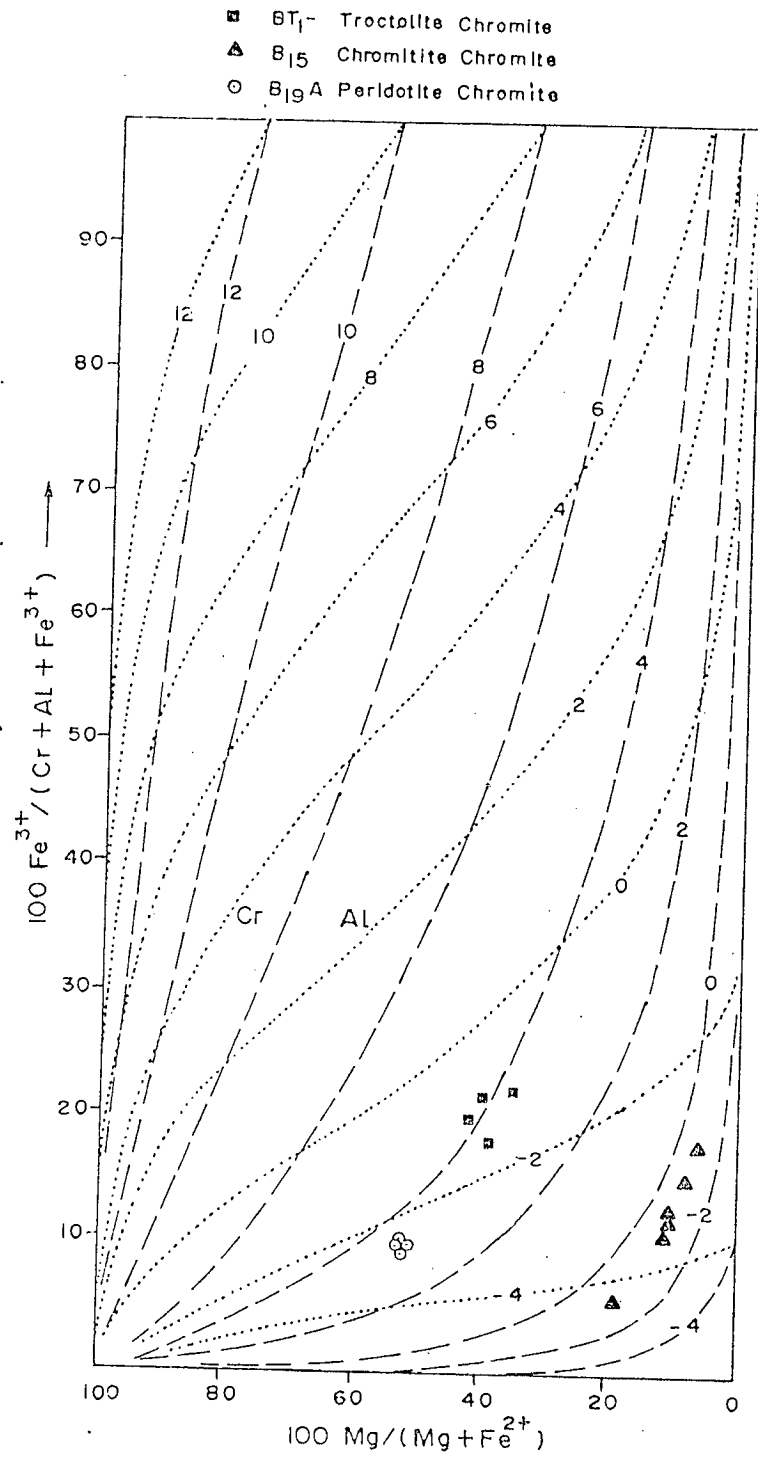
Fig.4.4   Fe3+ # vs Mg # diagram contoured with theoretical constant fo2 isobars from Irvine (1965) showing plots of Bondla chromites. Dashed lines-isobars for Al-free system, dotted lines isobars for Cr-free system.

plots of Bondla chromites. The chromitite chromites (B15) show low fo_2 than those in peridotite (B19A) and troctolite (BT1). The chromites from stratiform complexes are normally formed under low fo_2 (Jan and Windley, 1990). Cr and Fe^{+3} contents are related to the percentage of cumulus chromite to cumulus olivine. The chromitite chromites is bound to contain more Cr and less Fe^{+3} than peridotite chromites (Olivine-chromite cumulate) (Jackson, 1969). The trend of increasing Fe^{+3} shown by chromitite chromites is largely the result of an increase in fo_2 due to crystallization (Roeder and Reynolds, 1991) and replenishment, however, in this case the increase could be related to alteration. It is seen from the diagram that Fe^{+3} is highest in the accessory chromites (BT1) and decreases in peridotite chromites (B19A). Chromitite chromites (B15) show a range of Fe^{+3} spanning from peridotite chromites (B19A) to troctolite chromites (BT1). An opposite behaviour is observed in chromites from Alpine-peridotites wherein Fe^{+3} is higher in spinels from chromitites and spinel-rich dunites than in accessory spinels (Dick, 1977). In the present case however, the increase in Fe^{+3} may be ascribed in part to secondary alteration, given the altered nature of the rocks. This is also supported

94

by the trend shown by the Mg # which is reverse to that normally encountered.

Classification of Chromites

The continental geological setting of the Bondla complex, the repetitive nature and way up stratigraphy of the chromite layers alternating with those of olivines, the cumulate textures shown by chromites and associated silicates are all consistent with the stratiform nature of chromites. Mineralogically, the chromites show features which are typical of layered chromites. Mineral chemical features such as high Cr_2O_3 (more than 45 wt%), TiO_2 more than 0.51 wt.% and FeO more than 17 wt.% in chromites containing over 45 wt.% Cr_2O_3, Al_2O_3 more than MgO, Cr/Fe ratio (between 1 and 2) which decreases upwards, are features which are characteristics of stratiform chromites. However, in order to distinguish them from segregated layered chromites in ophiolites, the Bondla chromites could be classified as `Bushveld type' following Stowe (1994). The high Cr # ranging from 0.63 to 0.96 and low Al_2O_3 content between 7.0 and 17.0 wt.% (excluding altered rim compositions) permit them to be classified as

Archaean greenstone-hosted chromites (LeBlanc, 1984;
Stowe, 1994).

As pointed out by Irvine (1967) spinels can be used
as petrogenetic indicators. Using spinel compositions,
Dick and Bullen (1984) divided the Alpine-type peridotites
into three groups: Type-I peridotites and associated
volcanics having spinels with Cr # less than 0.6, Type-III
peridotites and associated volcanics containing spinels
with Cr # more than 0.6 and Type-II peridotites and
volcanics, those spanning the range of spinels in Type-I
and Type-III peridotites.   The chromites from Bondla show
Cr # more than 0.60 and therefore, they show similarities
to spinels in Type-III peridotites of Dick and Bullen
(1984).   Such high chrome spinels analogous in Type-III
peridotites are reported from arc - related lavas from SE
Alaska and from continental layered intrusions (Dick and
Bullen 1984).

The rock association chromitite-dunite-peridotite
(Thayer, 1969) permits the Bondla chromites to be classi-
fied as early magmatic segregation deposits (Park and Mac
Diarmid, 1975; Jensen and Bateman, 1979). The chromites

can also be categorised as high grade ores (more than 45 wt.% Cr2O3) suitable for the metallurgical industry however, their Cr:Fe(t) ratio is slightly lower than the recommended value of 2.5.

The associated mafic-ultramafic complex can be classified as a medium - and small - sized sheet-like or funnel shaped intrusion emplaced in non-orogenic area (Jensen and Bateman, 1979; Edwards and Atkinson, 1986) similar in form to the Skaergaard and Rhum intrusions (Wager and Brown, 1967). Considering the zonal distribution of the rocks - ultramafics forming the Lower Zone and the mafics forming the Upper Zone, the complex shows similarities to the Great Dyke Complex, Zimbabwe where chromites are confined to the lower ultramafic zone (Page, 1977; Wilson, 1982).

Sulphide Mineralisation

The sulphide mineralisation is confined to the NW-SE trending zone of mylonite. Along this zone the rocks are converted to quartz-sericite-schist. They are intruded by three sets of quartz-calcite veins which are described earlier.

The sulphides are confined to the quartz-calcite veins. The intersections of veins are the favourable locales for the sulphides. The sulphides occur as lenticles, segregations, clots, stringers, disseminations and also as thin veinlets.

Ore Petrography

The sulphide ore assemblage was studied under incident light. The sulphides are made up of pyrite, pentlandite, chalcopyrite, pyrrhotite with subordinate galena, millerite and Ni- and Co-sulphoarsenides.

Pyrite is the predominant phase in the mineral assemblage. It belongs to two generations. Pyrite-I is euhedral and occurs as megacrysts showing compositional zoning (Plate XIII Photo 1). It is invariably fractured and shows intergrowth with chalcopyrite. Pyrite-II is fine grained, interstitial and spongy in appearance. At places, it replaces pyrite-I. Pyrite-II shows intergrowth with pentlandite (Plate XIII Photo 2). Pentlandite also occurs as discrete grains and as exsolution lamellae in pyrrhotite (Plate XIV Photo 1). The latter is replac-

ing pyrite. The sulphoarsenides are represented by Ni-
and Co-gersdorffite. Ni-gersdorffite either occurs as
discrete grains or is seen to vein pyrite. Co-gersdorf-
fite often occurs as euhedral grains (Plate XIV Photo 2)
often zoned and is intergrown with pyrite. Galena and
millerite have restricted occurence and are generally
associated with pentlandite.

Mineral Chemistry

The sulphide minerals were analysed by standard
electronprobe technique using an energy dispersive system
at C.S.I.R.O., Australia. Between 5 and 15 analyses were
performed on each mineral phase from each ore sample.
Fifteen represensentative chemical analyses from about 50
analyses performed in total, are presented in Table No
4.2. These are the first mineral analyses published on the
sulphides from Bondla (Dessai, *et al.*, 1994). It is seen
from the table that intergrain compositional variation in
pyrite within a sample is not very significant. Considera-
ble variation in element concentrations is however ob-
served between pyrites of two generations. Pyrite-I con-
tains between 0.78 and 1.23 wt.% Co whereas, in pyrite-II

99

Table No. 4.2 Electronprobe Microanalysis of Sulphides from Bondla

Element (%)	Pyrite I		Pyrite II		Chalcopyrite			Pentlandite			Pyrrhotite	Millerite	Ni-Gersdorffite		Co-Gersdorffite
	KM1	KM2	KN	KN	KM1	KM2	KN	KM1	KM2	KN	KN	KM2	KM1	KM2	KM1
As	0.75	0.41	0.17	0.06	0.06	0.09	0.08	0.05	0.06	0.04	0.06	0.00	41.55	42.02	40.90
Fe	44.46	44.82	45.10	45.16	29.47	30.33	29.88	24.87	25.72	32.81	57.74	1.73	4.97	3.49	5.34
Co	1.23	0.78	0.88	0.01	0.02	0.04	0.02	6.29	0.20	0.09	0.01	0.24	9.85	8.22	22.17
Ni	0.22	0.39	0.05	0.81	0.00	0.02	0.05	34.25	39.66	31.77	0.72	62.02	21.28	24.83	8.88
Cu	0.01	0.02	0.01	0.01	33.08	32.83	33.23	0.02	0.01	0.01	0.06	0.00	0.01	0.01	0.01
S	53.19	52.67	53.68	52.78	35.02	35.14	34.99	33.35	33.56	34.56	39.74	35.77	20.60	20.42	21.02
Total	99.86	99.09	99.89	98.83	97.65	98.46	98.24	98.76	99.20	99.28	98.34	99.76	98.26	98.60	98.32

Co percentage varies from 0.01 to -0.88 wt.%. Ni in pyrite-I varies between 0.22 and 0.39 wt.%, whereas in pyrite-II it is between 0.05 to 0.81 wt.%. The percentage of Cu in both pyrites is insignificant. Pyrite-I shows higher percentage of arsenic (0.41 to 0.75 wt.%) than pyrite II (0.06 to 0.17 wt.%). Thus it is seen that pyrite is significantly richer in Co and As and poorer in Ni whereas, pyrite-II is richer in Ni and has insignificant concentrations of Co and As.

Chalcopyrite contains 29 to 30 wt.% Fe and between 32 and 33 wt.% Cu. The concentrations of other elements such as Ni, Co and As are insignificant.

Pyrrhotite contains about 57.74 wt.% Fe and 0.72 wt.% Ni. In Pentlandite, the Fe percentage varies from 24.8 to 32.8 wt.% and Ni from 31.7 to 39.6 wt.%. Some samples contain significant amount of Co which may be upto 6 wt.%. The Ni percentage in Ni-gersdorffite varies from 21.2 to 24.8 wt.%. As is between 41.5 and 42 wt.% and Fe is between 3.4 and 4.9 wt.%. Co-gersdØrffite contains about 22 wt.% Co, 40 wt.% As and 8 wt.% Ni.

Discussion

With the limited data available it is not intended here to go into the details of the genesis of the sulphides. However, pending detailed work certain broad deductions can be made within the realm of the available information.

It is widely believed that base metal mineralisation in Archaean greenstones is the result of deposition from hydrothermal solutions. However, there seems to be no consensus of opinion among different workers on the nature and origin of ore fluids. Hutchison and Burlington (1984) and Viljon (1984) considers sea-water derived exhalative fluids as carriers of the base and precious metals. Philips *et al.*, (1984) Fyfe and Kerrisch (1984) advocate metamorphically derived fluids as the transporter of metals whereas, Burrows *et al.* (1986) and Rock and Groves (1988) suggest magmatically derived fluids as the prime ore carriers.

The sulphide mineralisation at Bondla is controlled along the weak zone within a network of veins and veinlets

of quartz-calcite and sulphides indicating that the mineralized area could represent a focus of hydrothermal solutions which were guided towards the surface along the fracture system. The latter may have served as a feeder system for the mineralizing solutions. The vein mineralogy, the presence of significant amount of calcite, the abundance of Ni and Co in the ores are all consistent with CO_2 rich hydrothermal fluids. The presence of hydrothermal epidote in the alteration haloe may indicate as a first approximation a temperature of about 250 - 270o C (Browne,1978). This temperature range is also corroborated by the experimental phase relations of the assemblage pyrrhotite - pentlandite which indicates temperature less than 310oC. The low temperature of ore formation is also supported by the presence of millerite in the ore assemblage. In most documented exhalative deposits, precipitation temperatures are commonly below 300oC (Sato, 1972). At temperatures of 300oC and below there is considerable uncertainity regarding phase relations in the Cu - Fe - S system (Vaughan and Craig, 1978). Nevertheless a H_2S dominant ore fluid should successively precipitate pyrite - pyrrhotite - pentlandite with decreasing Fe activity and temperature. Absence of magnetite and haematite with

102

quartz may indicate low oxygen fugacity conditions. High Co/Ni ratios and high Co and Ni content of pyrite may indicate volcanogenic derivation. The mineralisation bears some similarities with the fracture controlled stringer ores of Kuchiganehal of Ingaldhal sulphide zone from Chitradurga schist belt. The latter mineralisation has been suggested as of volcanogenic, hydrothermal derivation (Anant Iyer and Vasudev, 1985). However, further detailed work on the sulphide mineralisation of Bondla is essential before any definite conclusions on the nature of mineralisation could be drawn.

CHAPTER V

PETROGENESIS

CHAPTER V

PETROGENESIS

Petrologists working on mafic-ultramafic layered complexes have been confronted with a number of problems. Foremost among these are the nature of parent magma, the characteristics of source rocks, the factors responsible for magma generation, the mode of emplacement, the conditions of crystallization and the tectonic environments.

In this chapter an attempt is made to answer some of these questions, in the light of the data presented in the earlier chapters and on the basis of the information available in the literature. It may be pointed out though, that precise evaluation of some of these problems was not possible due to the constraints of systematic chemical data. In addition to the basic problems addressed above, the genesis of chromite has been discussed.

Parent Magma

The rocks of the Bondla mafic-ultramafic complex are cumulates. Therefore, the chemical data, although can be used to decipher the magmatic process and to underline the compositional differences and the relationship of rocks with each other, they will have to be utilised with caution to determine the composition of the parent magma. The difficulty is further aggravated by the absence of either a chilled margin or closely related mafic dykes. Thus there is no direct evidence of the composition of the parent magma.

In such cases the parent magma composition can be estimated by application of mineral-melt partition coefficient to the most primitive cumulates. Such an approach was adopted by DeBari (1994) in case of the Fiambala gabbroic intrusion, northwest Argentina. She made use of FeO/MgO olivine-liquid partition coefficient [Kd(ol/liq)=0.30] of Roeder and Emslie (1970) and concluded that the most primitive olivine from the ultramafic cumulates (Fo90-91.5 and 0.40 NiO) crystallised from a liquid with Mg # between 0. 73 and 0.74. As the Fo con-

tent of the olivines from the troctolites of the Lower
Zone at Bondla is very close to the olivines from the
Fiambala intrusion, by analogy it is inferred that the
troctolite (BT2) with whole rock Mg # between 0. 73 and 0.
74 (MgO 12.5 wt.%) may represent the most primitive parent
magma of the Bondla mafic- ultramafic complex. Moreover
primary magmas in equilibrium with typical mantle mineral-
ogies should have high Mg #, Cr and Ni values. The Bondla
rocks have Mg # between 0.72 to 0.74, Cr more than 400
ppm. Ni about 370 ppm. and SiO_2 between 50 and 51 wt %.
These values lie within the ranges generally accepted for
primitive and even primary magmas (Rhodes,1981) except for
Ni values which are slightly lower.

Magma Type

The sequence of crystallisation is olivine $\pm$ spin-
el, pyroxene and plagiocase. Olivine and spinel (Cr- Al)
are cotectic phases as observed in Hawaiian tholeiitic ba-
salts. Pyroxenes from basaltic rocks have been studied in
an effort to relate compositional trends and the magma
type. The nature of pyroxene assemblage is considered to
be one of the criteria for the recognition of the parental

affinity of basaltic rocks although this has been questioned by Barberi et al.,(1971).

The tholeiitic magma type is mainly characterised by two pyroxene assemblages (one Ca-rich pyroxene and the other Ca-poor) both commonly show exsolution lamellae and crystallise together in the early and middle stages of differentiation of tholeiitic magma (Carmichael, 1960; Brown and Vincent, 1963; Brown, 1967; Atkins, 1969).

Pyroxenes from the Bondla gabbroic rocks are also characterised by two phases Ca-rich pyroxene in the sub-calcicaugite-augite range and Ca-poor pyroxene in the bronzite-pigeonite range. Both these show variation in iron content, and frequently contain exsolution lamellae and coexist with olivine suggesting a tholeiitic magma. The crystallisation trend of coexisting pyroxenes show a trend of iron enrichment, however, it is noteworthy that these pyroxene pairs are somewhat different than those from Skaergaard (Brown and Vincent, 1963) and Bushveld (Atkins, 1969). The wollastonite content of Ca-rich pyroxene is higher than that of Skaergaard and Bushveld, and Fe

and Ca content of the Ca-poor pyroxenes are lower than those of the equivalent pyroxenes from the mentioned intrusions. This may be due to the difference in crystal-lisation conditions (eg. lower equilibration temperature and possibly a slower cooling rate). The Bondla pyroxenes are poorer in alumina and titania and richer in silica than those from the above intrusions. The concentration of Al in tetrahedral sites (Al_z) is relatively low and typi-cal of tholeiitic type pyroxenes.

On AFM plot an iron enrichment trend characteris-tic of tholeiitic basalts is shared by the mafic-ultramaf-ic rocks and the associated metabasalts. Enrichment of ferrous iron during late to intermediate stages of magmat-ic differentiation is best exemplified by the mafic and ultramafic rocks of the complex as there is a complete spectrum of rocks from ultramafic to leucograbbroic which evolved from a tholeiitic basalt magma with subalkaline affinities (Irvine and Baragar, 1971). The iron enrichment trend shown by the rocks is more iron-rich compared with a typical tholeiite and slightly less iron-rich than the liquid trends of Skaergaard layered intrusion (Wager and Brown, 1967) which illustrates the extreme case of iron

enrichment. The iron-rich character of the mafic rocks is accompanied by slightly higher silica content. The silica saturated nature of the rocks is reflected in their quartz normative compositions in early differentiates indicating that the magma evolved from the tholeiitic side of the thermal barrier. Low silica and high iron are features typical of Fenner trend of crystallisation (Fenner, 1929).

In addition to high iron, the mafic rocks also con tain higher alumina concentrations. Some of the samples are fairly high in Al_2O_3 (16.5 wt.%) to be classified as high-alumina basalts. However, the enrichment in alumina is due to plagioclase accumulation. The samples are compared with field defined for high-alumina and high-iron basalts from the Archaean Blake River Group, Canada. The high-iron rocks are more alumina-rich than are typical Fe-basalts (Pearce and Birkett, 1974) and Fe-Ti basalts (Christie and Sinton, 1981) and the high-alumina rocks have more iron than typical high-alumina basalts (Kuno, 1960).

The crystallisation sequence olivine, pyroxene,

plagioclase is characteristic of tholeiitic melt and results in the formation of large amounts of pyroxene-rich ultramafic cumulates and gabbronorites very conspicuously seen in the Bondla complex.

The REE content of the Bondla rocks progressively increases from the Lower Zone ultramafics to the Upper Zone gabbros which is a consequence of olivine dominated crystallisation which causes the REE and the La/Lu ratio to incease with progressing fractionation. It is also supported by absence of Eu anomaly in the Lower Zone rocks whereas, the overlying gabbros exhibit a small positive Eu anomaly due to the accumulation of plagioclase. In the case of large intrusive complexes such as Skaergaard, Bushveld, Stillwater etc. the early cumulates tend to have a positive Eu anomaly and smaller La/Lu ratio than the presumed parent melts of the chill zone gabbro (Haskin and Haskin, 1968). The REE increases progressively in the stratigraphic sequence which could be ascribed to clinopyroxene crystallisation at low pressure (Cullers and Graf, 1984).

Nature of Source Rocks

The major and the trace element geochemistry indi-
cate that the Bondla magma was tholeiitic in character
and that it originated at mantle depths. It is generally
agreed that tholeiitic magmas originate at the upper
plagioclase stability limits. The Bondla magma can be
modelled as a low-Ti, high-Mg basaltic magma. It is widely
accepted that the generation of such a magma requires
melting of a severely depleted residual mantle source.
Experimental petrology arguments restrict the genesis of
low-Ti basalts and boninites to high degree (25-35%) of
water saturated melting of peridotitic mantle (Serri,
1981; Sun and Nesbitt 1978) at low pressures of less than
10 kb. However, the MgO content of the Bondla magma is
rather low to be the product of partial melting of a
primitive undepleted mantle source.

Mysen and Kushiro (1977) showed that melts produced
by extensive partial melting of lherzolite contain about
20% MgO. High pressure melting experiments on peridotitic
komatiite by Bickle and Ford (1977) also suggest that
liquids in equilibrium with olivine and orthopyroxene

(residue of extensive partial melting) at 10 kb contain 18-19 % MgO. If the Bondla rocks had generated by extensive partial melting their MgO should have been higher which is not the case. Furthermore extensive partial melting should produce LREE-depleted melts unlike the LREE-enriched melts found at Bondla. This is because LREE decrease with increasing degree of partial melting while the HREE remain constant (Nicholls and Harris, 1980). The Bondla rocks also show low concentrations of High Field Strength Elements (HFSE). Sun and Nesbitt(1978) suggested that the low content of HSFE is due to remelting of a mantle source already depleted in these elements. It is suggested that the low-Ti magmas at Bondla involved the remelting of a residual depleted mantle source with fractional crystallisation of derivative melts prior to magma emplacement. Such a model would explain the relatively high Cr, Ni and high Mg #s of olivine, Ca-poor - and Ca-rich - pyroxene in the Bondla rocks and also allows for somewhat lower levels of these elements than would be expected of partial melting of a primitive mantle source.

In order to know the nature and the type of source rocks the chemical data were plotted in Al_2O_3 /TiO_2 vs

TiO$_2$ (Fig.5.1a) and CaO/TiO$_2$ vs TiO$_2$ (Fig.5.1b) binary
diagram. In the Al$_2$O$_3$ /TiO$_2$ vs TiO$_2$ diagram majority of
the rocks show affinities towards arc- and MORB- type of
source. In the CaO/TiO$_2$ vs TiO$_2$ diagram majority of the
samples plot in the depleted arc- type of source. A few
which have higher content of TiO$_2$ as a result of magmatic
differentiation, plot in the undepleted - MORB field. Thus
it is clear that the chemical characteristics are more
consistent with a depleted arc- type source.

Tectonic Analogies

In the earlier sections the nature of the parent
magma and the source characteristics have been outlined.
In this section it is attempted to identify the tectonic
analogies of the Bondla magma with the help of High Field
Strength Elements (HFSE). Discriminant diagrams based on
less mobile elements such as Ti, Zr, Y, Hf, Nb, etc. are
currently being increasingly used for identifying the
tectonic environments of volcanic suites (Pearce and Cann,
1973; Floyd and Winchester, 1975). However, when these
diagrams are used to interpret the tectonic environments
of Precambrian rocks, it is necessary to take into account

113
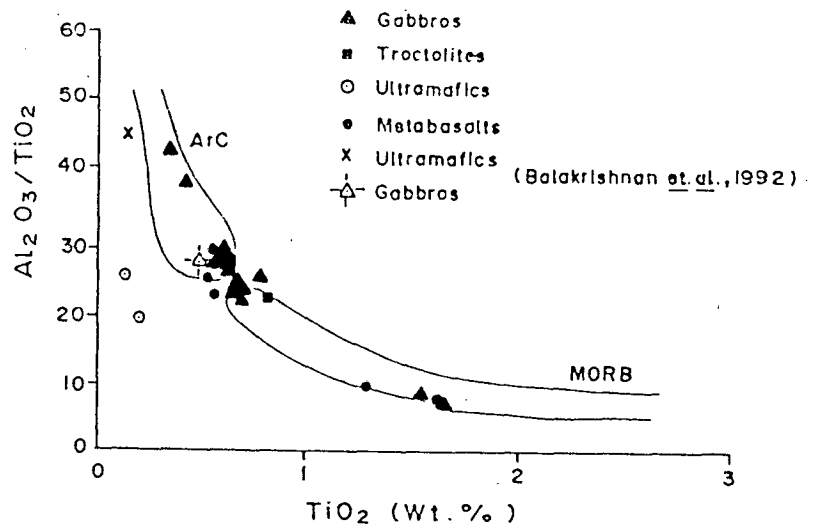
Fig.5.1a Plot of Bondla rocks in Al2O3/TiO2 vs TiO2 wt.% diagram [(after Sun and Nesbitt, (1978)].
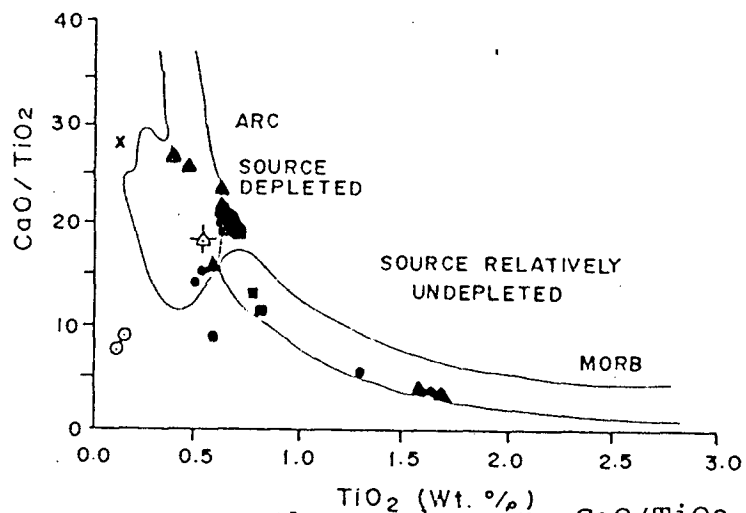
Fig.5.1b Plots of Bondla rocks in CaO/TiO2 vs TiO2 wt.% diagram [(after Sun and Nesbitt, (1978)].

the changes in chemistry the rocks have undergone due to secondary alteration and weathering. In fact most of these diagrams are based on and adopted for the Phanerozoic volcanic suites and their validity as discriminants particularly for the Precambrian plutonic rocks could be a matter of speculation and debate. Pharaoh and Pearce, (1984) discuss the efficacy of HFSE in characterisation of tectonic environments vis-a-vis mantle evolution and they conlude that even though time related changes occur in mantle evolution, they do not change the efficacy of the discriminant itself (also Condie,1976b).

In the Ti vs V plot, most of the samples plot in the field of arc- tholeiites, and MORB and continental tholeiites (Fig. 5.2a). The Ti/V ratio is less than 10 which is typical of arc-tholeiites (Shervais, 1982). The V/Ti ratio of igneous rocks reflects the oxygen fugacity of the magma (Shervais, 1982). In general the oxygen fugacity of arc-tholeiites is higher than that of MORB and continental tholeiites. In the Zr vs TiO_2 diagram (Fig. 5.2b) majority of the analyses occupy the field of arc-tholeiites. Two samples plot in the overlapping field of arc-tholeiites and MORB. In the Zr-(Ti/100)- (Yx3) tecton-
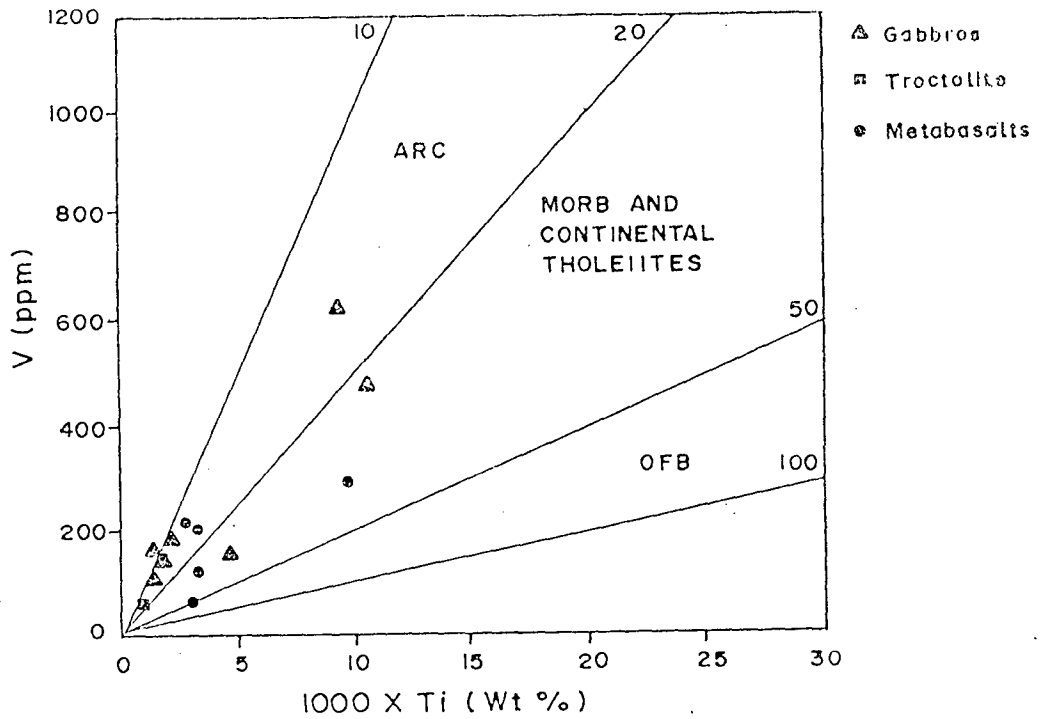
Fig.5.2a   Plots   of   Bondla   rocks   in   1000xTi   wt.%   vs   V
(ppm) [after Shervais, (1982)].
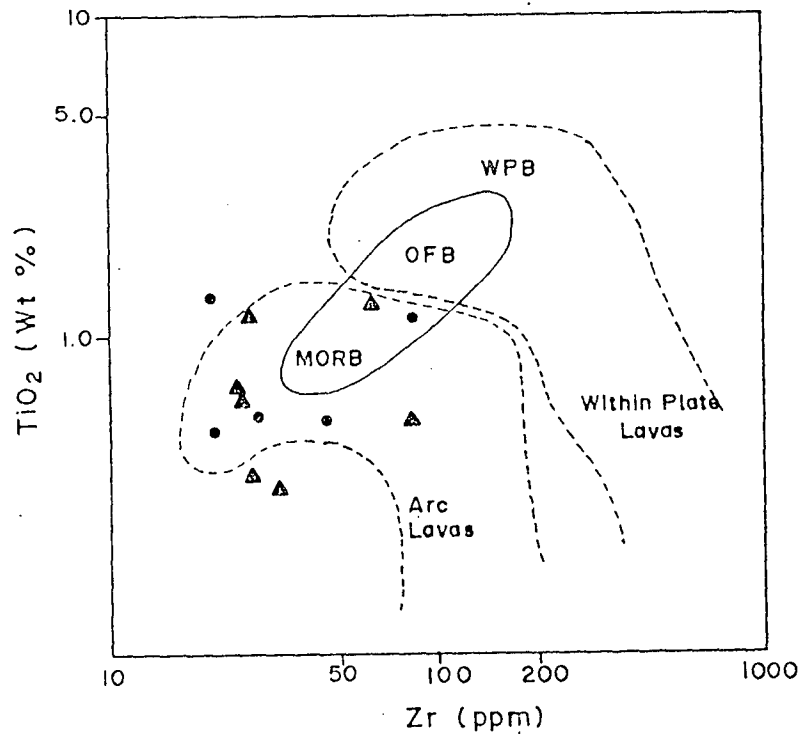
Fig.5.2b   Plots   of   Bondla   rocks   in   TiO2   wt.%   vs   Zr
(ppm)   [after   Pearce   and   Norry   (1979),
Pearce (1979)].

ic discriminant diagram (Fig. 5.3a) (Pearce and Cann, 1973) majority of the Bondla rocks plot in the ocean floor basalt (OFB) and low-K tholeiite fields. Similarly in Zr/4-2Nb-Y triangular plot (Fig. 5.3b), the Bondla rocks either plot in the N-type MORB field or lie in the vicinity of it. From the various discriminant diagrams it is apparant that the Bondla magma is identical to an arctholeiite having some similarities to MORB.

Chemical characteristics of the Bondla complex provide further evidence for an island-arc type of magma. The island-arc rocks are typically characterised by enrichment of LILE over MORB. These enrichments are not dependent on any prior fractionation of parent magma (De Bari, 1994). In comparison with MORB the island-arc rocks show depletion in HFSE. The trace element patterns of the most primitive Bondla rock (BT2) is depicted in a MORB normalised pattern (Fig.5.4). The pattern of a typical island-arc basalt from Talkeetna is also shown for comparison. The Bondla rock shows a characteristic arc-like signature with enrichment in LILE and depletion in HFSE relative to MORB. It is seen that the LILE concentrations in the most primitive Bondla rock are higher than average
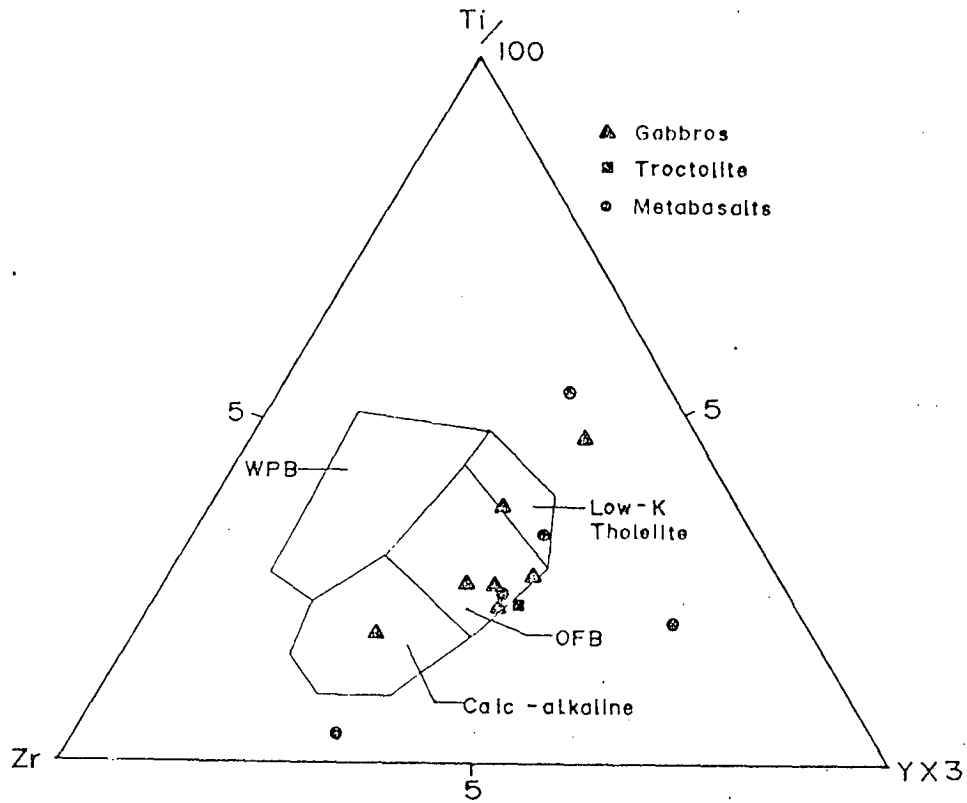
Fig.5.3a Plots of Bondla rocks in Zr-(Ti/100)-(Yx3) diagram [after Pearce and Cann, (1973)]. WPT-within Plate tholeiites,OFB-Ocean floor basalts.
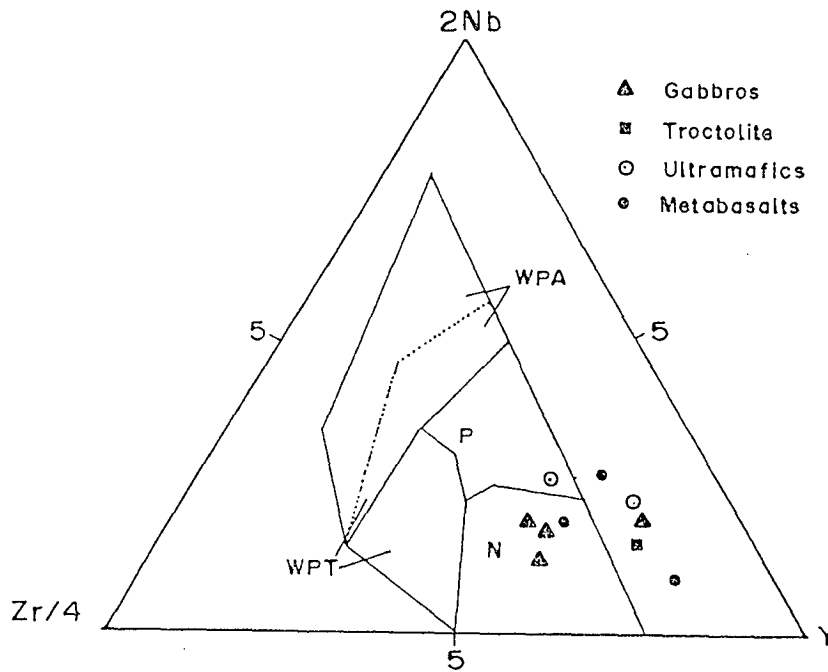
Fig.5.3b Plots of Bondla rocks in Zr/4-2Nb-Y diagram [after Meschede, (1986)]. WPT- Within plate tholeiites, WPA-Within plate alkali, P- p-type MORB, N-N-type MORB.
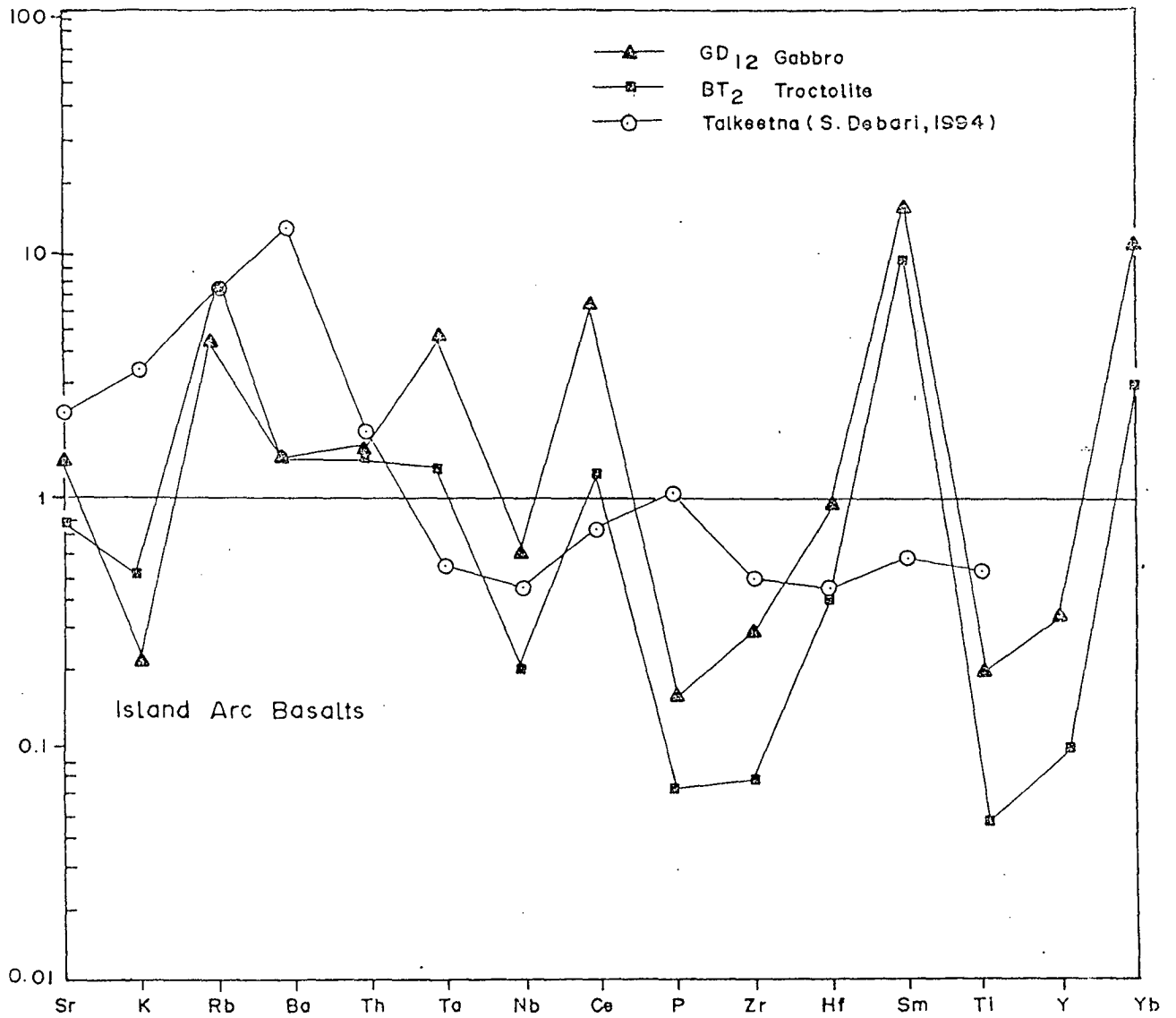
Fig.5.4   MORB normalised incompatible element pattern
          of troctolite and gabbro from Bondla and of
          island arc basalt, Talkeetna [from De Bari,
          (1994)].

MORB whereas the HFSE are typically lower. Basalts erupted in continental margin arcs exhibit similar patterns as their oceanic counterparts but have higher absolute trace element abundances. They are also richer in HFSE. These features have been attributed to their derivation from metasomatised subcontinental lithosphere (Pearce, 1983). Although this interpretation could be valid in case of Bondla, it seems more likely that the higher concentrations could have been developed by a combination of progressive crystal fractionation and replenishment during in situ crystallisation of magma. Thus it can be concluded that the most primitive of the Bondla magma closely resembles a typical primitive island arc-type tholeiitic magma. The magma generated in continental environments, and evolved from a primitive tholeiite with island-arc-type trace element characteristics.

Mode of Emplacement

The Bondla mafic-ultramafic complex shows a close similarity to the Great Dyke complex of Zimbabwe as far as the layered sequence is concerned . At Bondla the Lower Zone is made up of ultramafic rocks (olivine- chromite

cumulates) and the Upper Zone of gabbros and norites (plagioclase, clinopyroxene cumulates). The two zones are distinctly separated by a horizon of pyroxenite and troctolite although these are laterally not persistent in all sections. Texturally all rocks are cumulates and no chilled margin has been observed along the contacts of the intrusion. The ultramafic zone is best exposed in the NW where the layering dips northeasterly by about 30 to 35o. The gabbronorites are exposed both in the north and south, however, they are better exposed in the south where isomodal layering is seen. This indicates that the complex is made up of two subchambers which were interconnected.

The western contact of the complex with Precambrian metasediments is marked by a fault zone (zone of mylonite) whereas, the eastern margin is largely concealed under laterite. Along the western contact small coarse grained gabbro bodies are locally intruded along the fault zone. This bears testimony to the layered rocks being uplifted to their present position subsequent to consolidation. Subsequent tilting towards southeast and erosion has exposed the deeper ultramafic part of the layered series in the northwest. The absence of thermal metamorphic

effects in the vicinity of the fault zone suggest that the country rock metasediments must have been well above the immediate roof of the intrusion. Hence the uplift of the layered rocks must have been considerable.

Sequence of Crystallisation

The Bondla parent magma is a low-Ti, high-Mg tholeiitic in composition. Such a magma is capable of precipitating olivine, chrome-spinel, pyroxene and plagioclase. Olivine and chrome-spinel are likely to have crystallised slightly earlier than pyroxene and plagioclase. Stratigraphy shows that the latter two minerals are absent from the Lower Zone ultramafites. The layering could be explained as due to mechanical sorting. However, the difficulty is of the size of the chrome spinels relative to density due to which they would not be expected to sink faster than pyroxene. Secondly the size and density of pyroxene is similar to that of olivine yet they do not occur as cumulate phases along with olivine. This suggests that the order of crystallisation rather than mechanical sorting was the prime factor responsible for the formation of

macro- units. The distribution of minerals, repetition of layers in relation to stratigraphy, presence of a thick chromitite layer, reversal of cryptic variation in chromites all point to there being an underlying set of causes which were repeated many times during the process of crystallisation. The conditions necessary for the development of repeated units were initiated by periodic replenishment of the magma chamber by a fresh pulse of genetically related basaltic magma from a deeper source (Irvine, 1977; von Gruenewaldt and Worst, 1986; Eales, 1987; Hatton and von Gruenewaldt, 1987; Eales et al.,1990).

The Ni, and Cr vs Mg # correlation is consistent with the early fractionation of olivine and chromite from the magma (that resulted in low concentration of these elements in later differentiates) in the initial magma pulse at the same time driving the magma towards silica saturation which led to the precipitation of Ca- poor pyroxene in preference to Ca-rich pyroxene. Normally mantle derived magmas should crystallize Ca- rich pyroxene before Ca-poor pyroxene at crustal pressures (Campbell, 1985). The prevalence of Ca-poor pyroxene over Ca-rich pyroxene in the ultramafic part of the Bushveld has been

ascribed to elevated SiO_2 at the time of emplacement, as a result of pre-emplacement crustal contamination (Campbell 1985, Barnes, 1989) although continental boninite associations have been suggested. In the present case, however, the increase in silica is ascribed to olivine separation. The presence of Ca-poor pyroxene also indicates the anhydrous nature of the melt at this stage.

Subsequent to the crystallisation of pyroxenites the water content in the magma increased due to which olivine got stabilised relative to pyroxenes which led to the formation of the troctolite layer. The anorthitic nature of the troctolite plagioclase can also be attributed to the presence of water in the melt during crystallization (Helz, 1973).

The later more primitive pulse mixed with the resident magma (from the previous unit) to give a homogeneous liquid. A part of the residual magma may have been extruded from the chamber as lava at a surface volcano to form the metabasalts associated with the mafic-ultramafic rocks.

This situation was operational in the deeper north-western magma sub-chamber which gave rise to the olivine chromite cumulates. This seems to be more likely because in the early stages of magma chamber formation the tectonic conditions may have been unstable and resulted in periodic flooding of the chamber with fresh supplies of more primitive magma. Such a process of magmatic integration has been suggested by Wager and Brown (1967) in case of the Bushveld Complex of South Africa. Towards the close of the integration stage a magma replenishment occurred that gave rise to the main chromitite layer. Further differentiation occurred by crystal fractionation and gravity separation with the development of more regular cryptic layering and subdued rhythmic layering. This is observed in the southern magma sub-chamber where more regular cryptic variation is seen in the gabbro, gabbronorite and leucogabbro (Fig.5.5).

The southern sub-chamber was relatively shallow as deduced from the dominance of medium grained rocks. Lower MgO content of the rocks and greater degree of LREE enrichment than the rocks of the northwestern sub-chamber indicate more fractionated nature of the magma in the
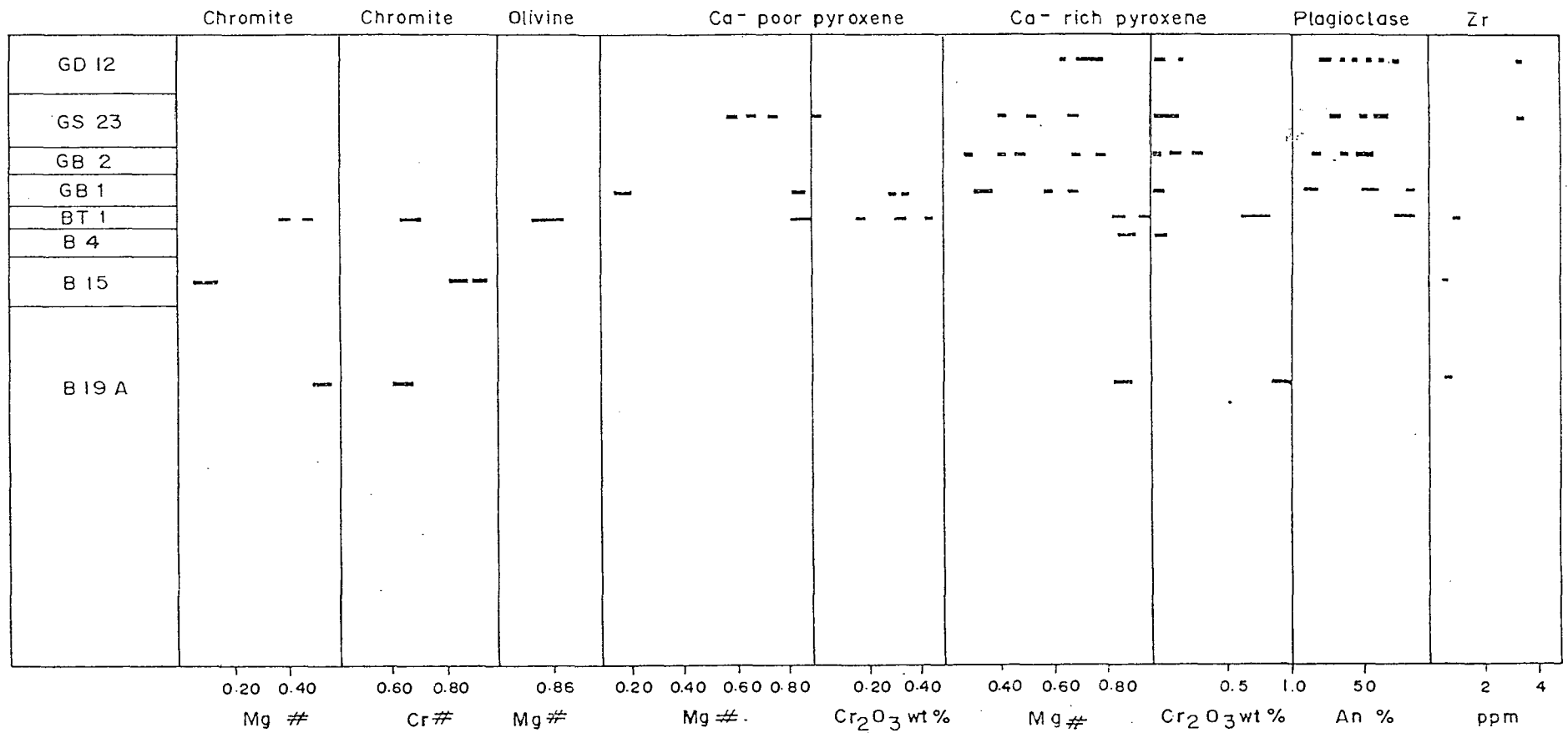
Fig. 5.5   A schematic stratigraphic column (not to scale) showing variations in mineral composition and whole-rock Zr content of representative rocks from Bondla.

southern sub-chamber. In this zone the plagioclase and the pyroxenes show a trend of crystallisation towards low temperature compositions. The magma became progressively richer in iron probably accompanied by increase in oxidation state leading to the precipitation of titaniferous magnetite. The melanocratic layers grade upwards into felspar-rich layers indicating rhythmic layering. Fractionation led to precipitation of plagioclase of andesine composition, Ca-rich pyroxene to ferroaugite composition and Ca-poor pyroxene to ferropigeonite. Upwards the rocks become leucogabbros with occasional granophyric textures.

Role of Water during Crystallisation

Several features of the Bondla intrusion indicate that the parent magma was hydrous in nature but it was not water saturated. This is supported by co-existance of olivine which is stable under hydrous conditions and orthopyroxene which is unstable under water saturated conditions. Continued crystallisation of anhydrous minerals may have led to water enrichment in the magma which stabilised anorthitic plagioclase. A minimum water content

122

can be inferred from the work of Holloway and Burnham (1972) who showed that amphibole will only crystallise from a basaltic melt that contains more than 3 wt.% water at the time of crystallisation . As amphibole is absent in the Bondla rocks it may be inferred that water content was much less than 3 wt.% originally, but may have increased at the time of plagioclase crystallisation .

Crystallisation Temperatures

The crucial factor in understanding the evolution of the rock suite is the knowledge regarding the temperature conditions under which the rocks crystallised. The only evidence of this is provided by the minerals contained in the rocks. Here it is considered that coexisting mineral phases are in the equilibrium, in the absence of evidence to the contrary. Although the estimated temperatures may not be exactly those at which the minerals crystallised, it is not unreasonable to consider them at least as lower limits at which the minerals crystallised or re-equilibrated.

It has been attempted here to make qualitative

assesment of the temperatures of crystallisation of the gabbroic rocks from the Bondla complex from the chemistry of pyroxenes. The efficacy of coexisting Ca- rich and Ca-poor pyroxenes to provide temperature information is well recognised. However, the lack of directly measured Fe^{+2} and Fe^{+3} creates a problem while using these geothermometers. The problems involved in applying experimental data from simple synthetic systems to complex natural mineral assemblages have been reviewed by Boyd (1973).

Temperature estimates were computed using the empirical geothermometers on experimentally determined Ca-Mg-Fe pyroxene phase relations following Lindsley (1983). The clinopyroxene mole fractions have been plotted in the experimentally contoured pyroxene quadrilateral (Lindsley, 1983) at 5 kb and 10 kb (Fig.5.6a and Fig.5.6b). The Ca-rich pyroxenes from troctolites (BT1) indicate temperatures between 1000 to 1200°C whereas, Ca-poor pyroxenes give temperatures between 1200 and 1300°C. The Ca-rich pyroxenes from gabbro (GS23) give temperatures of about 1000°C.

Textural evidence indicates that the cumulates in
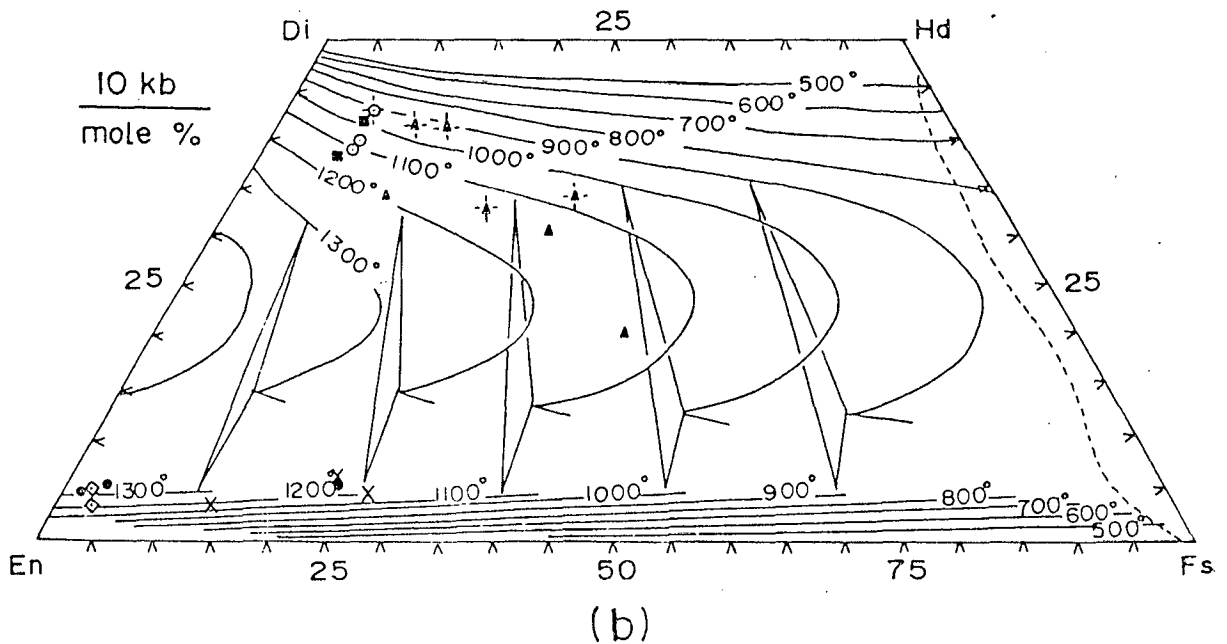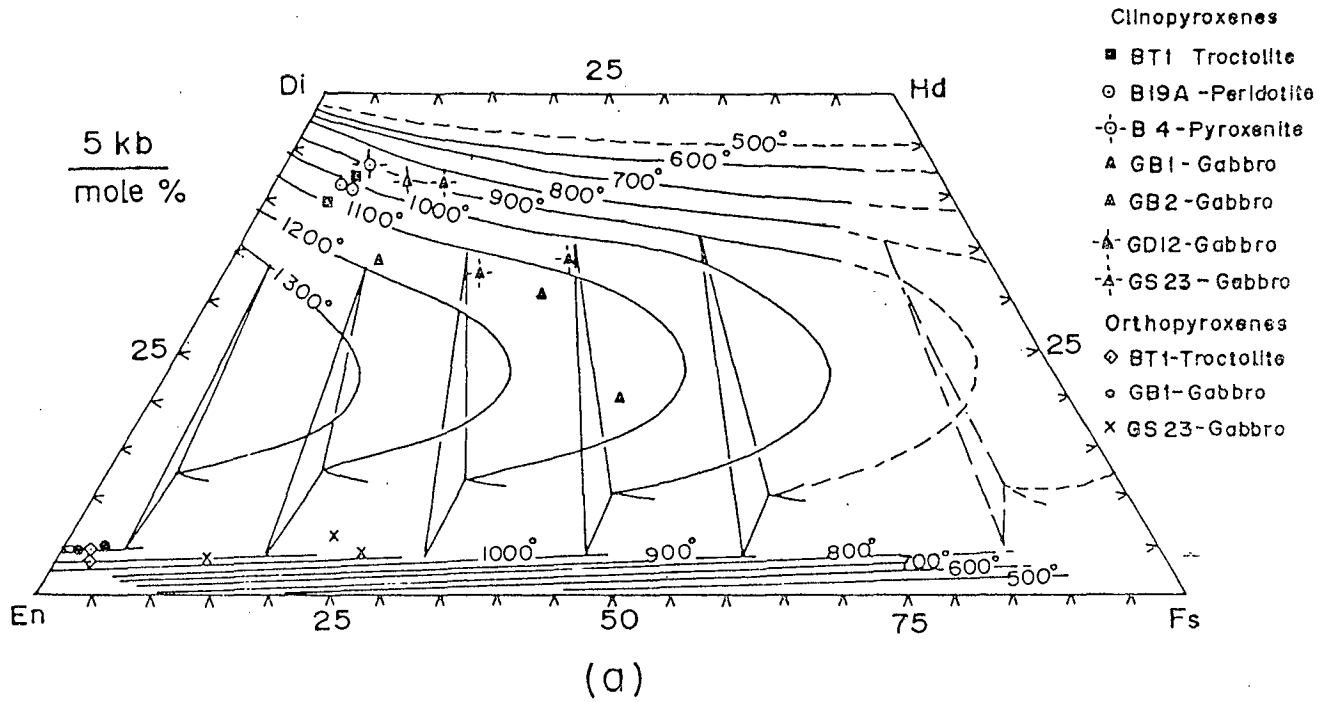
Fig. 5.6   Plot of Ca-poor and Ca-rich pyroxenes from Bondla
            rocks   in   pyroxene   quadrilateral   contoured   at
            100°C   interval   for   use   in   geothermometry
            [Lindsley, (1983), (a) 5kb, (b) 10kb].

gabbroic rocks (GS23) crystallised very close to the inversion temperature of pigeonite. The orthopyroxene formed by apparent inversion of pigeonite with a Mg # varying between 0.6 to 0.7. It has been shown by Barnes and Hoatson (1994) in case of the inverted pigeonites of the Munni Munni complex, Western Australia that orthopyroxene with Mg # in the range of 0.60 to 0.63 correspond to crystallisation temperature of $1100^{\circ}C$ (Lindsley, 1983). Balhaus and Glikson (1989) in Wingellina Hills intrusion, Central Australia suggest that olivines with Fo_{89} should have a melt with Mg # 0.72 and estimate the liquidus temperature of the parent melt at about $1350^{\circ}C$. By similar reasoning, it may be suggested, that the liquidus temperature of the primitive melt (BT2) at Bondla may have been approximately between 1200 and $1300^{\circ}C$, at pressures aproximately 6-10 kb. These values appear to be fairly in conformity with most basaltic compositions.

Depth of Crystallisation

Tholeiitic magmas in general originate at the upper plagioclase stability limits which broadly correspond to a

pressure of about 10 Kb. Low-Ti basalts and boninites under water saturated melting conditions originate at low pressures of less than 10 Kb (Serri, 1981; Sun and Nesbitt, 1978). The crystallisation in the nothwestern sub-chamber may have taken place approximately at 10 Kb. However, in the southern sub-chamber the crystallisation possibly occurred at a pressure of less than 10 kb, as plagioclase - the dominant phase of this zone, becomes unstable at 10 kb (Kushiro and Yoder, 1966; Green and Hibberson, 1970). Experimental studies on the system anorthite-potassium feldspar at 10 kb by Ai and Green (1989) showed that maximum solubility of K-felspar in plagioclase is about 18% at 10 kb. As the plagioclase at Bondla contains about 0.2 mole % K-felspar, it is contented that they are of low pressure origin.

Heat Source for Magma Generation

It has been shown that the Bondla magma was generated by partial melting of depleted mantle pyrolite source, in the shallower part of the mantle where the water content is sufficient to induce melting.

126

For melting to occur at relatively low pressures it is necessary that the geothermal gradient should be fairly steep and temperatures of about 1300°C be attained. Hence, it is essential to define the source of heat. From the currently available data on heat flow measurements from the Indian shield, it is possible to have a rough estimate of the conditions prevailing during Archaean. Heat flow in the Dharwar area is approximately 1×10^{-6} cal/cm2/sec and it increases in the northern part to 1.5 to 2×10^{-6} cal/cm2/sec (Naqvi and Rogers, 1987). Average heat flow from the Indian peninsula appears to be slightly higher than other Archaean shields (Jessop and Lewis, 1978). If this difference is valid then it can be ex-plained that the heat production in the crustal rocks may have been higher in the Archaean rocks in India than in similar rocks elsewhere (Rao et al., 1976). If these gradients have persisted for large part of geologic time then it can be visualised that enhanced melting might have taken place in the mantle (Naqvi and Rogers, 1987) during the Archaean. The close spatial association of rocks of komatiitic chemistry also hints at the unusually high geothermal gradient in the uper mantle before 2,500 Ma (Srikantappa et al., 1984).

127

A high geothermal gradient and a crustal thickness of about 35-40 km in Peninsular India (Naqvi and Rogers, 1987) could have suplied the required heat to bring about melting.

In summing up it is suggested that, the Bondla mafic-ultramafic complex represents an open system magma chamber which was periodically replenished by pulses of fresh primitive melt from below with concurrent fractionation at a pressure of approximately 10 kb. The complex comprises two subchambers, the northwestern and the southern. The northwestern chamber is deeper, wider and represents the main chamber (conduit). The southern chamber is shallower, narrower, and represents a higher level of the magma chamber. The main chamber shows rhythmic layering marked by olivine and chromite with a main chromitite horizon at the top of the ultramafic pile. In the southern chamber a layered gabbro sequence developed by convection and gravitational differentiation of a more evolved magma at a more shallow level after the stabilisation of the magma chamber.

The parent magma is a low-Ti, high-Mg tholeiitic

magma that was generated from a slightly metasomatised subcontinental lithosphere having trace element characteristics similar to continental arc-type lavas.

Genesis of chromite

In discussing the genesis of chromites some of the features appear to be significant. (i) The chromites occur as layers 0.5 to 5 cm in thickness which alternate with olivine-rich layers. (ii) Towards the top of the ultramafic pile the chromite occurs forming a thick chromitite layer 300 m wide (iii) Cr # of chromite increases from peridotite chromite to chromitite chromite and an opposite behaviour is shown by Mg #. Cr # shows inverse relationship with Al #. (iv) Fe^{+3} increase from peridotite chromite to chromitite chromite to troctolite chromite.

The $Cr/(Cr +Al+ Fe^{+3})$ ratio of Bondla chromites increases from peridotite chromite to chromitite chromites and then decreases further up in the troctolite chromite. The upward increase in Cr # could be related to enrichment of Cr^{+3} in the magma brought about by replenishment in the magma chamber. It could also be related to early clinopy-

roxene crystallisation which decreases the Cr/(Cr+Al) of the associated chromites as Cr/Al of clinopyroxene is higher than that of the melt (Roeder and Reynolds, 1991). This could also explain the absence of chromites in the gabbro pile above the troctolites. The absence of chromites in the gabbros in one sense is comparable to the stratigraphic gap observed in the Bushveld complex where no chromites are recorded.

Further upward decrease in Cr # from the chromitite chromite to troctolite chromite is largely dependent on the available Cr^{+3} in the magma. Fisk and Bence (1980) have shown that the $Cr/(Cr+Al+Fe^{+3})$ ratio of chromite co-precipitating with olivine decreases with decreasing temperature and that this trend may be related to a gradual decrease of Cr^{+3} in the magma with continued spinel crystallisation.

A different behaviour is however, shown by $Fe^{+3}\#$. It increases progressively upwards from peridotite chromite to chromitite chromite to troctolite chromite and also shows an inverse relationship with Mg #. In general chromites that crystallise early from basaltic magmas in

nature generally have Fe^{+3} # below 0.15 (Roeder and Reynolds, 1991) which is also the case with the Bondla chromites. The upward increase in Fe^{+3}# need be explained. Roeder and Reynolds (1991) have experimentally shown that ferric content of chromites increases with increasing fo_2. The upward increase in Fe^{+3}# shown by Bondla chromites could be related to increase in fo_2 brought about by the fresh pulse of magma, however, such a conclusion has to be taken with considerable reservations owing to the altered nature of the chromites.

Increase in fo_2 promotes crystallisation of spinel at the expense of silicates (Yoder and Tilley ,1962). Hill and Roeder (1974) have experimentally shown that increase in fo_2 promotes crystallisation of spinel however, Al_2O_3 content, Cr/Fe and Mg/R^{+2} ratio decreases at the same time as also seen in case of Bondla chromites. The decrease of Cr # of chromites is slightly affected by falling tempera-ture because although total Cr content of basaltic melt is very sensitive to fo_2 the composition of coexisting chromites is relatively insensitive to fo_2 value near and below that of FMQ buffer (Roeder and Reynolds, 1991). The reason being that Cr^{+3} content of the melt controls the

chromite composition and not the total Cr dissolved in the melt. Experimental studies (Elthon et al.,1982) and petrological investigations (Bodimier, et al.,1987; Suen and Frey, 1987) suggest that under sufficiently high pressure, pyroxene, olivine and spinel crystallise from basaltic magma to the exclusion of plagioclase. Thus Elthon et al.,(1982) concluded that ultramafic cumulates in the North Arm Mountain massif of the Bay of Island ophiolite crystallised at pressure of >10 kb. DeBari and Coleman (1989) reported a thick sequence of ultramafic rocks overlain by cumulate gabbros from Tonsina, Alaska. They have also been interpreted as high pressure cumulates. Some analogies with these rocks could be drawn in explaining the crystallisation of the Bondla rocks. It is tempting to suggest that the Bondla ultramafic pile with the chromite layers represent high pressure crystallisation (> 10 kb) of a basaltic magma. This is supported by experimental observations of Roeder and Reynolds (1991) wherein they have shown that increasing pressure leads to decrease in stability of plagioclase with a consequent increase of alumina both in the melt and coexisting chromites. Thus the chemical variation shown by chromites is not due to solubility of Cr in basaltic melts but it is the effect of

Al2O3 content of the melt and are not direct effects of pressure on the chromite- melt equilibrium as also shown by Fugi and Scarfe (1985) and Fallon and Green (1987).

Cyclicity of layering

Cyclicity of layering could be considerably modified and diversified simply through the blending of batches of liquid of the same parentage at diferrent stages of differentiation . Such a process can readily be visualised as occurring in subvolcanic intrusions and passageways through eruptive processes whereby fresh magma is repeatedly added to residues of earlier liquids that have been differentiated by partial crystallisation.

The dominant process of layer formation seems to have been sudden repetitive changes in supply of crystallisation products (settled crystals). It is essential, however, to explain the deposition of a thick chromitite layer. The petrogenesis of such a monomineralic layer of chromite remains a debated issue. One explanation is that the chromitite layer was formed by fractional crystallisation . Irvine and Smith (1969) explain that fractional

crystallisation by itself cannot yield a concentrated deposit of chromite once silicate minerals begin to form , but some additional process is required .Several hypothesis have been put forth by different workers to explain the mechanism for the origin of chromite-rich layers in stratiform intrusions.

On the basis of silicate inclusions in chromite from the Bushveld chromites, McDonald (1965) suggested the existance of a chrome-rich immiscible liquid. This interpretation was however, criticised by Jackson (1966) who argued that it is unlikely   that such a liquid would form in a basic magma. Cameron and DesBorough (1969) and Ulmer (1969) explaining the chromitites of Bushveld critical zone suggested that an increase in oxygen fugacity brought about by the assimilation of wall rocks could be the responsible factor. Whereas, according to Cameron, (1977, 1978) tectonically induced changes in total pressure in the magma chamber could bring about deposition of chromitite layers of great extent.

Contamination of the parental magma with granite melt derived from salic roof rocks was proposed by Irvine

134

(1975) as a possible mechanism by which chromitites formed in the Muskox and other intrusions. In the case of Stillwater Complex, Campbell and Turner (1986) opined that early emplacement of magma brought about extensive melting of th. floor leading to contamination of the magma which mixed with the following fresh input of a primitive magma to form the chromitite layer. Mixing between a relatively fractionated (evolved silicious) magma with a chromite - saturated primitive liquid is also suggested by Irvine (1977). The variation in chemistry exhibited by the Bondla chromites is consistent more with the latter possibilty.

Syntering of grains

One of the major problem concerning the origin of chromitite layers is how chromite cumulate with a calculated and expertimentally determined porosity of 30 to 45% (Jackson, 1961; Cameron and DesBorough, 1969) became densified to form a massive chromitite with less than about 10% silicates . Various hypothesis have been proposed to explain this feature . Cameron and Emerson (1959) suggested partial melting of cumulus chromite. McDonald (1967) proposed the existence of chromite rich liquid.

Both possibilities were rejected by Jackson because a chromite-rich liquid would require a temperature of 1700 to 2000º C.

Spry (1969) points out that simplest mechanism of crystal enlargement is by annealing or syntering of fine grained aggregates of strained grains to form a coarse grained aggregate of unstrained grains. The driving force for the growth being the lattice strain energy plus grain boundary energy. By this process polygonal texture can develop. The syntering process is greatly enhanced by the presence of a capillary fluid. The presence of a liquid phase can enhance the rearrangement of the particles in the aggregate to get the most effective packing and can produce maximum number of grain boundary contacts. The weight of the overlying crystal mush can provide the desired pressure. The process in this case is referred to as pressure syntering. Under thermodynamic equilibrium conditions the shape of the grains is polygonal with straight to slightly curved grains boundaries meeting in 120º at triple junctions. The development of polygonal grains with triple junctions in adcumulates such as chromitites was condidered by Voll (1960) to be due to synter-

136

ing. Golding (1975) considers such a mechanism to explain chromitites in podiform chromites from the Coolec ultramafic belt in New South Wales. A similar process is considered by Reynolds (1985) to have caused the densification of the magnetite layers in the upper zone of the Bushveld complex.

CHAPTER VI

SUMMARY
AND
CONCLUSIONS

CHAPTER VI

SUMMARY AND CONCLUSIONS

The thesis embodies the results of the field and laboratory investigations carried out by the author to study the geological setting, the structural features, the petrography, the geochemistry, the mineral chemistry and the petrogenesis of the Bondla mafic-ultramafic complex from central Goa. The associated chromites have also been investigated with regard to their textures and structures, mineralogy and mineral chemistry. On the basis of these studies the genesis of chromite has been discussed.

The Bondla mafic-ultramafic complex is exposed over an area of 60 sq km. It was geologically mapped on 1:25000 scale. The boundaries of the lithological units and the major structural features such as the folds, fracture zones, shear zones were demarcated on (1:60000) black and white aerial photographs and were checked in the field.

The area forms a part of the western Dharwar Craton of peninsular India (Naqvi and Rogers, 1987). It is pre-

dominantly occupied by the Archaean greenstones which constitute the Goa-Shimoga schist belt. The lithological units exposed in the area include metasediments with interlayered metavolcanics. The former are represented by quartz-chlorite-sericite-schists with bands of quartzite and phyllite. The lithounits belong to the Barcem Formation of the Goa Group (Gokul *et al.*, 1985) which has been correlated with the Chitradurga Group of the Dharwar Supergroup.

The rocks are folded into a NW-SE trending antiform which is overturned towards SW and is plunging due NW. A prominent shear zone 20 km long and about 2 km wide traverses the western limb of the fold. Along this zone the rocks are crushed and mylonitised.

Along the axis of the fold the mafic-ultramafic complex is intruded. The complex is layered and can be subdivided into two zones. The Lower Zone consists of ultramafic rocks represented by layerd dunite and peridotite which alternate with chromite layers. A thick chromitite layer occurs at the top of the Lower Zone. The Upper Zone comprises gabbros and gabbronorites which grade

139

upwards into leucogabbros. A layer of pyroxenite and troctolite serves as a marker horizon to separate the Lower Zone from the Upper Zone. The Lower Zone shows well developed rhythmic layering marked by cumulus olivine and chromite. The Upper Zone exhibits uniform layering. The ultramafic rocks are best-exposed in the northwestern part of the area between Nanus and Bondla whereas, the gabbros are exposed at Bondla and to the southeast at Durgini. The dunites, the peridotites and the chromitite are meso-cumulates and heteradcumulates. The pyroxenites show adcumulate texture. The troctolites and gabbroic rocks dominantly show orthocumulate texture.

The major element compositions show a subalkaline, low-Ti, high-Mg tholeiitic magma type. The evolutionary trends exhibited by the different elements can be at-tributed to progressive differentiation by fractional crystallisation. The compatible elements show depletion with differentiation indicating olivine, pyroxene and spinel controlled fractionation. The LILE and LREE show enrichment trends that parallel trends shown by FeO and MnO. The general smooth change in the shape of the pat-terns is consistent with the magma being related to par-

tial melting of a common source and/or crystal fractiona-
tion. The trend of increasing Ce/Yb ratio with differenti-
ation fits favourably with the crystal fractionation
process.

The chemistry of the silicate minerals also sup-
ports differentiation by fractional crystallisation. The
olivines from troctolites show compositional zoning. The
core Fo is 86.2 and it decreases slightly towards the
rims. The Ca-poor pyroxenes from the troctolite has a
composition varying between $Ca_{2-4.5}Mg_{82.5-85.4}Fe_{12.5-13.1}$
with Mg #s about 0.86 and 0.87. In the overlying gabbros
the Ca-poor pyroxene ranges in composition from
$Ca_{3.8}Mg_{84.0}Fe_{12.1}$ to $Ca_{4.1}Mg_{82.7}Fe_{13.0}$ with Mg# about
0.86. The pyroxene becomes iron-rich upsection. It co-
exists with ferrian-pigeonite ($Ca_{15.01}Mg_{15.4}Fe_{69.4}$) with
Mg # 0.17. The latter represents intercumulus phase. The
Ca-rich pyroxene from peridotite has a composition
$Ca_{43.0}Mg_{50.1}Fe_{6.7}$ with Mg # ranging from 0.87 to 0.97. In
comparison with this, the Ca-rich pyroxene from the
gabbroic rocks has a composition varying between $Ca_{28.8-}$
$_{43.8}Mg_{48.0-44.1}Fe_{23.1-11.9}$ with Mg #s ranging from 0.33 to
0.79. Lower Mg #s are shown by intercumulus pyroxene. The

cumulus pyroxene is strong y zoned with core Mg # varying from 0.70 to 0.79 and rim Mg # between 0.40 and 0.46. The intercumulus pyroxene has core Mg # 0.50 and rim Mg # 0.40. The Mg # decreases upsection. The cumulus plagioclase makes its first appearance in the troctolite at the top of the ultramafic zone. Here its An content is between An_{87} and An_{88}. It decreases in the overlying gabbros to An_{84} and An_{60}. The intercumulus plagioclase shows a much wider variation from An_{46} to An_{15}.

The chromite mineralisation is confined to the Lower Zone ultramafites. It is well exposed at two localities, namely Nanus and between Bondla and Poikul. At the former locality it occurs as layers 1-3 cm thick. The layers strike N40o and dip by 30-35o due N130o. Between Bondla and Poikul the chromite occurs as a massive chromitite layer which is more than 300 m wide. At places it can be traced intermittently over a distance of more than 1 km.

The chromites exhibit a variety of textures such as layered, disseminated, massive, micro-reticulate, occluded silicate, schlieren and myrmekitic. The chromites show

142

alteration to ferrit-chromit along the borders.

The massive ores from chromitites show maximum percentage of Cr_2O_3 which varies between 51 and 54 wt.%. The total Fe (FeO) ranges from 30 to 45 wt.%. Cr_2O_3 decreases in layered ores in peridotite to about 40 to 45 wt.% with 24 to 25 wt.% total Fe (FeO). Such a behaviour is characteristic of layered ores. The chromite shows compositional zoning with Cr # and Fe^{+3}# increasing from core to rim whereas, Mg # decreases. This compositional zoning can be attributed to secondary alteration and development of `ferrit- chromit' (Spangenberg, 1943). All chromites in general contain more than 0.5 wt.% TiO_2 which is a characteristic feature of stratiform chromites. The chromites show higher Al_2O_3 over MgO which is again a feature typical of layered chromites. The Cr # and Fe^{+3}# increase stratigraphically upwards. The increase of the former is related to enrichment of Cr^{+3} in the magma brought about by periodic replenishment. Fe^{+3} increase could be either related to increase in fo_2 brought about by replenishment or more likely it is related to the development of the `ferrit-chromit' attendant with alteration.

In various discrimination diagrams, the Bondla chromites either plot in the field of stratiform chromites or occupy the overlapping fields of stratiform and SE Alaskan-type complexes. Chromites can be categorised as early magmatic segregation deposits and belong to Type - III peridotites of Dick and Bullen (1984).

In the light of field characters, minerology and mineral chemistry and taking into account the various theories put forth by earlier workers to explain the genesis of chromites, a genetic model for the Bondla chromites has been suggested. The model involves differentiation by crystal fractionation and settling of crystals under the action of gravity. This process was aided by periodic replenishment and blending of batches of magma of similar parentage. It has also been suggested that the main-chromitite layer was formed as a result of crystal enlargement by annealing and sintering of fine grained chromites to form coarse grained aggregates. The driving force for the growth being the lattice strain energy plus the grain boundary energy (Spry, 1969). The process being enhanced by the presence of capillary fluids.

144

In discussing the petrogenesis of the Bondla mafic-ultramafic complex it is suggested that the troctolite (BT2) with Mg # between 0.73 and 0.74 (MgO - 12.5 wt.%) is the most primitive parent magma. It has a high Mg # (more than 0.73), more than 400 ppm Cr and about 370 ppm Ni with SiO_2 between 50 and 51 wt.%. These values lie within the range accepted for primitive magmas (Rhodes, 1981).

The sequence of crystallisation olivine, spinel, Ca-poor pyroxene, Ca-rich pyroxene, plagioclase, and coexistence of two pyroxenes, both showing exsolution lamellae indicate that the magma was tholeiitic in composition. The pyroxenes also show a trend of iron enrichment and are comparable in some respects with those of Skaergaard (Brown and Vincent, 1963) and Bushveld (Atkins, 1969) although their wollastonite content is little higher. This could be related to equilibration temperature and cooling rate.

The sub-alkaline tholeiitic nature of the magma is also supported by an iron enrichment differentiation trend shown by whole-rock compositions (Irvine and Baragar, 1971). The silica saturated nature of the magma is re-

flected in the quartz normative composition of early differentiates. The magma originated at mantle depths at about the upper plagioclase stability limit. It can be modelled as a low-Ti, high-Mg magma which was derived from a depleted mantle source. This is supported by the lower MgO content, slightly LREE enriched patterns and lower concentrations of incompatible elements. The melting may have taken place under hydrous conditions (Serri, 1981; Sun and Nesbitt, 1978) at low pressures of less than 10 kb. The heat required to bring about melting could have been provided by the Archaean rocks of south India which show higher heat flow values than other shield areas (Jessop and Lewis, 1978). This is also supported by the existence of rocks of komatitic chemistry in south Goa (Dessai and Deshpande, 1979 b, 1979c) and in other parts of the western Dharwar Craton. The geochemical data support a depleted MORB-type source with arc-like trace element characteristics. The discriminant diagrams based on HFS elements are inconclusive. They indicate arc-tholeiite and MORB and continental tholeiite type of tectonic environments. It can be surmised that the magma was identical to a depleted MORB with arc-like trace element characteristics and that it originated in continental environments.

The stratigraphy and distribution of the layered rocks - ultramafic rocks with some gabbros showing rhythmic layering in the northwest and gabbroic rocks with a better developed cryptic layering in the south indicate that the complex is made up of two sub-chambers which were interconnected. The complex was uplifted to its present position and was emplaced along a fault zone. Subsequent tilting towards SE and erosion has exposed a deeper ultramafic part in the northwest and a shallower gabbroic part in the south. The rhythmic layering and reversals in the cryptic variation shown particularly by chromites of the ultramafic zone can be explained as due to periodic replenishment of the magma chamber by more primitive genetically related magma from a deeper source. The Bondla magma was hydrous in nature due to which olivine-rich rocks formed during the early stages of crystalization driving the magma to silica saturation which stabilized Ca-poor pyroxene. The separation of anhydrous minerals led to increase of water content in the melt stabilising anorthitic plagioclase which is the dominant constituent of the Upper Zone. The water content may have been less than 3 wt.% as indicated by the absence of amphibole. The tectonic conditions in the initial stages may have been unstable

147

and resulted in periodic flooding of the magma chamber with fresh supplies of more primitive magma. During this stage of magmatic integration the ultramafic pile with chromite layers was formed. Towards the close of the magma integration stage, magma replenishment occurred that gave rise to the main chromitite layer.

Further differentiation occurred by crystal fractionation and gravity settling with more regular cryptic layering, by crystallisation of the more evolved resident magma. This is better seen in the south sub—chamber. The lower MgO content and the greater concentration of LREE in these rocks than those of the northwestern sub-chamber indicate more evolved nature of the magma and its crystallisation at lower temperatures, and at shallower depths.

The crystallisation in the northwestern sub-chamber may have taken place at about 10 kb. In the south sub-chamber the pressure was still lower as indicated by the presence of plagioclase (Kushiro and Yoeder, 1966; Green and Hibberson, 1970). Lower pressure is also supported by the lower content of potash feldspar in plagioclase. The Bondla magma may have been derived from a slightly metaso-

matised sub-continental lithosphere. The magma evolved from a primitive parental basalt with trace element characteristics typical of continental arcs. The Bondla intrusion provides a good example of an advancing, periodically replenished magma chamber (O'Hara, 1977) in the deep lower crustal environments.

REFERENCES

REFERENCES

Agata, T.,(1988). Chrome spinels from the Oura complex, central Japan. *Lithos*, V.21, pp.97-108.

Ahmed, Z., (1984). Stratigraphic and textural variations in the chromite composition of the ophiolitic Sakhakot-Quila complex, Pakistan. *Econ. Geol.*, V.79, pp.1334-1359.

Ahmed, Z., and Hall, A., (1981). Alteration of chromite from the Sakhakot-Quila complex, Malakand Agency, Pakistan. *Chem. Erde*, V.40, pp.209-239.

Ai, Y., and Green, D.H., (1989). Phase relations in the system anorthite-potassium feldspar at 10kb with emphasis on their solid solution. *Miner. Mag.*, V. 53, pp.337-345.

Anantha Iyer, G.V., and Vasudev, V.N., (1985). Copper metallogeny in the Jogimardi volcanics, Chitradurga greenstone belt. *Jour. Geol. Soc. Ind.*, V.26, pp.580-598.

Atkins, F. B., (1969). Pyroxenes of the Bushveld Intrusion, South Africa. *J. Petrol.*, V.10, pp.222-249.

Auge, T., (1987). Chromite deposits in the northern Oman ophiolite: mineralogical constraints. *Miner. Deposi-*

ta., V.22, pp.1-10.

Balakrishanan, S., Abbas, M. H., Vidyadharan, K. T., and Raghunandan, K. R., (1992). Chromite and sulphide mineralisation in the mafic-ultramafic complex of Usgaon, Goa./*Ind. Miner.,* V.41, pp.303-322.

Ballhaus, C.G., and Glikson, A.Y., (1989). Magma mixing and intraplutonic quenching in the Wingellina Hills intrusion, Giles complex, Central Australia. *J. Petrol.,* V.30, pp.1443-1469.

Barberi, F., Bizonard, H., and Varet, J., (1971). Nature of clinopyroxenes and iron enrichment in alkalis and transitional basaltic magmas. *Contr. Miner. Petrol.,* V.33, pp.93-107.

Barnes, S.J., (1989). Are Bushveld U-type parent magmas boninites or contaminated komatiites? *Contr. Miner. Petrol.,* V.101, pp.447-457.

Beckinsale, R.D., Drury, S.A., and Holt, R.W., (1980). 3,360-My-old gneisses from the South Indian craton. *Nature,* V.283, pp.469-470.

Bickle, M.J., and Ford, C.E., (1977). The petrogenesis of peridotitic komatiites: evidence from high pressure melting experiments. *Earth Planet. Sci. Lett.,* V.37, pp.97-106.

Bilgrami, S. A., (1969). Further data on the chemical

composition of the Zhob valley chromites- II. *Sind.*
Univ. Sci. Res. J. Spec. No. (Geol. Symp.), pp.31-
50.

Bird, M. L., and Clark, A. L., (1976). Microprobe study
of olivine-chromitites of the Goodnews Bay ultra-
mafic complex, Alaska and the occurrence of the
platinum. *U. S. Geol. Surv. J. Res.,* V.4, pp.
717-725.

Bliss, N.W., and MacLean W.H., (1975). The paragenesis
of zoned chromite from central Manitoba. *Geochim.*
Cosmochim. Acta., V.39, pp. 973-990.

Bodinier, J.L., Guiraud, M.,Fabries, J., Dostal, J., and
Dupuy, C., (1987). Petrogenesis of layered pyroxe-
nites from the Lherz, Freychinede and Prades
ultramafic bodies (Ariege, French Pyrenees).
Geochim. Cosmochim. Acta., V.51, pp.279-90.

Bonavia, F.F., Diella, V., and Ferrario, A., (1993).
Precambrian Podiform Chromitites from Kenticha Hill,
Southern Ethopia. *Econ. Geol.,* V.88, pp.198-202.

Boyd, F.R., (1973). A pyroxene geothermometer. *Geochim.*
Cosmochim. Acta., V.37, pp.2533-2546.

Brown, G.M.,(1967). Experimental studies on inversion
relations in natural pigeonite pyroxenes. *Ann.*
Rept. Geophys. Lab. (Carnegie Inst. Yrbk. 66).,

pp.347-353.

Brown, G.M.., and Vincent, E.A., (1963). Pyroxenes from late stages of fractionation of the Skaergaard intrusion, East Greenland. *J. Petrol.,* V.4, pp. 175-197.

Browne, P.R.L., (1978). Hydrothermal alteration in active geothermal fields: Ann. Reviews *Earth Planet. Sci. Lett.,* V.6, pp.229-250.

Brunn, J.E., (1956). Contribution a` l'e`tude ge`ologique du pinde septentrionate et d`unepartie` de la Mace`donie Occidentale, Ann. Geol. Pays Helle`niques 1st ser 7. In Sapountzis E.S. (1979). The Thessaloniki gabbros. *J. Petrol.,* V.20, pp.37-70.

Buddington, A.F., (1936). Gravity stratification as a criterion in the interpretation of the structure of certain intrusives of the Northwestern Adironacks. *Rept. 16th Inter. Geol. Congr.* , Washington.

Burns, R.G., (1973). The partitioning of trace transition elements in crystal structure: a provocative review with applications to mantle geochemistry. *Geochim. Cosmochim. Acta.,* V.37, pp.2395-2403.

Burrows, D.R., Wood, P.C., and Spooner, E.T.C., (1986).

Carbon isotope evidence for a magmatic origin for Archaean gold-quartz vein deposits. *Nature*, V.321, pp.851-854.

Cameron, E.N., (1975). Postcumulus and subsolidus equilibration of chromite and coexisting silicates in the eastern Bushveld complex. *Geochim. Cosmochim. Acta.*, V.39, pp.1021-1033.

Cameron, E.N., (1977). Chromite in the central sector of the Eastern Bushveld Complex. *S. Africa. Am. Mineral.*, V.62, pp.1082-1096.

Cameron, E.N., (1978). The lower zone of the eastern Bushveld complex in the Olifants River trough : *J. Petrol.*, V.19, pp.437-462.

Cameron, E.N., (1979). Titanium-bearing oxide minerals of the critical zone of the eastern Bushveld Complex. *Am. Miner.*, V.64, pp.140-140.

Cameron, E.N., and Desborough, G.A., (1969). Occurrence and characteristics of chromite deposits - Eastern Bushveld Complex, in *Magmatic Ore Deposits*, H.D.B. Wilson, (Ed.), Econ. Geol. Mono. 4, pp.23-40.

Cameron, E.N., and Emerson, M.E., (1959). The origin of certain chromite deposits in the eastern part of the Bushveld Complex. *Econ. Geol.*, V.54, pp.1151-1213.

Campbell, I.H., (1985). The difference between oceanic and continental tholeiites: a fluid dynamic explanation. *Contr. Miner. Petrol.,* V.91, pp.37-43.

Campbell, I.H., and Turner, J.S., (1986). The role of convection in the formation of platinum and chromite deposits in layered intrusions. *Mineralog. Assoc. Canada Short Course Handbook.* V.12, pp.236- 278.

Carmichael, I.S.E., (1960). The pyroxenes and olivines from some Tertiary acid glasses. *J. Petrol.,* V.1, pp.309-336.

Cheng Chung, (1969). Genetic types of chromite deposits based on their textures and structures. *Int. Geol. Rev.,* V.11(4), pp.428-439.

Christie, D.M., and Sinton, J.M., (1981). Evolution of abyssal lavas along propagating segments of the Galapagos spreading center. *Earth Planet. Sci. Lett.,* 56, 321-335.

Condie, K.C.., (1976a). Trace-element geochemistry of Archaean greenstone belts. *Earth Sci. Rev.,* V.12, pp.393-417.

Condie, K.C., (1977b). Trace element models for the origin of Archaean volcanic rocks: In Windley, B. F. (Ed.) *Early History of the Earth,* London, John Wiley and

Sons, pp.419-424.

Cox, K.G., (1980). A model for flood basalt vulcanism. *J. Petrol.*, V.21(4), pp.629-650.

Cullers, R.L., and Graf, J.L., (1984). Rare earth elements in igneous rocks of the continental crust: predomi antly basic and ultrabasic rocks. In: Henderson, P.(Ed.) *Rare Earth Element Geochemistry: Developments in Geochemistry 2.*, Elsevier, Amsterdam, pp.235-274.

DeBari , S.M., (1994). Petrogenesis of the Fiambal'a gabbroic Intrusion, Northwestern Argentina, a deep crustal syntectonic pluton in a continental magmatic arc. *J. Petrol.*, V.35, pp.679-713.

DeBari, S.M., and Coleman, R.G., (1989). Examination of the deep levels of an island are: evidence from the Tonsina ultramafic-mafic assemblage, Tonsina, Alaska. *J. Geophys. Res.*, V.94, pp.4373-91.

Dessai, A.G., (1978). Thermal study of manganese oxide and hydroxide minerals from Sanguem district, Goa, India. *Jour. Mines Metals and Fuels,* V.26, pp.193-196.

Dessai, A.G.,(1980). Infrared and thermal studies on the Iron ores from parts of Goa, *Jour. Mines, Metals and Fuels,* V.28, pp.166-169.

Dessai, A.G., (1984). Lithomarges from Goa a study based on infrared spectroscopy and differential thermal analysis. *Jour. Geol. Soc. Ind.,* V.25, pp.598-603.

Dessai, A.G., (1985a). An Appraisal of the Manganese Ore Deposits of Goa, India. *Proc. Ind. Nat. Sci. Acad.,* V.51, A; pp.1021-1032.

Dessai, A. G., (1985b). Mineralogy and genesis of clay deposits from Sanvorde Goa, India. *Proc. Ind. Nat. Sci. Aca.,* V.51, pp.432-440.

Dessai, A.G., and Deshpande, G.G., (1977a). Occurrence of Nsutite (gamma-MnO2) in the Manganese Ores, Sanguem district, Goa, India. *Curr. Sci.,* V.46, pp.816-817.

Dessai, A.G., and Deshpande, G.G., (1977b). Chrysotile Asbestose occurrence in the ultramafic rocks of Sanguem district, Goa, India. *Curr. Sci.,* V.16, pp.816-817.

Dessai, A.G., and Deshpande, G.G., (1978). Manganese Ore Deposits of India. *Berg u Huttenmannische Monatschefte,* V.123. pp.465-468.

Dessai, A.G., and Deshpande, G.G., (1979a). Mode of Occurrence, controls of localisation and genesis of the manganese Ore deposits from Sanguem district, Goa, India. *Geoviews,* V.5, pp.21-29.

Dessai, A.G., and Deshpande, G.G., (1979b). Komatiites from Sanguem area, Goa, India. *N. Jb. Miner. Abh.*, V.135, pp.209-220.

Dessai, A.G., and Deshpande, G.G., (1979c). Komatiite dykes from Sanguem area, Goa, India. *Bull. Earth Sci.*, V.7, pp.5-15.

Dessai, A.G., and Peshwa, V.V., (1982). Manganese Mineralisation in a tropical forest area, Goa, India: A study based on aerial photographs and Landsat-1 imagery interpretation. In: Haming, D.J.C. and Gibbs, A.K. (Ed.) *Hidden Weath: Mineral Explotation Techniques in Tropical Forest areas*, pp.170-175.

Dessai, A.G., and Warrier, S., (1986). Mineralogy of clays from laterites on gneissic rocks, Colva, Goa, India. *Gond. Geol. Mag.*, V.1, pp.25-33.

Dessai, A.G., French, D. and Arolkar, D.B., (1994). Mineralogy of polymetallic sulphide mineralisation in Archaean greenstones at Tisk-Usgaon, Goa, India. *Curr. Sci.*, V.66, pp.824-825.

Dhepe, P.D., (1963). A note on the geology and iron and manganese ore deposits of Goa. *Jour. Univ. Poona*, V.4, pp.28-29.

Dhoundiyal, D.P., Paul, D.K., Sarkar, A., Trivedi, J.R.,

Gopalan, K., and Potts, P.J., (1987). Geochronology and Geochemistry of Precambrian Granitic Rocks of Goa, Southwest India. *Precambrian Research,* V.36, pp. 287-302.

Dick, H.J.B., (1977). Partial melting in the Josephine peridotite: B 1, The effect on mineral composition and its consequences for geobarometry and geothermometry. *Am. J. Sci.,* V.277, pp.801-32.

Dick, H.J.B., and Bullen, T., (1984). Chromian spinel as petrogenetic indicator in abyssal and alpine-type peridotit/es and spatially associated lavas. *Contr. Miner. Petrol.,* V.86, pp.57-76.

Dickey, J.s., Jr., (1975). A hypothesis of origin for podiform chromite deposits. *Geochim. Cosmochim. Acta,* V.39, pp.1061-1074.

Dickey, J.S.,Jr., Yoder, H.S., Jr. (1972). Partitioning of chromium and aluminium between clinopyroxene and spinel. *Carnegie Inst. Wash. Yearb.,* V.73, pp.384-392.

Dunn, J.A., (1942). Manganese Ore. *Geol. Surv. Ind. Rec.,* V.76, pp.53.

Eales, H.V., (1987). Upper Critical Zone chromite layer at RPM Union Mine, Western Bushveld complex, in Stowe C.W. (Ed). *Evolution of chromium Ore fields: New*

York, Van Nostrand-Reinhold, pp.144-168.

Eales, H.V., and Marsh. J.S., (1983). Al/Cr ratios of coexisting pyroxenes and spinellids in some ultramafic rocks. *Chem. Geol.,* V.38, pp.57-74.

Eales, H.V., and Reynolds, I.M., (1985). Factors influencing the composition of chromite and magnetite in some Southern African rocks. *Geol. Soc. S. Afr. Spec. Pub.,* V.7, pp.5-20.

Eales, H.V., de Klerk, W.J., and Teigler, B., (1990). Evidence for magma mixing processes within the critical and lower zones of the northwestern Bushveld complex, *Chem. Geol.,* V.88, pp.261-278.

Edwards, R., and Atkinson, K., (1986). *Ore Deposit Geology.* Chapman and Hall. 466p.

Elthon, D., Casey, J.F., and Komor, S., (1982). Mineral chemistry of ultramafic cumulates from the North Arm mountain massif of the Bay of Islands ophiolite: evidence for high pressure crystal fractionation of oceanic basalts. *Geophys. Res.,* V.87, pp.8717-8734.

Evans, B.W., and Frost, B.R., (1975). Chromian spinel in progressive metamorphism - a preliminary analysis. *Goechim. Cosmochim. Acta.,* V.39, pp.959-972.

Evans, B.W., and Wright, T.L., (1972). Composition of liquidus chromite from the 1959 (Kilauea Iki) and

1965 (Makaopuhi) eruptions of Kilauea volcano, Hawaii, *Am. Mineral.*, V.57, pp.217-230.

Fallon, T., and Green, D.H., (1987). Anhydrous partial melting of MORB pyrolite and other peridotite compositions at 10 kbar: implications for the origin of primitive MORB glasses. *Miner. Petrol.*, V.37, pp.181-219.

Fenner, C. N., (1929). The crystallisation of basalts. *Am. J. Sci.*, V.18, pp.225-253.

Fermor, L.L., (1909). Manganese Ore deposits of India. *Geol. Surv. Ind. Mem.*, V.37, pp.1-371.

Fermor, L.L., (1936). An attempt at the correlation of the ancient schistose formations of Peninsular India. *Mem. Geol. Surv. Ind.*, V.70, pp.53-218.

Fisk, M. E., and Bence, A.E., (1980). Experimental crystallisation of chrome spinels in FAMOUS basalt 527-1-1. *Earth Planet. Sci. Lett.*, V.75, pp.111-23.

Flannagan, F. J., (1967). U. S. Geological Survey silicate rock standards. *Geochim. Cosmochim. Acta.*, V.31, pp.289-308.

Floyd, P. M., and Winchester, J. A., (1975). Magma type and tectonic setting discrimination using immobile elements. *Earth Planet. Sci. Lett.*, V.27, pp.211-218.

←Foote, R. B., (1876). Geological features of the south Mahratta country and adjacent districts. *Mem. Geol. Soc. Ind.,* V.12, pp.1-268.

Fugi, T., and Scarfe, C. M., (1985). Compositions of liquids coexisting with spinel lherzolite at 10kb and the genesis of MORBs. *Earth Planet. Sci. Lett.,* V.90, pp.18-28.

Fyfe, W.S., and Kerrich, R., (1984). Gold: natural concentration processes. *In Gold' 82.* A.A. Balkema, Rotterdam, The Netherlands, pp.99-127.

Gast, P. W., (1968). Trace element fractionation and the origin of tholeiitic and alkaline magma types. *Geochim. Cosmochim. Acta.,* V.32, pp.1057-1068.

Gokulam, A.R., (1972). Iron Ore deposits of Goa. *Geol. Surv. Ind. Bull.,* V.37, pp.1-186.

Gokul, A.R., (1985). Structure and tectonics of Goa. *Earth resources for Goa's development. Goa Seminar Volume, Geol.Surv.Ind.,* pp.14-21.

Gokul, A. R., and Srinivasan, M.D., (1976). Chandranath Granite, Goa. *Rec. Geol. Surv. Ind.,* V.107, pp.38-45.

Gokul, A. R., Srinivasan, M. D., Gopalkrishnan, K., and Vishwanathan, L. S., (1985). Stratigraphy and structure of Goa. *Earth Resources for Goa's*

development. *Goa Seminar Volume, Geol. Surv. Ind.,* pp.1-13.

Golding, H.G., (1975). Relict Textures of chromitites from New South Wales; *Geol. Soc. Australia Jour.,* V.22, pp.397-412.

Gopalkrishnan, K., (1976). Canacona granite and its relation to the schistose rocks, Canacona taluk, Goa. In Karunakaran C., (Ed.) Seminar on Precambrian Geology of the Peninsular Shield . Geol. Surv. Ind. Calcutta, 1971, V.51, *Geol. Surv. Misc. Publ.,* V.23(2), pp.375-379.

Green, D.H., and Hibberson, W., (1970). The instability of plagioclase in peridotite at high pressure. *Lithos,* V.3, pp.209-21.

Greenbaum, D., (1977). The chromitiferous rocks of the Troodos ophiolite complex, Cyprus. *Econ. Geol.,* V.72, pp.1175-1194.

Hall, A. L., (1932). The Bushveld Igneous Complex of the Central Transvaal. *Mem. Geol. S. Afr.* No.28, 554pp.

Haskins, L. A., and Haskin, M.A., (1968). Rare-earth elements in the Skaergaard intrusion. *Geochim. Cosmochim. Acta.* V. 32, pp.433-447.

Hatton, C.J., and von Gruenewaldt, G., (1987). The Geological setting and petrogenesis of the Bushveld chromite

layers. In: Stowe, C.W. (Ed). *Evolution of Chromium Ore Fields*. Van Nostrand-Reinhold, New York, pp.109-143.

Helz, R. T., (1973). Phase relations of basalts in their melting range at PH_2O = 5kb as a function of oxygen fugacity: Part I. Mafic phases. *J. Petrol*. V.14, pp.249-302.

Henderson, P., (1975). Reaction trends shown by chrome-spinels of the Rhum layered intrusion. *Geochim. Cosmochim. Acta.*,V. 39, pp.1035-1044.

Herbert, R., (1982). Petrography and Mineralogy of oceanic peridotites and gabbros: Some comparisons with ophiolite complexes. *Ofioliti*.V.7, pp.299-324.

Hill, R., and Roeder, P., (1974). The crystallisation of spinel from basaltic liquid as a function of oxygen fugacity. *J. Geol.*, V.82, pp.709-729.

Hoffman, M.A., and Walker, D., (1978). Textural and chemical variations of olivine and chrome spinel in the East Dover ultramafic bodies, Vermont. *Geol. Soc. Am. J. Sci.*,V.280-A, pp.232-268.

Holloway, J. R., and Burnham, C. W., (1972). Melting relations of basalt with equilibrium water pressure less than total pressure. *J. Petrol.*,V.13, pp.1-29.

164

Hopson, C. A., (1964). "Crystalline rocks", in Geology of Howard and Montgomery Counties. *Maryland Geol. Surv. County Rept.*, 257 p.

Hutchison, R. W., and Burlington, J. L., (1984). Some broad characteristics of greenstone belt lodes. In Foster, R.P. (Ed.) *Gold' 82:* The Geology, Geochemistry and Genesis of Gold Deposits, Geological Society of Zimbabwe, A.A. Balkema, Rotterdam, pp.339-369.

IMA (1988). Nomenclature of pyroxenes. *Mineral Mag.*, V.52, pp.535-550.

Ingerson, E., (1935). Layered peridotitic laccoliths of the Trout River area, Newfoundland. *Amer. J. Sci.*,V. 33, pp. 389-392.

Irvine, T. N., (1967). Chromian spinel as a petrogenetic indicator, Part 2, Petrologic applications. *Can. J. Earth Sci.,* V.4, pp.71-103.

Irvine, T. N., (1975). Origin of chromitite layers in the Muskox intrusion and other stratiform intrusions: a new interpretation. *Geology,* V.5, pp.273-277.

Irvine, T. N., (1977). Chromite crystallisation in the join $Mg_2SiO_4-CaMgSi_2O_6-CaAl_2Si_2O_8-MgCr_2O_4-SiO_2$. *Carnegie Inst. Washington Yearb.,* V.75, pp. 597-611.

Irvine, T.N., (1982). Terminology for layered intrusions. *J. Petrol.*, V.23, pp.127-162.

Irvine, T. N., and Baragar, W. R. A., (1971). A guide to the chemical classification of the common volcanic rocks. *Can. J. Earth Sci.*, V.8, pp.523-548.

Irvine, T. N., and Smith, C. H., (1969). Primary oxide minerals in the layered series of the Muskox intrusion, In Wilson, H.D.B.,(Ed.), *Magmatic Ore Deposits, Econ. Geol. Mon.*, V.4, pp.76-94.

Jackson, E. D., (1961). Primary textures and mineral associations in the Ultramafic Zone of the Stillwater complex, Montana. *U.S. Geol. Surv. Prof. Paper*, V.358, pp.1-106.

Jackson, E.D., (1966). Liquid immiscibility in chromitite seam formation - a discussion. *Econ. Geol.*, V.61, pp.777-780.

Jackson, E. D., (1967). Ultramafic cumulates in the Stillwater, Great Dyke, and Bushveld intrusions. In: Wyllie, P.J. (Ed.), *Ultramafic and Related Rocks,* John Wiley and Sons, New York, pp.20-38.

Jackson, E.D., (1969). Chemical variation in co-existing chromite and olivine in chromite zones of Stillwater complex. In Wilson, H.D.B. (Ed.), *Magmatic Ore Deposits,* pp.41-71.

Jan, M. Q., and Windley, B. F., (1990). Chromian spinel -silicate chemistry in ultramafic rocks of the Jijal complex, Northwestern Pakistan. *J. Petrol.,* V.31, Part-3, pp.667-715.

Jan, M.Q., Windley, B.F., and Abbas, S.G., (1984). Microprobe analytical data on chromites from the Muslim-bagh Ophiolite, Pakistan, *Geol.Bull. Univ. Peshawar,* V.17, pp.1-16.

Jan, M.Q., Windley, B.F., and Khan, A.A., (1985). The Waziristan Ophiolite, Pakistan. General geology and geochemistry of chromite and associated phases: *Econ. Geol.,* V.80, pp.249-306.

Jena, B. K., (1985). Usgaon ultramafic - gabbro complex, Goa. *Jour. Geol. Soc. Ind.,* V.26, pp.492-495.

Jensen, M.L., and Bateman, A.M., (1979). *Economic Mineral Deposits.* John Wiley and Sons, New York. 593p.

Jessop, A. M. and Lewis, T., (1978). Heat flow and heat generation in the Superior Province of the Canadian Shield. *Tectonophysics.* V.50, pp.55-77.

Karunakaran, C., (1970). Ultramafic and related rocks of Peninsular India. Proc. *2nd Symp. Upper Mantle, Nat. Geophy. Research Inst.,* pp.370-376.

Keith, M. L., (1954). Phase equilibria in the system

MgO-Cr$_2$O$_3$-SiO$_2$. *J. Am. Ceram. Soc.*, V. 37, pp.490-496.

Krishnan, M. S., (1968). *Geology of India and Burma* Higginbotham's Ltd., Madras, 536 p.‖Kuno, H.,(1960). High - alumina basalts. *J. Petrol.*, V.1, pp.121-145.

Kushiro, I., (1960). Si - Al relations in clinopyroxenes from Igneous Rocks. *Am. J. Sci.*, V.258, pp.548-554.

Kushiro, I., and Yoder, H. S., (1966). Anorthite-forsterite and anorthite-enstatite reactions and their bearing on the basalt-eclogite transition. *J. Petrol.*, V. 7, pp.373-362.

Leblanc, M., (1985). Les gisements de spinelles chromife`res. *Bull. Mineral.*, V.108, pp.587-602.

Leblanc, M., Dupuy, C., Cassard, D., Moutte, J., Nicolas, A., Prinzhofer, A., Rabinovitch, M., and Routhier, P., (1980). Essai sur la gen'ese des corps podiformes de chromite dans les p'eridotites ophiolitiques: 'etude des chromites de Nouvelle-Cal'edonie et comparison avec celles de M'editerran'ee orientale. In: Panayiotou, A. (Ed.), Ophiolites, Proc. Intern. Ophiolite Symp., Cyprus, *Geol. Surv. Cyprus Publ.*, pp.691-701.

Le Maitre, R.W., (1976). The chemical variability of

some common igneous rocks. *J. Petrol.*, V.17, pp.589-637.

Lindsley, D.H., (1983). Pyroxene thermometry. *Am. Miner.*, V.68, pp.477-493.

Maclaren, M.A., (1904). General Reports. *Geol. Surv. Ind. Rec.*, pp.96-131.

Majumdar, A.K., (1965). Mineralogy of the iron and manganese ores of Sanguem district of Goa. *Mineral Wealth,* V.1, pp.14-20.

McDonald, J. A., (1965). Liquid immiscibility as a factor in chromitite seam formation in the Bushveld Complex. *Econ. Geol.*, V. 60, pp. 1674-1685.

Mc Donald, J.A., (1967). Evolution of the part of the lower critical zone from Reighock western Bushveld. *J. Petrol.*, V.8, pp.165-209.

Malpas, J., and Robinson., P.J., (1987). Chromite mineralisation in the Troodos Ophiolite, Cyprus, In: Stowe, C.W. (Ed). *Evolution of Chromium Ore Fields,* Van Nostrand-Reinhold, New York, pp.220-237.

Meschede, M., (1986). A method of discriminating between different types and mid-ocean ridge basalts and continental tholeiites with the Nb-Zr-Y diagram. *Chem. Geol.*, V.56, pp.195-205.

Middlemost, E.A.K., (1975). The Basalt Clan. *Earth Sci.*

Rev., V.11, pp.337-364.

Mysen, B. O., and Kushiro, I., (1977). Compositional variations of coexisting phases with degree of melting of peridotite in the upper mantle. *Am. Mineral.,* V.62, pp.843-865.

Naqvi. S. M., and Hussein, S. M., (1979). Geochemistry of meta-anorthosites from a greenstone belt in Karnataka, India. *Can. Jour. Earth Sci.,* V.16, pp. 1254-1264.

Naqvi, S. M., and Rogers, J. J. W., (1987). Precambrian Geology of India. *Oxford Monographs on Geology and Geophysics,* No.6, Oxford University Press, Oxford, 223p.

Nautiyal, S.P., (1967). Precambrians of Mysore Plateau. *Proc. Ind. Sci Congr.,* V.53, pp.1-14.

Nicholls, I.A., and Harris, K.L., (1980). Experimental rare earth element partition coefficients for garnet, clinopyroxene and amphibole coexisting with andesitic and basaltic liquids. *Geochim. Cosmochim. Acta.,* V.22, pp.287-308.

Nijagunappa, R., and Naganna, C., (1983). Nuggihalli schist belt in the Karnataka craton: An Archaean layered complex as interpreted from chromite distribution. *Econ. Geol.,* V.78, pp.507-513.

Oertal, G., (1958). A Geologia do Distrito de Goa. *Geological Services of Portugal,* Lisbon.

O'Hara, M. J., (1977). Geochemical evolutoin during fractional crystallization of a periodically refilled magma chamber. *Nature,* V.266, pp.503-507.

Page, N. J., (1977). Stillwater Complex, Montana: rock succession, metamorphism and structure of the complex and adjacent rocks. *U. S. Geol. Surv. Prof. Paper,* pp.1-79.

Park, C.F. Jr., and Mac Diarmid, R.A., (1975). *Ore Deposits.* W.H.Freeman and Company, San Francisco, 475p.

Pascoe, E. H., (1965). A Manual of Geology of India and Burma. Govt. of India, New Delhi 1, 485p.

Pearce, J.A., (1979). Geochemical evidence for the genesis and eruptive setting of lavas from Tethyan Ophiolites. In Panayiotou, A., (Ed.),*Ophiolites.* Edited by A. Panayiotou, Proc. Inter. Ophiolite Symp. Geol. Surv. Cyprus, Publ., pp.261-272.

Pearce, J.A., (1983). Role of the sub continental lithosphere in magma genesis at active continental margins. In Hawkesworth, C.J., and Norry, M.J., (Eds.),*Continental basalts and mantle xenoliths.* Shiva Publishing Limited, Nantwich, United Kingdom, pp.230-249.

Pearce, T.H., and Birkett, T.C., (1974). Archaean metavolcanic rocks from Thackeray Township, Ontario. *Can. Miner.*, V.12, pp.509-519.

Pearce, J.A., and Cann, J.R., (1973). Tectonic setting of basic volcanic rocks determined using trace element analyses. *Earth Planet. Sci. Lett.*, V.19, pp.290-300.

Pearce, J.A., and Norry, M.J., (1979). Petrogenetic implications of Ti, Zr, Y and Nb variations in volcanic rocks. *Contr. Miner. Petrol.*, V.69, pp.33-47.

Peoples, J.W., (1936). Gravity stratification as a criterion in the interpretation of the structure of the Stillwater, *Montana. Rept. 16th Inter. Geol. Congr.*, Washington, pp.353-360.

Pharaoh, T. C., and Pearce, J. A., (1984). Geochemical evidence for the geotectonic setting of early Proterozoic metavolcanic sequences in Lipland, *Precambrian Research*, V.25, pp.283-308.

Philips, G. N., Groves, D. I., and Martyn, J. E., (1984). A epigenetic origin for Archaean banded iron-formation-hosted gold deposits: *Econ. Geol.*, V.79, pp.162-171.

Pichamuthu, C.S., (1956). The problem of the ultrabasic rocks. *Proc. Mysore Geol. Assoc.*, pp.12.

Pichamuthu, C.S., (1968). The Precambrian of India. In

Rankama K. (Ed.) *Geological System*. Interscience, London.

Radhakrishna, B. P., (1974). Peninsular Gneissic Complex of the Dharwar Craton, a suggested model for its evolution. *Jour. Geol. Soc. India,* V.15, pp.439- 454.

Radhakrishna, B.P., (1983). Archaean granite-greenstone terrain of South Indian Shield. In Naqvi, S.M., and Rogers, J.J.W., (Ed.),*Precambrian of South India, Geol. Soc. India Mem. 4,* pp.1-46.

Rama Rao, B., (1940). Archaean complex of Mysore. *Bull. Geol. Dept.* No.17, pp.1-95.

Rama Rao, B., (1962). A Handbook of the Geology of Mysore State, Southern India, Bangalore Printing and Publishing Co., Bangalore, 264p.

Ramdohr, P., (1980). The ore minerals and their inter-growths, Oxford, Pergamon, Oxford, V.2, 207p.

Rammlmair, D., Raschka, H., and Steiner, L., (1987). Systematics of Chromite occurrences in Central Palawan, Phillipines, *Miner. Deposita,* V.22, pp.190-197.

Rao, R. U. M., Rao, G. V., and Narain, H., (1976). Radioactive heat generation and heat flow in the Indian shield. *Earth Planet. Sci. Lett.,* V. 30, pp.57-64.

Reynolds, I.M., (1985). The nature and origin of titaniferous magnetite-rich layers in the upper zone of the

Bushveld Complex: a review and synthesis. *Econ. Geol.*, V.80, pp.1089-1108.

Rhodes, J.M., (1981). Characteristic of primary basalt magmas. In: *Basaltic Volcanism on the terrestrial planets,* Pergamon, Oxford, pp.409-452.

Rivalenti, G., Garuti, G., Rossi, A., Siena, F., and Sinigoi, S., (1981). Chromian spinel in the Ivrea - Verbano layered igneous complex, Western Alps, Italy. *Tschermaks Miner. Petr. Mitt.,* V.29, pp.33- 53.

Rock, N.M.S., and Groves, D.I., (1988). Can lamprophyres resove the genetic controversy over mesothermal gold deposits? *Geology,* V.16, pp.538-541.

Rodgers, K.A., (1973). Chrome-spinels from the Massif du Sud, southern New Caledonia. *Miner. Mag.* V.39, pp.326-339.

Roeder, P. L., and Emslie, R. F., (1970). Olivine - liquid equilibrium. *Contr. Miner. Petrol.,* V.29, pp.275-289.

Roeder, P.L., and Reynolds, I., (1991). Crystallisation of chromite and chromian solubility in basaltic melts. *J. Petrol.,* V.32, pp.909-934.

Sahu, K.C., and Gurav, R.P., (1972). The nature and origin of the blue dust in Precambrian iron Ore. *Jour. Geol. Soc. Ind.,* V.13, pp.30-38.

Sapountzis, E. S., (1979). The Thessaloniki gabbros. *J.*

174

Petrol., V.20, pp.37-70.

Sato, T., (1972). Behaviour of ore forming solutions in sea water. *Mining Geology,* V.22, pp.31-42.

Serri, G., (1981). Petrochemistry of ophiolite gabbroic complexes: a key for the classification of ophiolites into low-Ti and high-Ti types. *Earth Planet. Sci. Lett.,* V.51, pp.203-212.

Shapiro, L., and Brannock, W.W., (1962). Rapid analysis of silicate, carbonate and phosphate rock. *U.S.Geol. Surv. Bull.,* V.1144-A, pp.1-56.

Shervais, J. W., (1982). Ti-V plots and the petrogenesis of modern ophiolitic lavas. *Earth Planet. Sci. Lett.,* V.59, pp.101-118.

Slemmons, D. B., (1962). Determination of volcanic and plutonic plagioclase using a three or four axis Universal stage. *Geol. Soc. Amer., Special paper,* 69p.

Smeeth, W. F., (1916). Outline of the geological history of Mysore. *Bull. Dept. Mines and Geol.,* Mysore State, No.6, pp.22.

Spangenberg, K., (1943). Die Chromitlager statte von Jampadal am Zobten E: *Zeitschr. Parakt, Geologie,* V.5, pp.13-35.

Spry, A., (1969). Metamorphic textures. Pergamon, Oxford. 350 p.

Srikantappa, C., Friend, C.R.L., and Janardhan, A.S. (1980). Petrochemical studies on chromites from Sindhuvalli, Karnataka, India. *Jour. Geol. Soc. Ind.*, V.94, pp.199-214.

Srikantappa, C., Hormann, P.K., and Raith, M., (1984). Petrology and Geochemistry of layered ultramafic-mafic complexes from the Archaean craton of Karnataka, south India. In Kroner, A., Hanson, G.N., and Goodwin, A.M., (Eds.), *Archaean Geochemistry,* Elsevier, pp.138-161.

Stowe, C.W., (1994). Compositions and tectonic settings of Chromite deposits through time. *Econ. Geol.*, V.89, pp.528-546.

Streckeisen, A. L., (1974). Classification and nomenclature of plutonic rocks. *Geol. Rundsch.*, V.63(2), pp.773-786.

Sudhakar, K.S., (1980). Pillow structures in serpentinites, Tagadur, Nuggihalli Schist belt, Karnataka. *Earth Planet. Sci. Lett.*, V.89, pp.117-119.

Suen, C. J., and Frey, F. A., (1987). Origin of the mafic and ultramafic rocks in the Ronda peridotite. *Earth Planet. Sci. Lett.*, V.85, pp.183-202.

Sun, S. S., and Nesbitt, R. W., (1977). Chemical hetero-
geneity of the Archaean mantle, composition of the
earth and mantle evolution. *Earth Planet. Sci.
Lett.,* V.35, pp.429-448.

Sun, S. S., and Nesbitt, R. W., (1978). Petrogenesis of
Archaean ultrabasic basic volcanics: evidence from the
rare earth elements. *Contr. Miner. Petrol.,* V.65,
301p.

Swami Nath, J., and Ramakrishan, M.,(1981). Early Precam-
brian Supracrustals of Southern Karnataka. *Mem. Geol.
Surv. Ind.,* V.112, pp.1-350.

Swami Nath, J., Ramakrishan, M.,and Vishwanatha, M. N.,
(1976). Dharwar stratigraphic model and Karnataka
cratonic evolution. *Rec. Geol. Surv. Ind.,* V.107,
pp.149-175.

Thayer, T. P., (1964). Principal features and origin of
podiform chromite deposits, and some observations on
the Gulemon-Soridag district, Turkey. *Econ. Geol.,*
V.59, pp.1497-1524.

Thayer, T. P., (1969). Gravity differentiation and magmat-
ic re-emplacement of podiform chromite deposits. In
Wilson, H.D. B., (Ed.), *Magmatic Ore Deposits , Econ.
Geol. Monogr.,* V.4, pp.132-146.

Thompson, R. N., (1982). Magmatism of the British

Tertiary Volcanic Province. *Scottish Journal of Geology,* V.18, pp.49-107.

Thompson, R. N., Hendry, G. L., and Parry, S. J., (1984). An assesment of the relative roles of the crust and mantle in magma genesis: an elemental approach. *Phil. Trans. R. Soc. Lond.,* V.A310, pp.549-590.

Ulmer, G. C., (1969). Experimental investigations of chromite spinels. *Econ. Geol., Monogr.,* No.4, pp.114-131.

Varadarajan, S., (1970). Emplacement of chromite-bearing ultramafic rocks, Mysore State, India. *Proc. Second Symp. on Upper Mantle Project, Hyderabad,* pp. 441-451.

Vaughan, D. J., and Craig, J. R., (1978). Mineral chemistry of metal sulphides: *Cambridge Univ. Press,* 493 p.

Vidyadharan, K.T., and Abbas, M.H., (1989). Preliminary investigation of base metals in Usgaon area, Goa. *Rec. Geol. Surv. Ind.,* V.122, pp.147-154.

Viljon, M.J., (1984). Archaean gold mineralisation and komatiites in Southern Africa. In Foster, R.P. (Ed). *Gold'82,* A.A. Balkema Pub., Rotterdam pp.595-628.

Vishwanathan, S., (1974). Basaltic komatiite occurrences in the Kolar Gold Field of India. *Geol. Mag.,* V.82,

pp.107-113.

Voll, G., (1960). New work on petrofabrics: *Liverpool and Manchester Geol. Jour.*, V.2, pp.503-567.

von Gruenewaldt, G., and Worst, B.G., (1986). The chromite depositioin at Zwartkop chrome mine, Western Bushveld complex, In Anhaeusser, C.R. and Maske, S. (Eds). Mineral deposits of South Africa, Johannesberg, *Geol. Surv. S.Afr.*, V.2, pp.1217- 1227.

Wager, L.R., (1968). Rhythmic and cryptic layering in mafic and ultramafic plutons, In Hess H.H and Poldervaart, A. (Eds). *Basalts,* V.2, Interscience Pub. London, pp.573-622.

Wager, L. R., and Brown, G. M., (1967). Layered Igneous Rocks. W. H. Freeman & Co., San Franscisco, 588p.

Wager, L.R., and Deer, W.A., (1939). Geological investigations in East Greenland, Pt. III. The Petrology of the Skaergaard Intrusion, Kangerdlugssauq, East Greenland. *Medd. om Gronland,*V.105, pp.1-352.

Wager, L.R., Brown, G.M., and Wadsworth, W.J., (1960). Types of igneous cumulates. *J. Petrol.*, V.1, pp.73-85.

Wilson, A. H., (1982). The geology of the Great `Dyke', Zimbabwe: the ultramafic rocks. *J. Petrol.*, V.23, pp.

240-292.

Wilson, M., (1989). Igneous Petrogenesis. Unwin Hyman, London, 446 p.

Yoeder, H. S., and Tilley, C. E., (1962). Origin of basalt magmas: an experimental study of natural and synthetic rock systems. *J. Petrol.*, V.3, pp.342-532.

ADDENDUM

Barnes, S.J., and Hoatson, D.M., (1994). The Munni Munni Complex, Western Australia. Stratigraphy, structure and petrogenesis. J.Petrol., V.35, pp.715-751.

Irvine, T.N., (1965). Chrome spinels as a petrogenetic indicator, Part 1, Theory. Can. J. Earth Sci., V.2, pp. 648-71.

Thayer, T.P., (1970). Chromite segregation as petrogenetic indicators. Spec. Publ. Geol. Soc. S. Africa, V.1, pp.533-65.

PLATE I

Photo 1 : Bondla mafic-ultramafic complex seen from

Tisk-Usgaon Road, (looking east).

Photo 2 : Silicification and brecciation seen between

Tisk and Usgaon, to the east of the road.

PLATE I
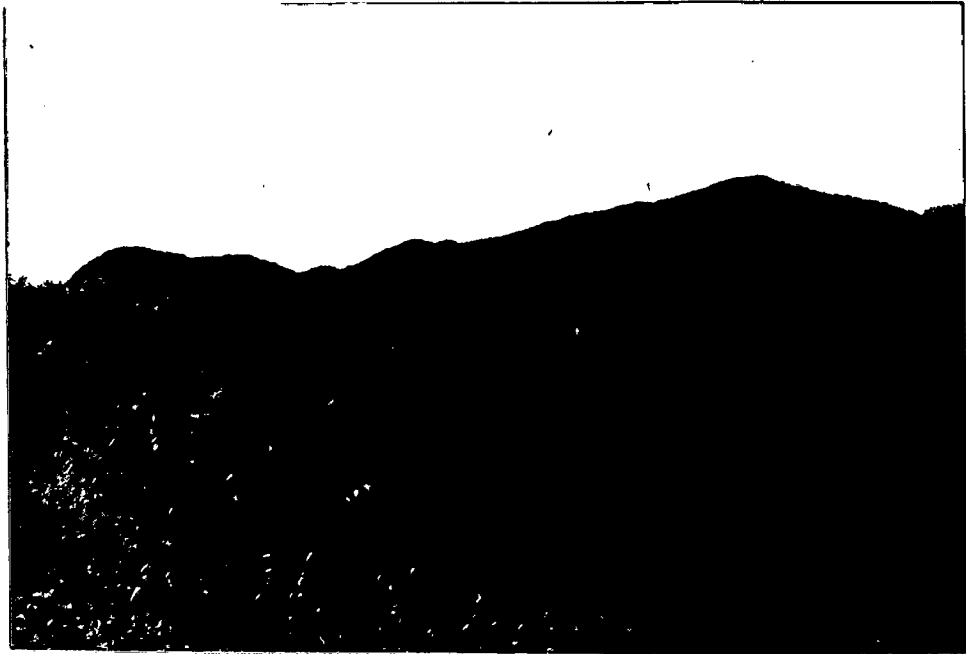
PHOTO 1

PHOTO 2

PLATE II

Photo 1 : Pinching and swelling quartz veins in the
            zone of mylonite seen between Tisk and
            Usgaon, 0.5 km east of the road.

Photo 2 : Thin chromite layers alternating with thick
            olivine-rich layers.

PLATE II

PHOTO I
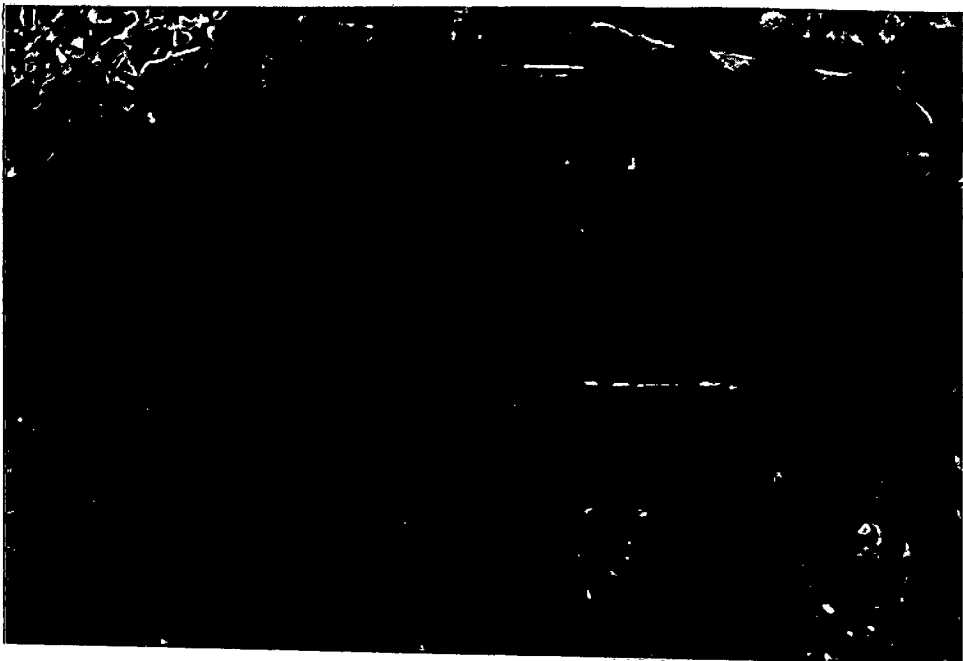
PHOTO 2

PLATE III

Photo 1 : Pulverised rocks from the zone of mylonite. (BXN)

Photo 2 : Sericite-and quartz-rich bands seen in mylonite. (BXN)

PLATE III

PHOTO 1

1200 μ

PHOTO 2

1200 μ
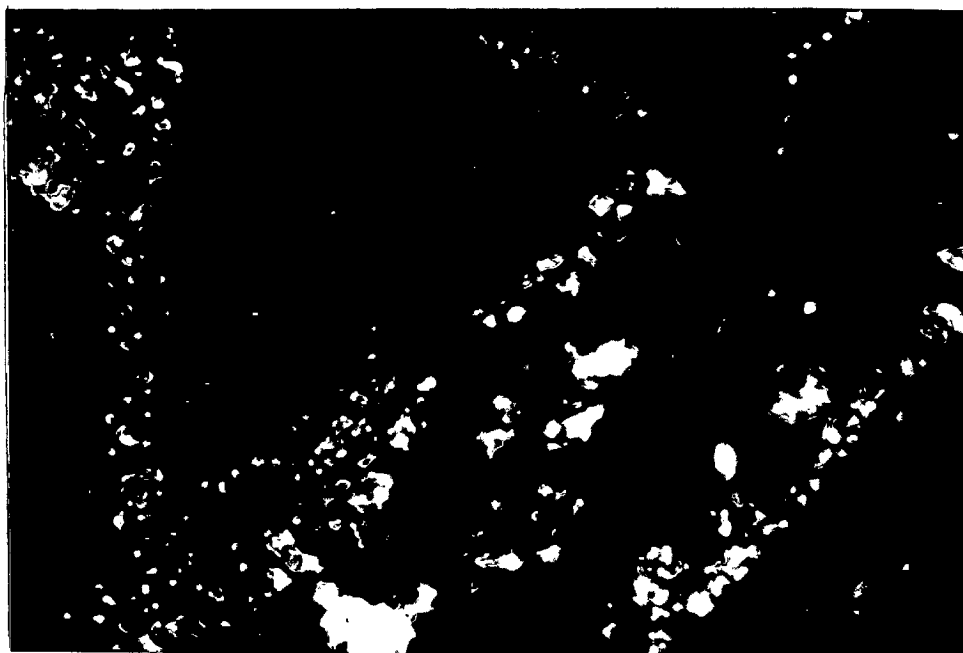
PLATE   IV

Plate 1 : Olivine (serpentinised) mesocumulate from
            dunite. (3XN)

Photo 2 : Alternating chromite and olivine-rich layers
            in peridotite.

PLATE IV

PHOTO 1

⊢————⊣
1200 μ

PHOTO 2

PLATE V

Photo 1 : Preferred alignment of olivine (serpentinised)
            within the plane of layering of peridotite.
            (BXN)

Photo 2 : Oikocrysts of Ca-poor pyroxene poikilitically
            enclosing rounded olivine and chromite.
            (BXN)

PLATE V

PHOTO 1   ⊢————⊣
200 µ
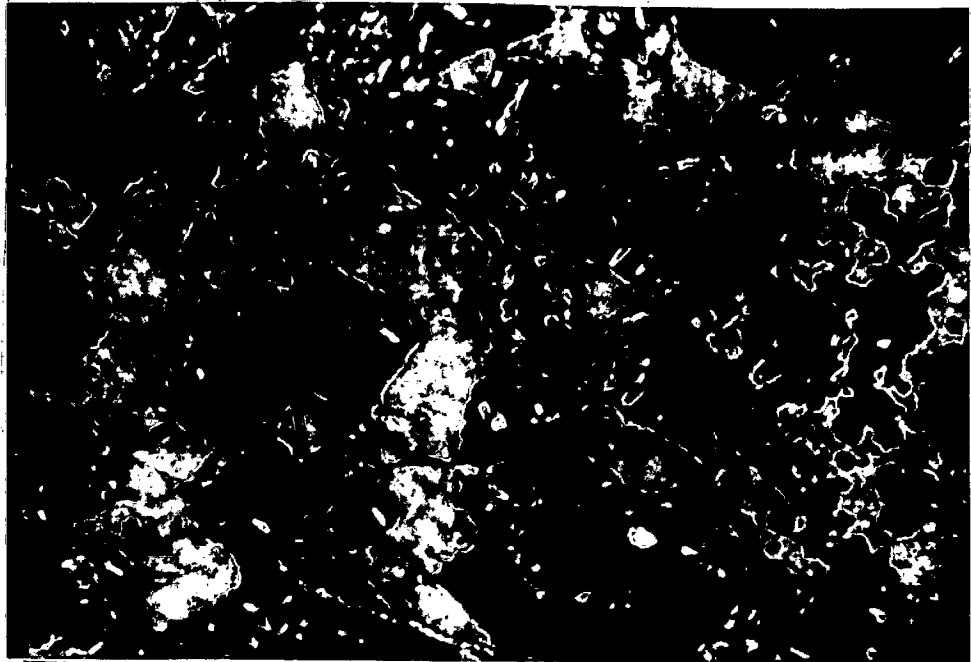
PHOTO 2   ⊢————⊣
150 µ

PLATE VI

Photo 1 : Vermicular silicates (pseudomorphs of
serpentine after olivine) poikilitically
enclosed by chromite in chromitite.
(BXN)

Photo 2 : Mosaic of subhedral chromite with rounded
silicates forming ring texture in chromitite.

PLATE VI

PHOTO I

900μ

PHOTO 2

450μ
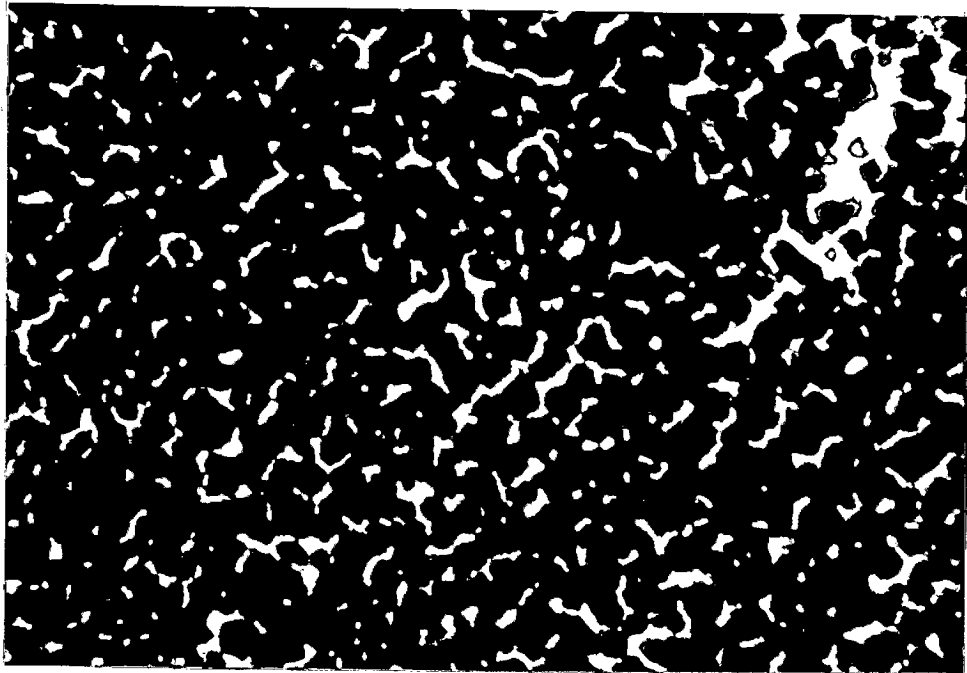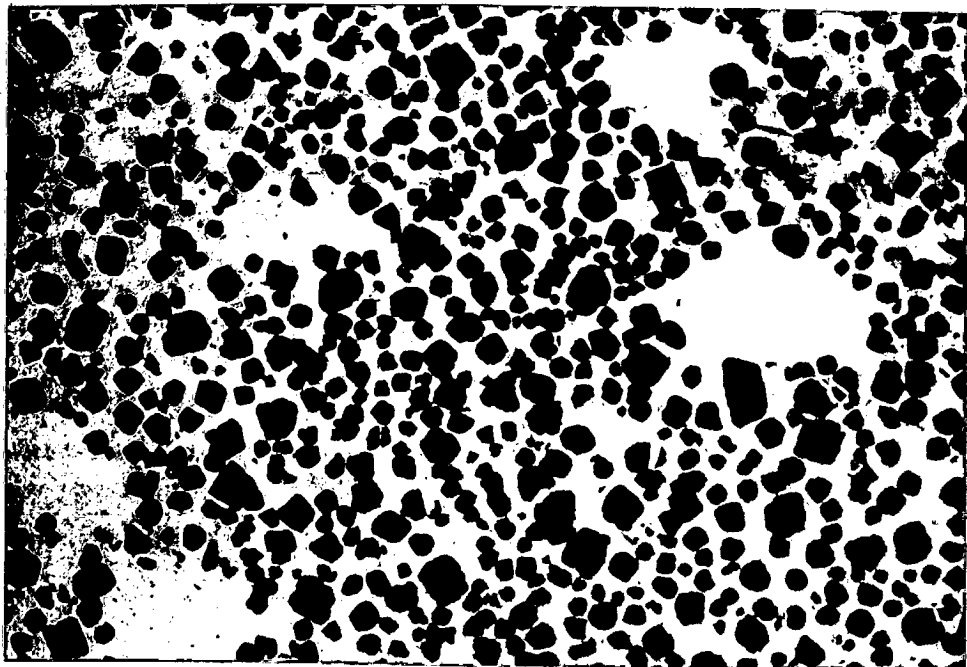
PLATE VII

Photo 1 : Exsolutions of rutile in clinopyroxene from
pyroxenite. (BXN)

Photo 2 : Rutile exsolutions at an angle to the
clinopyroxene cleavage.

PLATE VII

PHOTO 1 |—————|
                             200 µ
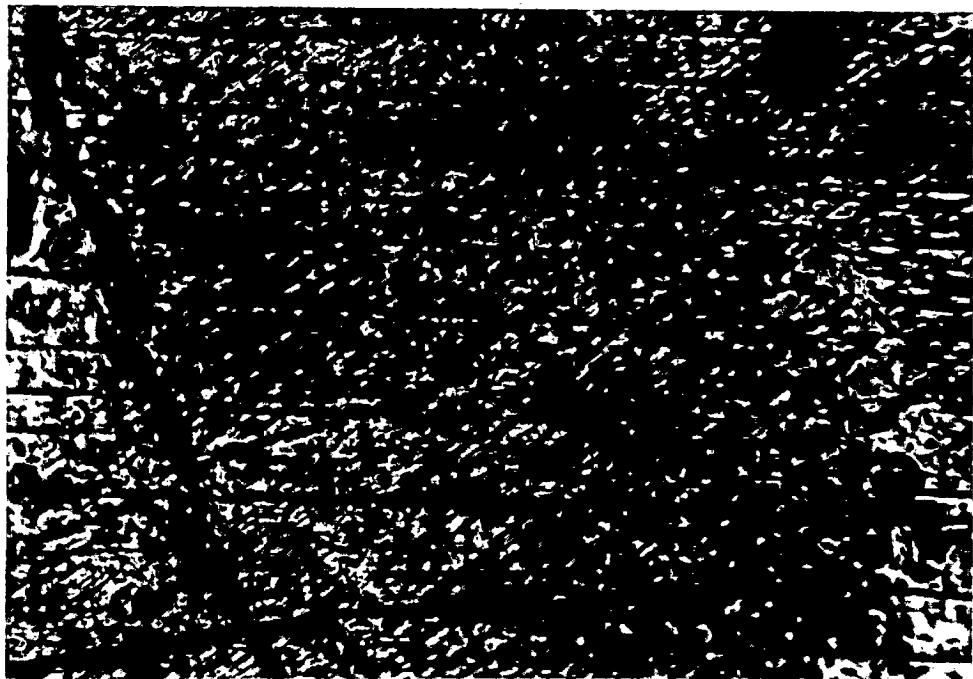
PHOTO 2 |—————|
                             200 µ

PLATE VIII

Photo 1 : Orthocumulate texture of troctolite.
              Plagioclase exhibit uniform core and
              zoned borders.(BXN)

Photo 2 : Mesocumulate texture in gabbronorite.
              Plagioclase show marginal zoning due
              to post-cumulus growth.(BXN)

PLATE VIII

PHOTO 1

150 μ

PHOTO 2

150 μ
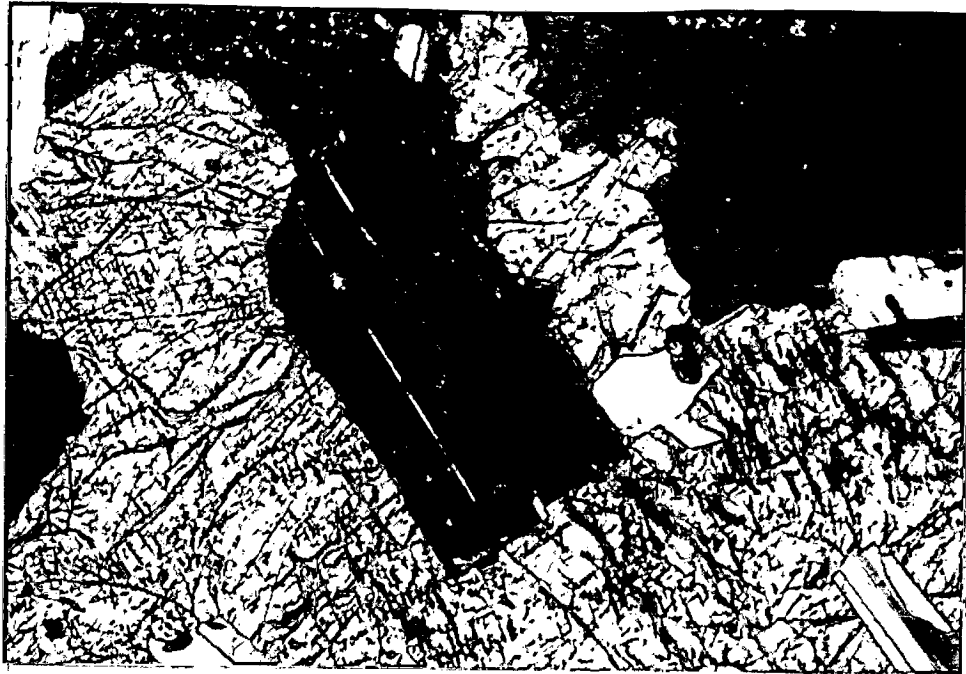
PLATE IX

Photo 1 : Exsolutions of clinopyroxene in Ca-poor
pyroxene. (BxN)

Photo 2 : Exsolution belbs of pigeonite and fine
exsolution lamallae of hypersthene in
clinopyroxene. (BxN)

PLATE IX
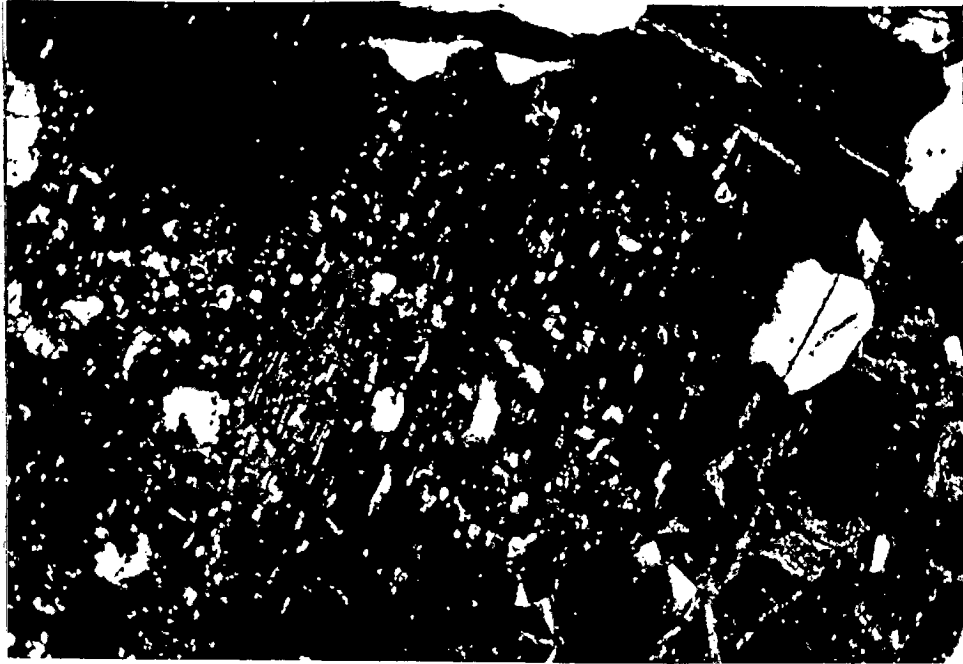
PHOTO 1   └──────────┘
100 ⋏

PHOTO 2   └──────────┘
110 ⋏

PLATE X

Photo 1 :   Reticulate texture exhibited by layered
            chromites.

Photo 2   : Aggregates of chromite with cuniform
            interstices occupied by serpentinised
            olivine.

PLATE X

PHOTO 1

PHOTO 2

700 μ
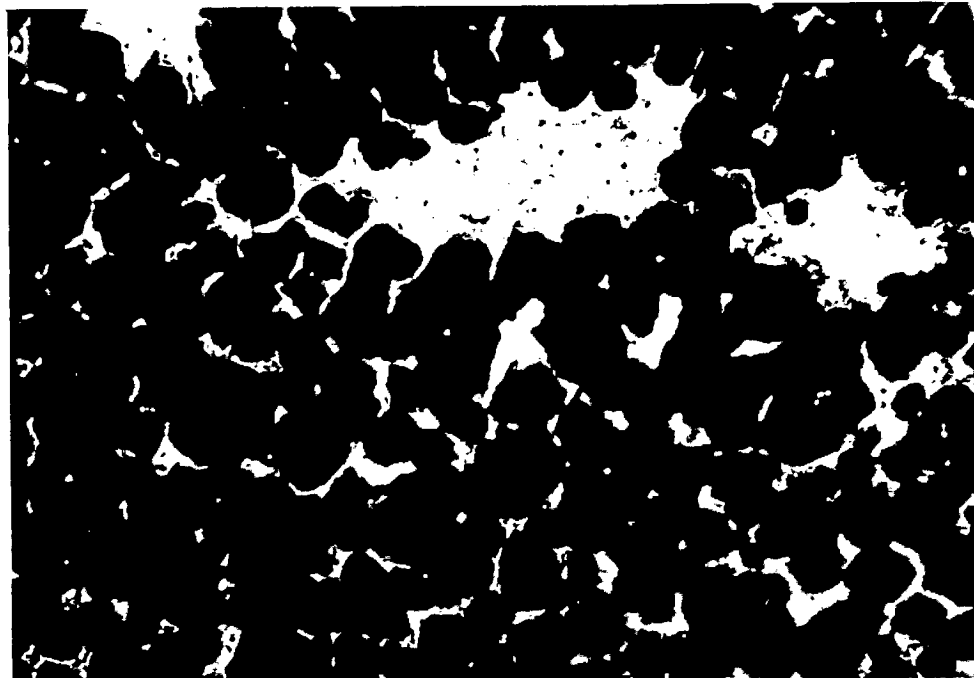
PLATE XI

Photo 1 : Pitted surface of chromite from chromitite.

Photo 2 : Exsolutions of ilmenite in chromite.

PHOTO 1

50 μ

PHOTO 2

50 μ
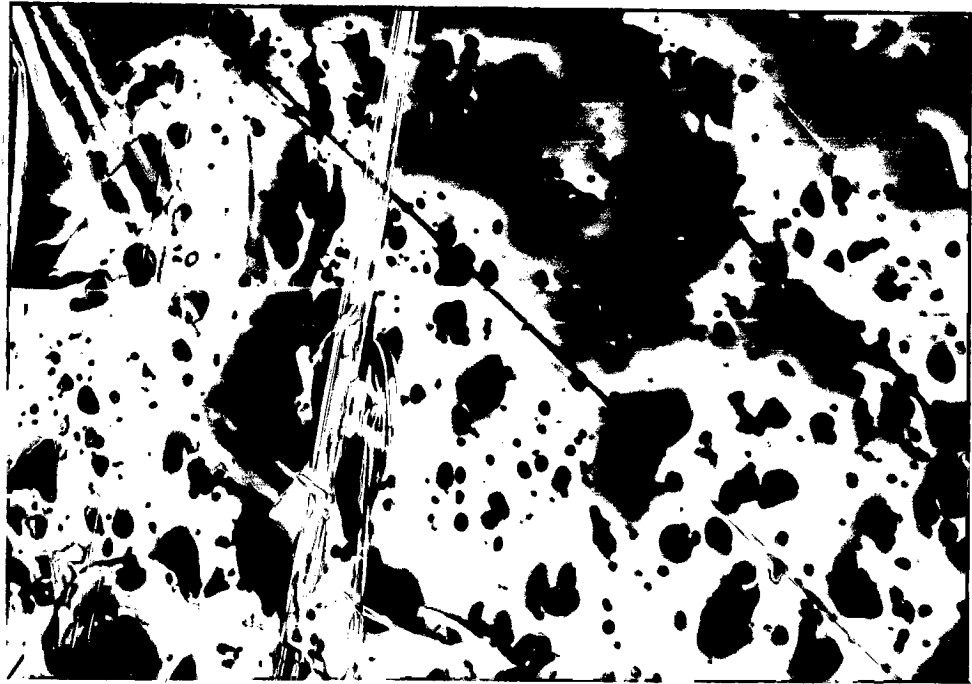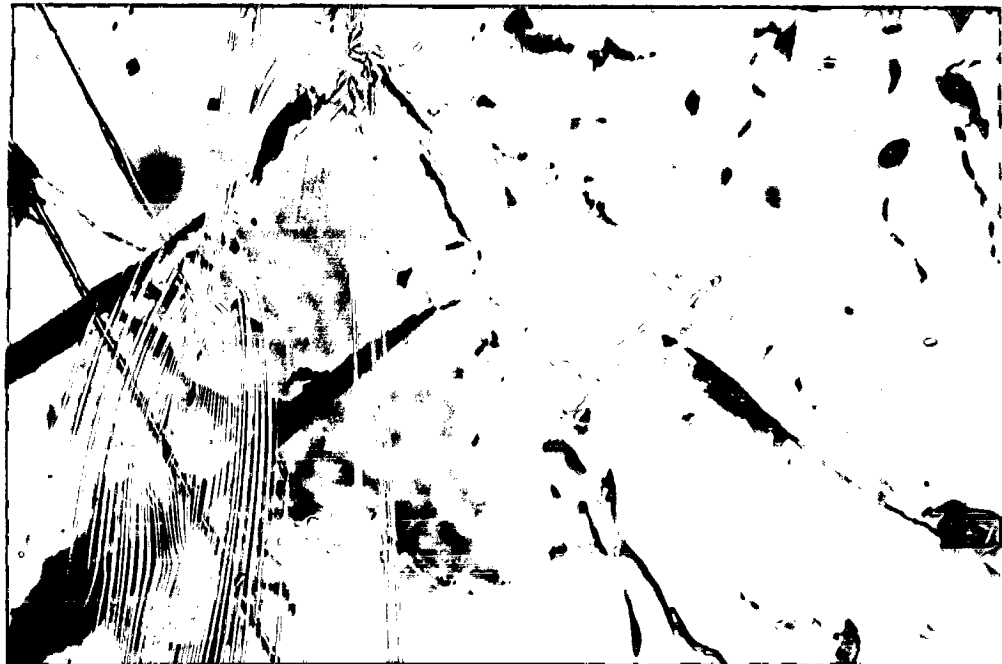
PLATE XII

Photo 1 :   Fibrous chlorite replacing chromite
            perpendicular to the layer.(BxN)

Photo 2 :   Rounded islands of serpentinised olivine in
            a ring of chromite grains.
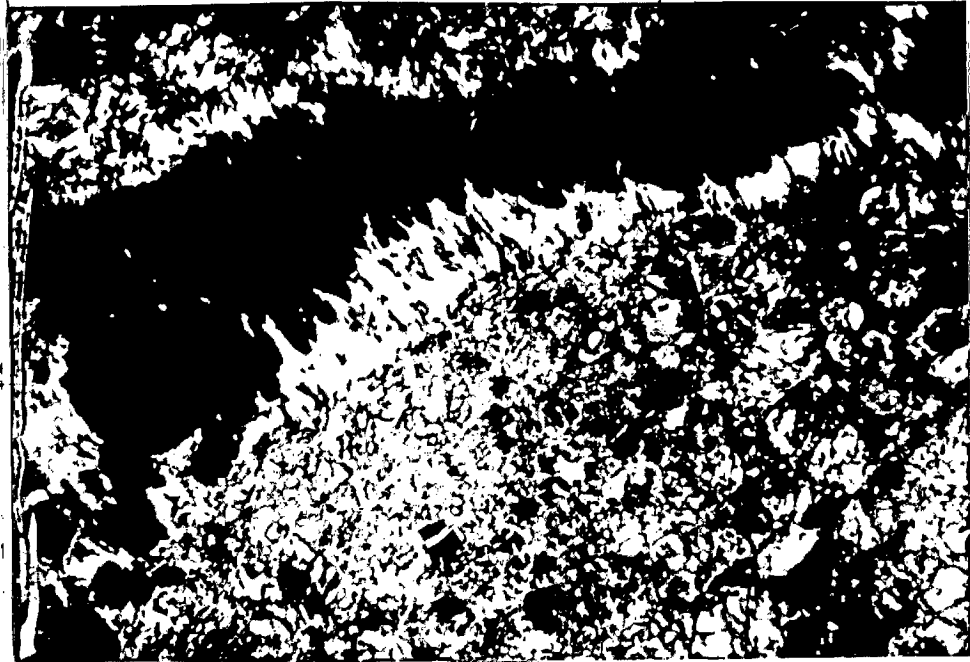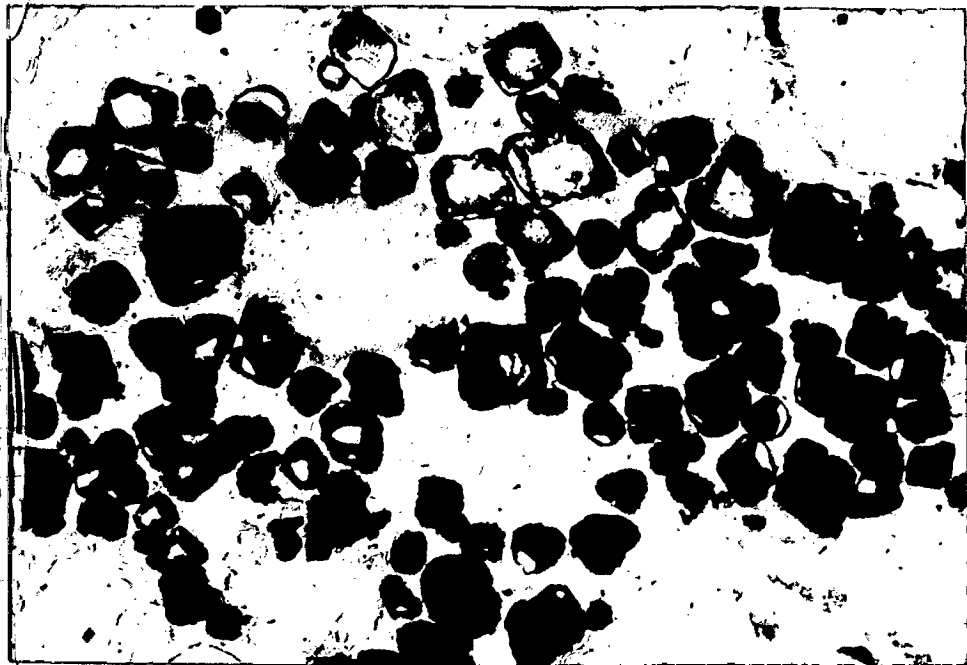
PLATE XII

PHOTO 1
900 μ

PHOTO 2
300 μ

PLATE XIII

Photo 1 : Megacrysts of euhedral pyrite sh~~w~~oing
compositional zoning.

Photo 2 : Intergrowth of pyrite-II and pentlandite
(pyrite-light   grey,   pentlandite   darker
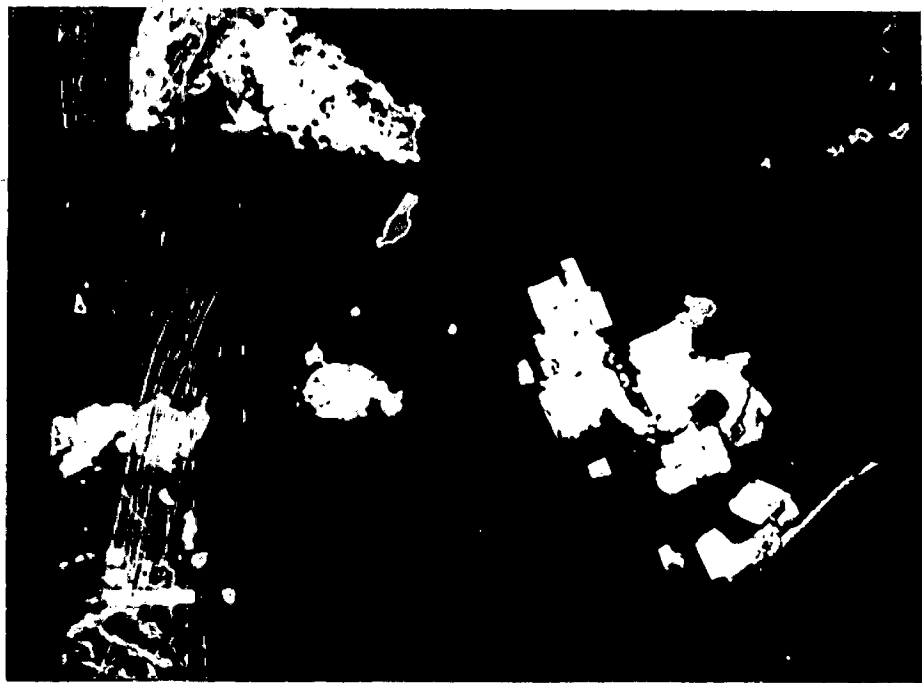grey).

PLATE XIII

PHOTO 1

PHOTO 2

PLATE XIV

Photo 1 : Exsolutions of pentlandite (light grey) in
pyrrhotite (medium grey).

Photo 2 : Euhedral crystal of Co-gersdorffite (light
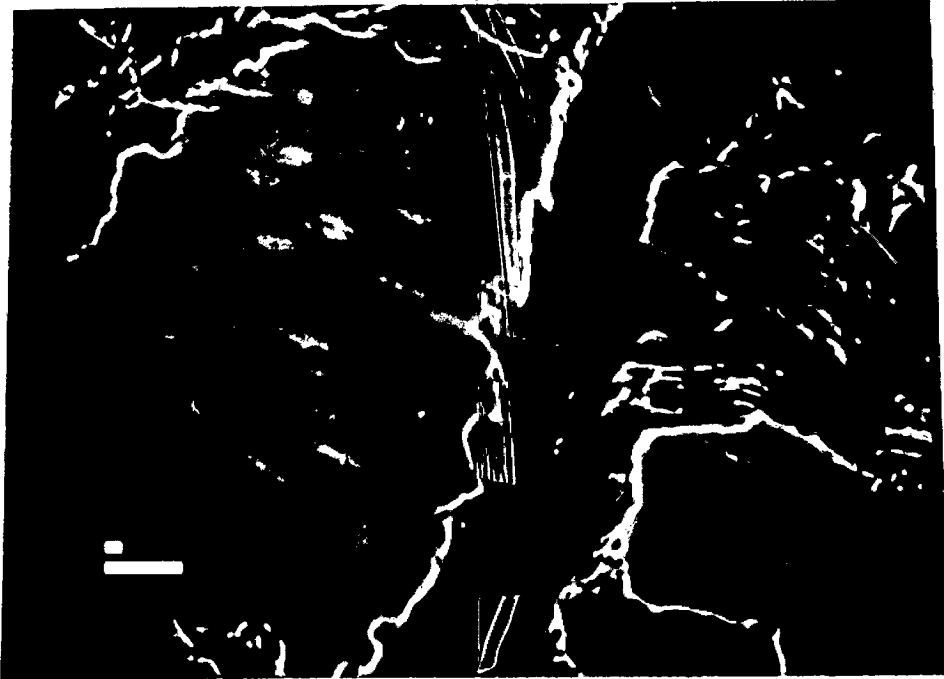grey) intergrown with pyrite (medium grey)

PLATE XIV

PHOTO 1

PHOTO 2